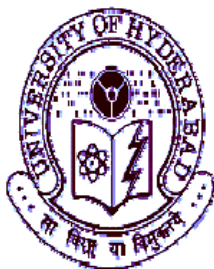


**SYNTHESIS, STRUCTURE AND PROPERTIES OF COPPER (II)  
AND NICKEL (II) PSEUDOHALIDE COMPLEXES WITH  
4,5-DIAZAFLUOREN-9-ONE**

A Thesis  
Submitted for the Degree of  
**Doctor of Philosophy**

By  
**BONIGE KISHORE BABU**



School of Chemistry  
University of Hyderabad  
Hyderabad – 500046  
India

DECEMBER 2010



*To*

**MY SAVIOUR JESUS CHRIST**





# CONTENTS

<b>TATEMENT</b>	i
<b>CERTIFICATE</b>	ii
<b>ACKNOWLEDGMENTS</b>	iii
<b>PREFACE</b>	v
<b>CHAPTER I</b>	
<b>A brief introduction of copper and nickel complexes</b>	
1.1. Coordination chemistry of copper (II) and nickel (II)	1
1.2 Copper complexes	2
1.2.1 Dopamine- $\beta$ -monooxygenase	2
1.2.2 Hemocyanins	3
1.2.3 Catechol oxidases	4
1.3 Copper(II) chemistry	6
1.3.1 Copper(II) dafone complexes	7
1.4. Nickel complexes	8
1.4.1 Nickel superoxide dismutase	9
1.4.2 Nickel carbon monoxide dehydrogenase	10
1.5 Ni(II) complexes	12
1.6 Pseudo halide chemistry of copper(II) and nickel(II) complexes	14
1.7 References	19
<b>CHAPTER II</b>	
<b>Tetranuclear copper azide complex of 4,5-Diazafluoren-9-one</b>	
2.1 Introduction	31
2.2. Experimental	32
2.2.1 Reagents	32
2.2.2 Synthesis of $(\text{Cu})_4(\text{dafone})_4(\text{N}_3)_8$ (1)	33

2.3. Measurements	33
2.3.1 Crystallographic data collection and structure determination	33
2.4. Crystal structure.	34
2.4.1 Crystal structure of $(\text{Cu})_4(\text{dafone})_4(\text{N}_3)_8$ (1)	34
2.5 Electronic spectra	39
2.6 Magnetic properties	40
2.7 Estimation of the Exchange Integrals by DFT Calculations	44
2.8 Conclusion	47
2.9 References	48

### CHAPTER III

#### Copper complexes of 4,5-Diazafluoren-9-one

3.1. Introduction	51
3.2. Experimental	51
3.2.1. Reagents	51
3.2.2. Synthesis	51
3.3. Measurements	53
3.3.1. Crystallographic data collection and structure determination	54
3.4. Crystal structure	56
3.4.1. Crystal structures of $\text{Cu}(\text{dafone})_2\text{NCS}_2$ and $\text{Cu}(\text{dafone})_2(\text{NCO})_2 \text{CH}_3\text{CN}$	56
3.4.2 Crystal structure of $[\text{Cu}_2(\text{dafone})_4(\text{OH})_2](\text{ClO}_4)_2$ (3)	63
3.4.3. Crystal structure of $[\text{Cu}_2(\text{dafone})_2(\text{oxalate})_2](\text{H}_2\text{O})_{0.5}$ (4)	66
3.5. Electronic spectra	69
3.5.1. $\text{Cu}(\text{dafone})_2\text{NCS}_2$	70
3.5.2. $\text{Cu}(\text{dafone})_2(\text{NCO})_2 \text{CH}_3\text{CN}$	70
3.5.3 $[\text{Cu}_2(\text{dafone})_4(\text{OH})_2](\text{ClO}_4)_2$	71
3.5.4. $[\text{Cu}_2(\text{dafone})_2(\text{oxalate})_2](\text{H}_2\text{O})_{0.5}$	72
3.6. Magnetic properties	73

3.7. Estimation of the Exchange Integrals by DFT Calculations	74
3.8 Conclusion	75
3.9 References	77

## CHAPTER IV

### Nickel complexes of 4,5-Diazafluoren-9-one

4.1. Introduction	79
4.2. Experimental	80
4.2.1. Reagents	80
4.2.2. Synthesis	80
4.3. Measurements	81
4.3.1. Crystallographic data collection and structure determination	81
4.4. Crystal structure	83
4.4.1. Crystal structures of Ni(dafone) <sub>2</sub> (NCS) <sub>2</sub> (1)	83
4.4.2. Crystal structure of [Ni(dafone)(H <sub>2</sub> O) <sub>4</sub> ](NO <sub>3</sub> ) <sub>2</sub> (2)	86
4.5. Electronic spectra	89
4.6. Conclusions	91
4.7. References	91

## CHAPTER V

### Nickel complexes of 1,10-phenanthroline ligand

5.1. Introduction	97
5.2. Experimental	98
5.2.1. Reagents	98
5.2.2. Synthesis	98
5.3. Measurements	99
5.3.1 Crystallographic data collection and structure determination	99
5.4. Crystal structure	101
5.4.1. Crystal structure [Ni(phen)(H <sub>2</sub> O) <sub>3</sub> Cl]Cl(H <sub>2</sub> O) (1)	101

5.4.2. Crystal structure of $[\text{Ni}(\text{phen})(\text{H}_2\text{O})_3\text{Br}]\text{Br}$ (2)	103
5.4.3. Crystal structure of $[\text{Ni}(\text{phen})_3](\text{Br}_3) \cdot \text{Br}_2$	106
5.5 Conclusion	109
5.6. References	110
<b>POSTERS AND WORKSHOPS</b>	115
<b>Manuscripts under preparation</b>	115

## **STATEMENT**

I hereby declare that the matter embodied in this thesis is the result of investigations carried out by me in the School of Chemistry, University of Hyderabad, Hyderabad, India under the supervision of Prof. M. V. Rajasekharan. In keeping with the general practice of reporting scientific observations, due acknowledgement has been made wherever the work described is based on the findings of other investigators.

**BONIGE KISHORE BABU**



## CERTIFICATE

Certified that the work embodied in this thesis entitled “*SYNTHESIS, STRUCTURE AND PROPERTIES OF Cu(II) and Ni(II) PSEUDOHALIDE COMPLEXES WITH 4,5-DIAZAFLUOREN-9-ONE*” has been carried out by **BONIGE KISHORE BABU**.  
under my supervision and the same has not been submitted elsewhere for any degree.

Hyderabad  
DECEMBER 2010

**M. V. RAJASEKHARAN**  
(Thesis Supervisor)

**DEAN**  
School of Chemistry





## ACKNOWLEDGEMENTS

I thank with immense pleasure Prof. M. V. Rajasekharan, supervisor of my thesis for his generous support and guidance. As a student, I am privileged to work with an admirable researcher and teacher. I am also grateful to him for the freedom of thought he has given me. I thank Prof. D. Basavaiah, the Dean, School of Chemistry and former Dean(s) for providing all the facilities of the School. I also thank Bhuyan A.K, Desiraju.G.R. and other faculty members in the School of Chemistry for their cooperation on various occasions.

I thank all the non-teaching staff of the School, for their help during the research work. A special word of thanks goes to Mr. Raghavaiah for his help in x-ray data collection, Ms. Asia Parvez for her help in IR measurements.

I thank Dr. J.-P. Tuchagues at Laboratoire de Chimie de Coordination du CNRS, Toulouse, France for the variable temperature magnetic susceptibility measurements. I gratefully acknowledged financial assistance provided by CSIR and UPE, India for carrying out my research.

I am also thankful to current (Dr. Bhargavi, Mr. Krishnachari and Mr.Mehaboob) and former labmate Dr. Sailaja for their assistance and timely help. My special thanks to Dr. Biju. A. R for his excellent co-operation to finish my thesis writing. My heartfelt thanks also go to all dear friends of the university. I thank all those who gave suggestions, advices and guidance before and in course of the research.

Special mention to Bro.Israel(God servant) and Bro. Katta Ravi, because they helped and motivated to join University of Hyderabad and Dr.Damodar Rao for his guidance to write M.Sc entrance. I should convey honest thanks to my classmates, Dr.Mukkanti, Dr.Prasanth, Dr.Satyanarayna, Dr.Prabhakar, Dr.Lenin, and Dr.Rinku radhika for their valuable suggestions and moral support during my M.Sc and M.phil Courses.

My sincere thanks to Hebron Church Members and the founder Bro. Bakth Singh, and other co-workers Bro.Andrew, Bro.Paul Abhishegum, Bro.Israel (Gannavaram),

Bro.Asirvadam, Bro.Israel (Macherla), Bro.Isaac (MRF) and prayer supporters Dr. Suseel Nirmala, Dr.Praveen Kumar,Pedda Ravi, Chinna Ravi Dr. Pedda Rataiah, Dr. Nageswara Rao, Dr.Pamu, Dr.James Raju, Prof.Sudhakar, Beesanna, Devaiah, VasanthaRao, Pradeep, M.Santhosh Kumar, Ch.Syam Kumar, M.RamaKrishna, Sk.Masthan, Krisna, Pintu, Koti, Sis.Swathi, Mrudula, Malleswari, Jansy, divya, santhi, sreelatha, swapna, rupa, grace, Sindhura, Dr.Rani, Dr.Karunakar, Dr. Kumar, swaroop, pradeep, Prashanth, Samuel, Chandra, Krimson and saints from Macherla(penuel), Bethesda(hyd), Gopanpalli, Gannavaram, and all other places, those who prayed for me in my joy, problems and sufferings.

My sincere gratitude to my dear family members, wife Swarna Latha and my beloved *children* John Samuel and Paul Jacob nana John Babu, *amma* Marthammma, *thamudu* Ramesh, *maradalu* Subbayamma, *daughters* cherry and china, *Chelli* Kavitha Priyanka, *Bavamaridi* Kiran, athama samdanam, mamaiah staynamdam, babai david raju, aunt indira, vineetha, jeevitha,ashi *akka* Padma and all other relatives for their encouragement and love towards me spiritually, economically throughout my career.

Last but not least, my adoration towards beloved God, Saviour of the sinners and heavenly father **Jesus Christ** for his spiritual and physical guidance, for His breath, for His grace which is abundant, for His unexplainable love, for His calvary's blood to wash my sins, for His promises in all times, for His forgiving character that never showed by any person on the earth and for constant encouragement to fulfil my education, ambitions and good desires. There is a word in **the Bible**, ***I will never leave thee nor forsake thee*** (Heb 13:5). That has been proved to be true in my life as God is with me in all the situations. I am thankful for all benefits such as His salvation and spiritual talents.

**BONIGE KISHORE BABU**

## PREFACE

The studies on copper(II) and nickel(II) pseudohalide 4,5-diazafluoren-9-one (dafone) complexes are of great interest due to their relevance in various biological systems like DNA intercalation studies and the importance in the field of molecular magnetism. 4,5-diazafluoren-9-one (dafone) is a bidentate ligand. It is a derivative of 1,10-phenanthroline (phen), having an exocyclic keto function. The thesis explores synthesis, structure and properties of various copper(II) and nickel(II) pseudohalide complexes.

Thesis is divided into five chapters. Chapter I gives a brief introduction to various copper(II) and nickel(II) pseudohalide complexes and their relevance to various fields including biological systems. Besides these, a brief account of the background work of mononuclear, dinuclear, tetranuclear and polynuclear complexes are also described. Chapter II deals with synthesis, structural analysis, reflectance spectra, molecular magnetism and DFT of tetranuclear copper(II) complex with azide ion. Chapter III deals with Synthesis, structure, reflectance spectra, of two mononuclear, and one polynuclear copper(II) pseudohalide complexes are discussed. Molecular magnetism and DFT studies of one dinuclear copper(II) hydroxy bridged complex also discussed. Chapter IV deals with synthesis, electronic spectra and structural characterisation of two mononuclear nickel (II) dafone complexes are discussed. In Chapter V, synthesis and structural characterisation of three 1,10-phenanthroline (phen) nickel(II) complexes are discussed.

In the thesis only essential crystallographic data and selected geometrical parameters of the compounds are given. Through out the thesis, in thermal ellipsoid plots atoms are represented as 30% probability ellipsoids and all hydrogen atoms and solvent molecules are omitted for clarity.

A copy of this thesis (.pdf), file containing crystallographic information (.cif) and a .cif file viewer is available in a CD-ROM at the back cover of the thesis.

Part of the work reported in this thesis has been published are given at the end of the thesis.

## Abbreviations and definitions

$$R1 = \Sigma ||F_o| - |F_c|| / \Sigma |F_o|$$

$$wR2 = \{\Sigma [w(F_o^2 - F_c^2)^2] / [\Sigma (w(F_o^2)^2)]\}^{1/2}$$

$$w = 1/[\sigma^2(F_o)^2 + (AP)^2 + BP]; P = [2F_c^2 + \text{Max}(F_o^2, 0)]/3$$

$$\text{GooF} = \{\Sigma [w(F_o^2 - F_c^2)^2] / (n-p)\}^{1/2}$$

$$\Delta\rho_{max}, \Delta\rho_{min} = \text{Maximum, minimum residual electron density on the final Fourier map.}$$

# CHAPTER 1

## A brief introduction of copper and nickel complexes

### 1.1 Coordination chemistry of copper (II) and nickel (II)

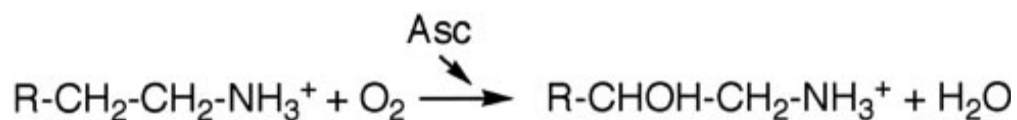
$\text{Cu}^{2+}$  and  $\text{Ni}^{2+}$  occupying adjacent position in the periodic table have considerable similarity in their coordination chemistry. There are also important differences, most of which can be traced to the electronic lability associated with the  $d^9$  configuration of  $\text{Cu}^{2+}$ . The present chapter briefly reviews these aspects. Much of the interest especially during the past two decades, arise from the biological role of these ions. Therefore, some aspects of the biological role of copper and nickel are also discussed even though the thesis is not directly concerned with bio-inorganic chemistry. This chapter also reviews the coordination modes of dafone as well as pseudo halide ligands as a prelude to the material presented in later chapters.

## 1.2 Copper complexes

The coordination chemistry of copper(II) has been increasingly studied in an effort to simulate various biological systems. Copper is present in the active site of several enzymes and play fundamental roles in living systems. This metal is coordinated to the protein forming mononuclear enzymes, e.g. dopamine- $\beta$ -monooxygenase, which catalyze the conversion of dopamine to norepinephrine with the insertion of an atom of oxygen into the benzylic position of the ethylamine side chain.<sup>1</sup> Binuclear enzymes, e.g. hemocyanins, transport dioxygen in various arthropods and molluscs.<sup>2</sup> Catechol oxidases are ubiquitous plant enzymes containing a dinuclear copper center. In the wound-response mechanism of the plant they catalyze the oxidation of a broad range of *ortho*-diphenols to the corresponding *o*-quinones coupled with the reduction of oxygen to water.<sup>3</sup>

### 1.2.1 Dopamine- $\beta$ -monooxygenase

Dopamine- $\beta$ -monooxygenase belongs to a small class of copper proteins found exclusively in eukaryotes. These physiologically important enzymes catalyze the transformation of dopamine to norepinephrine (D $\beta$ M). A schematic diagram of the D $\beta$ M unit is shown in Figure 1:1



This enzyme is localized in subcellular compartments: the chromaffin vesicles of the adrenal gland or synaptic vesicles of the sympathetic nervous system (D $\beta$ M)<sup>4</sup>. Low temperature EPR spectra of D $\beta$ M indicate a typical 'type 2' cupric ion pattern which is similar to Cu(II)-EDTA standards<sup>5</sup>. Spin counting of fully reconstituted enzyme shows two cupric ions per subunit.

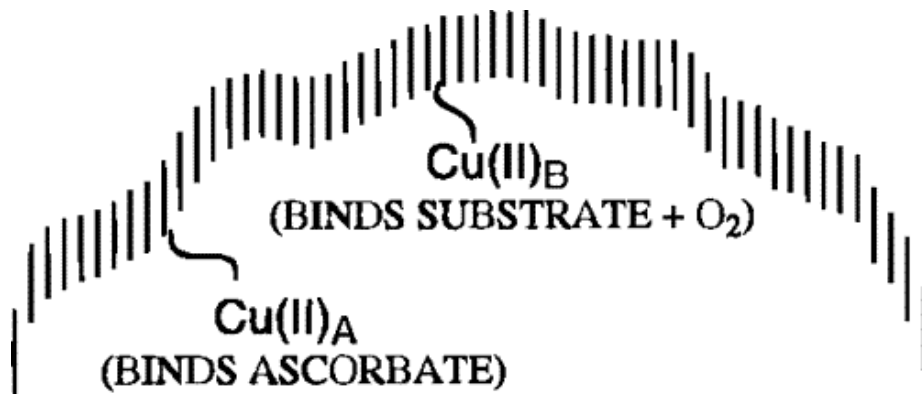


**Figure 1.1.** Schematic of the D $\beta$ M Subunit, Showing the Different Roles for Cu<sub>A</sub> (in Electron Transfer) and Cu<sub>B</sub> (in Substrate Hydroxylation)<sup>6</sup>

These data immediately ruled out a binuclear complex in which the active site coppers are connected by a bridging ligand.

### 1.2.2 Hemocyanins

Hemocyanins are giant oxygen transport proteins found in many arthropods and molluscs. Freely dissolved in the hemolymph, they are multisubunit proteins that contain many copies of the active site, a copper atom pair that reversibly binds oxygen. The active site is a pair of Cu atoms, designated CuA and CuB, (Figure 1.2) which are coordinated directly to the protein by histidine

side chains<sup>8</sup>. Upon reaction with oxygen, which binds as a peroxide ion, the Cu(I,I) state is oxidized to the Cu(II,II) state.

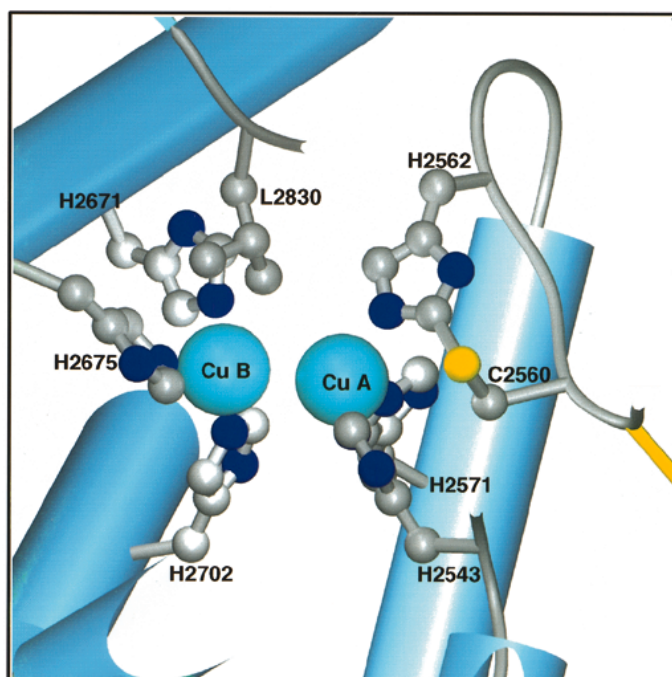


**Figure 1.2.** The oxygen-binding site. Odg (*Octopus dofleini* hemocyanin) is portrayed with  $\alpha$ -helices shown as cylinders,  $\beta$ -sheets as flat ribbons, and random coil as rope<sup>7</sup>. Copper atoms are shown as large spheres.

### 1.2.3 Catechol oxidases

Catechol oxidases are ubiquitous plant enzymes containing a dinuclear copper center which oxidises phenols into quinones. Catechol oxidase is also known as *o*-diphenol oxidase or polyphenol oxidase. This ubiquitous plant enzyme lacks hydroxylase activity, but catalyzes a two-electron transfer reaction during the oxidation of a broad range *o*-diphenols (like caffeic



acid) to the corresponding *o*-quinones by molecular oxygen<sup>9</sup>. The resulting highly reactive quinones auto-polymerize to form brown polyphenolic catechol melanins, a process thought to protect the damaged plant from pathogens or insects<sup>10</sup>. The turning of apple into flesh brown, darkening of cut potato tuber, turning tea leaves brown and producing the flavour of black tea when the green leaves are bruised and left in the presence of air for about an hour before drying etc are due to polyphenolic catechol melanins. The crystal structure of the enzyme from sweet potato shows that the active centre contains dicupric Cu(II)-Cu(II) state<sup>11</sup>. (Figure 1. 3)

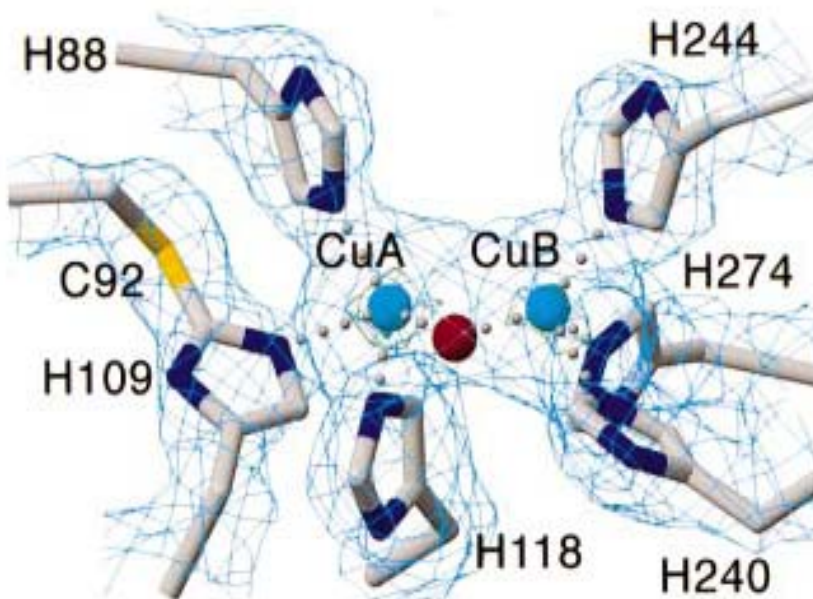


**Figure 1.3.** A sample of  $2[|F_o| - |F_c|]\Phi_{\text{calc}}$  electron density, for the oxidized catalytic dinuclear copper site.<sup>11</sup>

### 1.3 Copper(II) chemistry

Copper(II) readily forms coordination complexes involving mainly the coordination numbers four, five and six, but unlike the majority of the first-row metal ions, the copper(II) complexes are characterized by a seemingly infinite variety of distortions. The majority of six-coordinate copper(II) complexes involve an elongated tetragonal<sup>12</sup> or rhombic octahedral structure<sup>13</sup>, with only a few involving a compressed tetragonal<sup>14</sup> (or rhombic) octahedral structure. The tetrahedral geometry for the copper(II) ion always involves a significant compression along the  $S_4$  symmetry axis. Only the square planar geometry is regular for both the nickel(II) and copper(II) ions. Five-coordinated copper(II) ion rarely shows up a regular square pyramidal stereochemistry<sup>15</sup>.

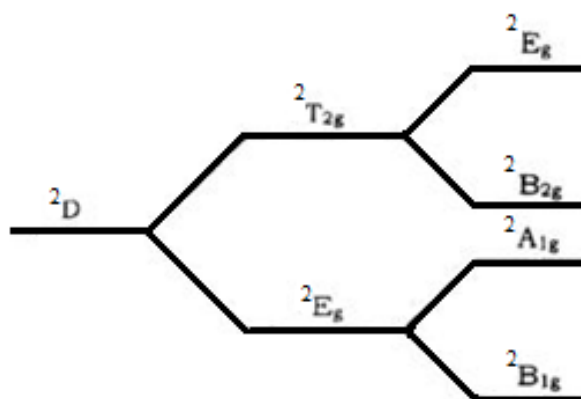
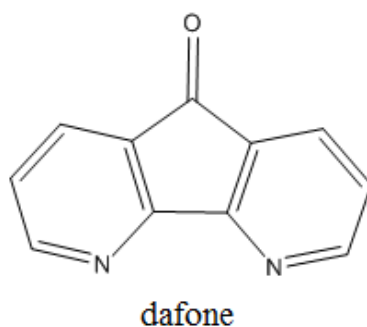


**Figure 1.4.** Splitting of  $^2T_{2g}$  and  $^2E_g$  states in Copper(II)

Copper(II) complexes are generally green or blue. Exceptions are usually caused by strong UV bands tailing off into blue end of the visible spectrum causing them to appear red or brown. The structural aspects in relation to its magnetic behaviour, electronic spectra and nature of bonding have been thoroughly reviewed<sup>16</sup>. The correlation between stereochemistry and  $d^9$  configuration has been well established by using single crystalline EPR spectra<sup>17</sup>. Since copper(II) is subjected to Jahn-Teller distortion a regular octahedron complex is not formed in all cases. The spectra is based on the splitting as shown in Figure 1.4

### 1.3.1 Copper(II) dafone complexes

4,5-Diazafluoren-9-one (dafone) is a bidentate ligand. It is a derivative of 1,10-phenanthroline (phen), having an exocyclic keto function<sup>18</sup>. Dafone attracted attention of researchers due perhaps to its DNA intercalation properties<sup>19</sup>. The reactive exocyclic keto function in dafone offers distinct advantages for further derivatization to yield multinuclear metal complexes having interesting catalytic and biological properties.



The bite distance (2.99 Å) of the donor N atoms dictates the overall geometry of the metal complexes. The rigid five-membered ring of dafone enlarges the N-N bite distances compared with the analogues 2,2'-bipyridine. Consequently the long N-N distance of the dafone has an unfavourable effect on the formation of a five-membered chelating ring with transition metal ions and so the coordination chemistry of dafone is still restricted to few metal complexes.<sup>17,20, 21</sup> While the  $\text{Cu(en)}_2\text{X}_2$  (en = ethylenediamine) complex have coplanar  $\text{CuN}_4$  chromophore,<sup>22</sup> the  $\text{Cu(bpy)}_2\text{X}_2$  complexes are prevented from assuming this coordination by the steric requirements of the bipyridyl hydrogen atoms<sup>23</sup>. However the large N-N bite distance (2.99 Å) enforced by the rigid five-membered central ring leads to unequal binding by the two N atoms with smaller metal atom ions, such as Cu(II) and thus  $\text{Cu(dafone)}_2\text{X}_2$  complexes form coplanar  $\text{CuN}_4$  chromophore.<sup>17b</sup> However dafone appears to overcome its preference for unsymmetrical chelation when its tris chelates was stabilized by extensive polyiodide networks<sup>20e</sup>. In most cases Cu(II) forms mononuclear complexes with dafone<sup>20</sup>, only one structure has been reported with a dinuclear core<sup>21</sup>.

#### 1.4. Nickel complexes

Nickel plays numerous roles in the biology of microorganisms and plants, the main constituent of various enzymes and coenzymes like carbon monoxide dehydrogenase<sup>24</sup>, superoxide dismutase<sup>25</sup> and glyoxalase.<sup>26</sup>

### 1.4.1 Nickel superoxide dismutase

Superoxide dismutases are metalloenzymes which disproportionate the  $O_2^-$  radical into molecular oxygen and peroxide ion. The superoxide radical is an inevitable by-product of aerobic metabolism which if not eliminated may cause significant cellular damage. To avoid such a harmful consequences, all oxygen metabolising organisms have metalloenzymes known as superoxide dismutases (SODs). X-ray crystallographic studies<sup>4</sup> of NiSODs from *streptomyces* have shown that the active site is mononuclear. The 1.30 Å resolution crystal structure of nickel superoxide dismutase (NiSOD) identifies a novel SOD fold, assembly, and Ni active site. NiSOD is a hexameric assembly of right-handed 4-helix bundles of up-down-up-down topology with N-terminal hooks chelating the active site Ni ions (Figure 1.5). The active site Ni geometry cycles from square planar Ni(II), with thiolate (Cys2 and Cys6) and backbone nitrogen (His1 and Cys2) ligands, to square pyramidal Ni(III) with an added axial His1 side chain ligand, consistent with electron paramagnetic resonance spectroscopy.

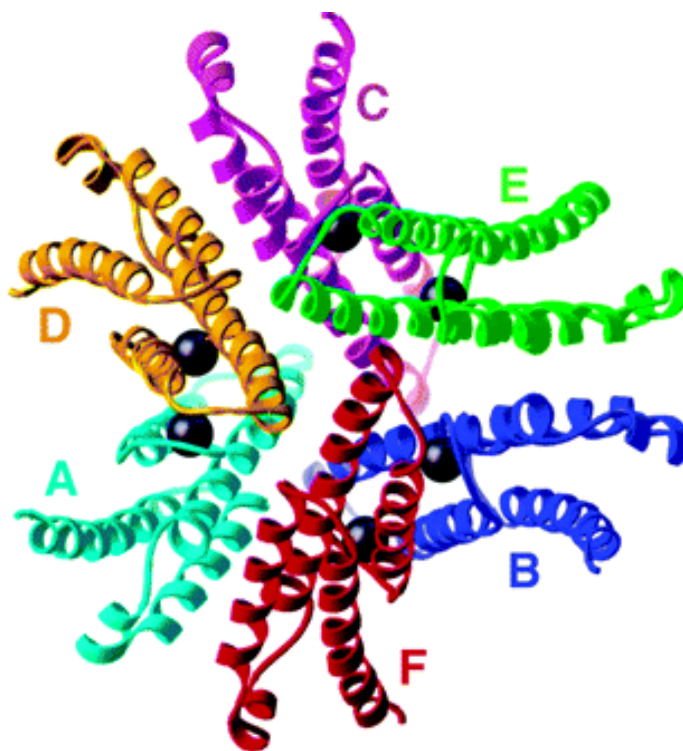


**Figure 1.5.** NiSOD subunit and hexameric structure<sup>4</sup>

### 1.4.2 Nickel carbon monoxide dehydrogenase

The capacity to oxidize carbon monoxide (CO) is a central metabolic feature of several groups of bacteria and archaea. Carbon monoxide dehydrogenases (CODHs) are the enzymes responsible for CO metabolism in microorganisms. The homodimeric nickel-containing CO dehydrogenase from the anaerobic bacterium *Carboxydotherrnus hydrogenofomans* catalyzes the oxidation of CO to CO<sub>2</sub>. A crystal structure of the reduced enzyme has been solved at 1.6 Å resolutions.

Figure 1.6

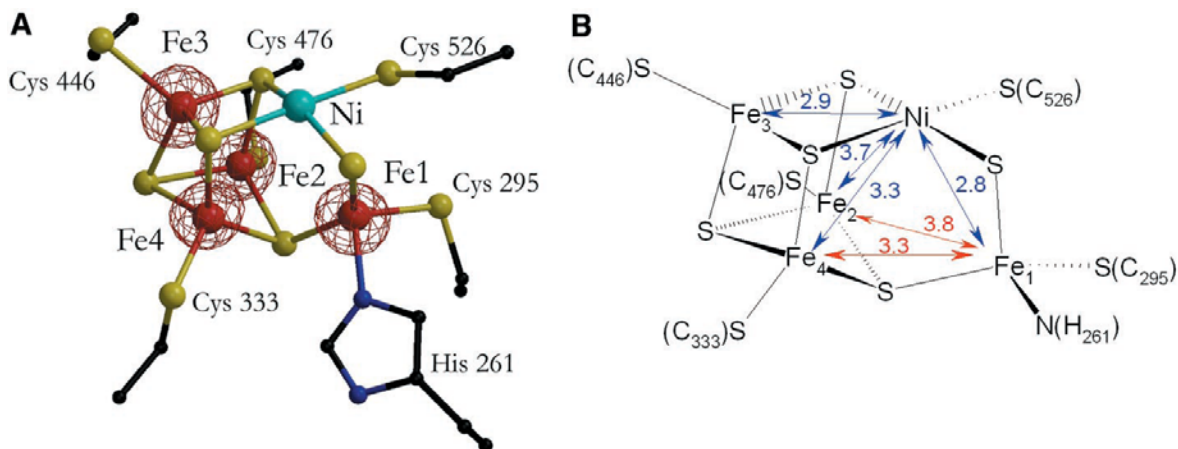


**Figure 1.6.** Cluster C, the active site of CO dehydrogenases. (A) View of the cofactor with its protein ligands. (B) Schematic presentation of cluster C with Ni-Fe (blue) and selected Fe-Fe (red) distances.<sup>24</sup>

This structure represents the prototype for Ni-containing CO dehydrogenases from anaerobic bacteria. It contains five metal clusters of which clusters B, B', and a subunit-bridging, surface-exposed cluster D are cubane-type [4Fe-4S] clusters. The active-site clusters C and C' are novel, asymmetric [Ni-4Fe-5S] clusters. Their integral Ni ion, which is the likely site of CO oxidation, is coordinated by four sulfur ligands with square planar geometry.

### 1.5 Ni(II) complexes

Nickel has a variety of oxidation states ranging from -1 to +4. The most common oxidation state is +2. Nickel(II) forms a large number of complexes with coordination numbers 4 to 6. Some examples are given in table.

---

Table.1.1 Various coordination modes adopted by Ni(II) complexes.

---

Coordination number	Geometry	Examples
4	Square planar	$[\text{Ni}(\text{CN})_4]^{2-}$ <sup>27</sup>
4	Tetrahedral	$[\text{Ni}(\text{Cl})_4]^{2-}$ <sup>28</sup>
5	Square pyramid	$[\text{Ni}(\text{CN})_5]^{3-}$ <sup>29</sup>
6	Octahedral	$[\text{Ni}(\text{NH}_3)_6]^{2+}$ <sup>30</sup>

---

A characteristic feature of nickel(II) complexes is that often a temperature dependent equilibrium exists among the various structures. This is due to the very small free energy difference between the various stereochemical forms<sup>31</sup>.



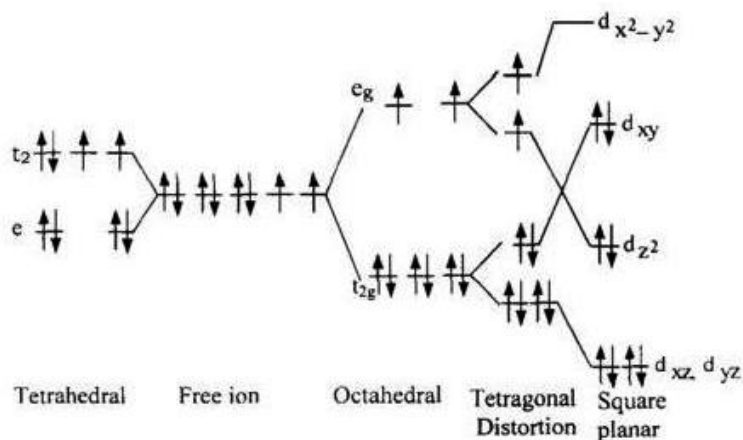


**Figure 1.7.** d-orbital splitting pattern for tetrahedral, octahedral and square planar complexes of Ni<sup>2+</sup>.

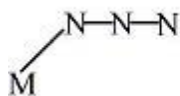
Figure 1.7 shows d-orbital splitting pattern for tetrahedral, square planar and octahedral Ni<sup>2+</sup>. While tetrahedral Ni(II) generally is paramagnetic, four-coordinate square planar Ni(II) is usually assumed to have a closed-shell (diamagnetic) ground state, which results from the large antibonding  $\sigma$ -interaction of the four ligands with the  $d_{x^2-y^2}$  metal orbital. This is not always true, however, since paramagnetic square planar Ni(II) complexes with a triplet ground state have been discovered.<sup>32</sup> Ni has a smaller radius in square planar geometry than in tetrahedral, which is assumed to result from the non-Aufbau electron filling in  $d^8$  square planar species. Even though many nickel(II) complexes of  $\alpha$ -diimine ligands like bpy<sup>33</sup> and phen<sup>34</sup> were reported only one dafone complex has been structurally characterized by X-ray crystallography.<sup>35</sup>

## 1.6 Pseudo halide chemistry of copper(II) and nickel(II) complexes

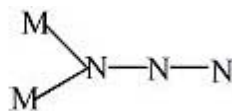
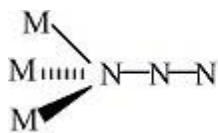
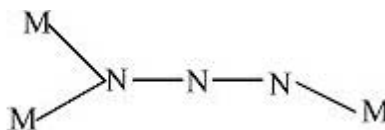
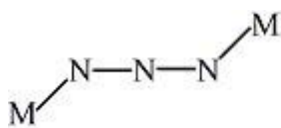
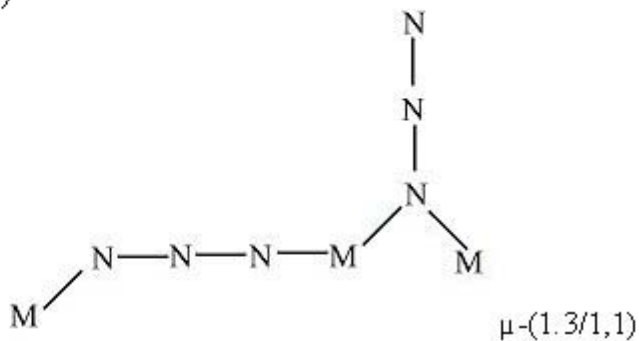
Pseudo halides can bind to range of transition metals and have a number of potential binding modes. This means that a range of structural diversity can be observed. Short bridging pseudo halide ligands such as azides, thiocyanates, isocyanates, cyanides and nitrile donors provide a convenient way of connecting transition metals in the solid state. They are extremely versatile ligands in coordination chemistry. Importantly pseudo halides are generally rigid with a somewhat defined directionality, so when combined with labile transition metals they are more disposed to form crystalline materials. Investigation into the structural and magnetic properties of the polynuclear transition metal complexes with pseudohalides has been a fascinating subject in the field of coordination chemistry.<sup>36</sup> Several magnetically active binuclear<sup>37</sup> and polynuclear<sup>38-44</sup> metal complexes containing pseudo halides has been reported. In the field of pseudohalide chemistry, the research in metal-azido systems has been mainly concentrated on the low dimensional molecules.<sup>45,46</sup> The high dimensional molecular networks of metal-azido derivatives are of particular interest because of their novel topology and enhancement of bulk magnetic properties as well as their magneto-structural correlations. Copper(II)-azide chemistry<sup>47,48</sup> is of considerable interest in recent years. And there have been extensive efforts focusing on the synthesis and properties of transition metal azide compounds. The azide ligand, despite the fact that strong magnetic couplings are common features of

transition metal-azido systems, is yet to yield many magnetic materials at room temperature and low temperature.

On the other hand, the many possible bridging modes of this ligand make its compounds a real challenge for crystal engineers. To date, the azido ligand has been found to bridge metal ions in the modes of 1,1-(end-on, EO)<sup>49</sup> 1, 3-(end-to-end, EE)<sup>50-52</sup>, 1,1,1<sup>53,54</sup>, 1,1,3<sup>55</sup>, 1,1,1,1<sup>56, 57</sup> and unusual 1,1,1,3,3,3 fashion<sup>58</sup>. Ferromagnetic interactions are usually transmitted by the EO bridging mode of the azido ligand and antiferromagnetic interactions are by the EE bridging mode<sup>59-62</sup>. DFT calculations on EO or EE azido bridged transition metal dimeric complexes provide good predictions and theoretical evidence for the magnetic properties.<sup>63-65</sup> Different bridging modes of azide as shown below.

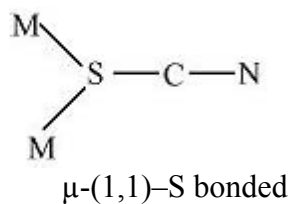
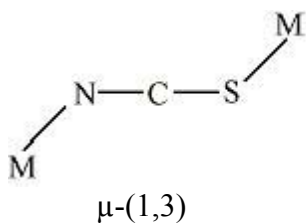
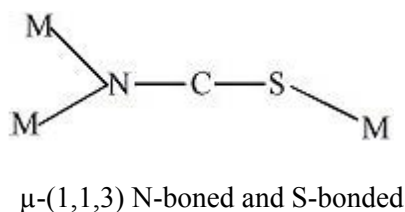
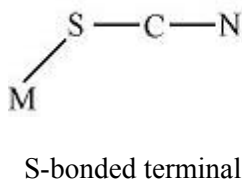
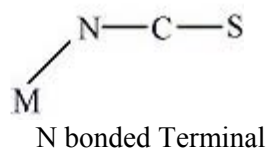
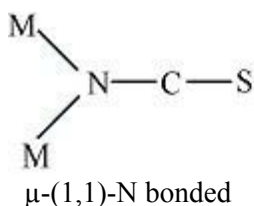


Terminal

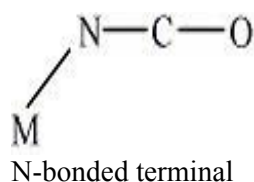
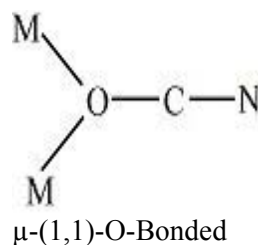
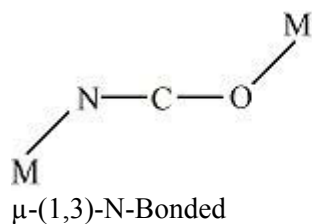
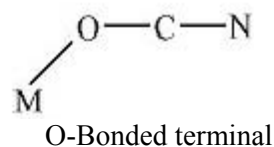
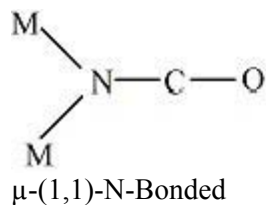
 $\mu$ -(1,1) $\mu$ -(1,1,1) $\mu$ -(1,1,3) $\mu$ -(1,3) $\mu$ -(1,3/1,1)

Thiocyanate (or isothiocyanate) complexes have attracted a great deal of attention due to their structural versatility and potential for development of optical, magnetic and conductive materials<sup>66-68</sup>. However, research efforts are primarily focused on their synthesis, magnetism and coordination isomerism. Noticeably, despite great significance as functional solid materials,

polymorphism of thiocyanate complexes remains little explored. Being an ambidentate ligand thiocyanate may coordinate the metal center through the nitrogen (M-NCS) or the sulfur (M-SCN) or both (M-NCS-M). The N-C and C-S bond distances of the thiocyanate ion are 1.149 and 1.169 Å, respectively. The coordination bond distance of N-bonded thiocyanate is less than S-bonded thiocyanate ion. The SCN group is an excellent polymer bridge, and the introduction of this anion to the compound can lead to the one-two-three dimensional nets.<sup>65</sup> Bridging thiocyanate-Cu(II) complexes includes  $\mu$ -N,S-NCS<sup>66,67</sup> and  $\mu$ -S,S-NCS<sup>68</sup> modes. Different ways of bridging moieties have shown in the below.



The linear cyanate ligand may coordinate the metal center through the nitrogen (M-NCO) or the oxygen (M-OCN) or both (M-NCO-M). The N-C and C-O bond distances of the thiocyanate ion are 1.17 and 1.23 Å respectively. Majority of the reported complexes are N-bonded. Different coordination modes of the cyanate are shown in the below scheme.



Furthermore, as a part of our research studies on our metal complexes of azide, thiocyanate and isocyanate bridges, we have obtained some interesting compounds as we discussed in the coming chapters.

## 1.7. References

1. (a) Winkler, H.; Apps, D. K.; Fischer-Colbrie, R. *Neuroscience* **1986**, *18*. (b) Stewart, L. C.; Klinman, J. P. *Annu. Rev. Biochem.* **1988**, *57*, 551. (c) Klinman, J. P. *Chem. Rev.* **1996**, *96*, 2541.
2. Magnus, K. A.; Ton-That, H.; Carpenter, J. E. *Chem. Rev.* **1994**, *94*, 727.
3. Klabunde, T.; Eicken, C.; James C.; Sacchettini, J. C.; Bernt, K. B. *Nature. Structural biology.* **1998**, *5*, 1084.
4. Stewart, L. C.; Klinman, J. P. *Annu. Rev. Biochem.* **1988**, *57*, 551.
5. Iones, T.; Skotland, T.; Lontie, R. *CRC Press: Boca Raton*, **1984**, 131.
6. Brenner, M. C.; Klinman, J. P. *Biochemistry* **1989**, *28*, 4664.
7. Evans, S. V. J. *J. Mol. Graph.* **1993**, *11*, 134.
8. Ling, J.; Nestor, L. P.; Czernuszewicz, R. S.; Spiro, T. G.; Fraczekiewicz, R.; Sharma, K. D.; Loehr, T. M.; Sanders-Loehr, J. *J. Am. Chem. Soc.* **1994**, *116*, 7682.
9. Cary, J. W.; Lax, A. R.; Flurkey, W. H. *Plant Mol. Biol.* **1992**, *20*, 245.
10. Dervall, B. J. *Nature.* **1961**, *189*, 311.
11. Klabunde, T.; Eicken, C.; James C. Sacchettini, J. C.; Krebs, B. *Nature Structural biology.* **1998**, *5*, 1084.
12. Moncol. J.; Mudra, M.; Lönnecke, P.; Hewitt, M.; Valko, M.; Morris, H.; Svorec, J.; Melnik, M.; Mazur, M.; Koman, M. *Inorg. Chim. Acta* **2007**, *360*, 3213.

13. Barquín, M.; Garmendia, M. J.; Larrínaga, L.; Pinilla, E.; Torres, M. R. *Inorg. Chim. Acta* **2009**, *362*, 2334.
14. Simmons, C. J.; Stratemeier, H.; Hanson, G. R.; Hitchman, M. A. *Inorg. Chem.* **2005**, *44*, 2753.
15. Wang, Z.; Reibenspies, J.; Motekaitis, J.; Martell, A. E. *J. Chem. Soc., Dalton Trans.* **1995**, 1511.
16. (a) Hathway, B. J.; Billing, D. E. *Coord. Chem. Rev.* **1984**, *57*, 55. (b) Hobbey, M. H.; Smith T. D.; *Coord. Chem. Rev.* **1972**, *9*, 311. (c) Yamad, S.; Takendii, A. *Coord. Chem. Rev.* **1982**, *43*, 87.
17. (a) Menon, S.; Balagopalakrishna, C.; Rajasekharan, M. V.; Ramakrishna, B. L. *Inorg. Chem.* **1994**, *33*, 950. (b) Balagopalakrishna, C.; Rajasekharan, M. V.; Bott, S.; Atwood, J. L.; Ramakrishna, B. L. *Inorg. Chem.* **1992**, *31*, 2843. (c) Balagopalakrishna, C.; Rajasekharan, M. V. *Phys. Rev.* **1990**, *B42*, 7794.
18. Henderson Jr, L. J.; Fronczek, F. R.; Cherry, W. R. *J. Am. Chem. Soc.* **1984**, *106*, 5876.
19. Pyle, M.; Rahman, R.; Meshoyrer, J. P.; Kumar, C. V.; Turro, N. J.; Barton, J. K. *J. Am. Chem. Soc.* **1989**, *111*, 3051.
20. (a) Li, B.; Li, B.; Zhu, X.; Zhang, Y. *Inorg. Chem. Commun.* **2003**, *6*, 1304. (b) Ren, Y.-G.; Chen, Z.-R. Li, H.-H.; Zhao, B.; Huang, C.-C.; Li, J.-Q. *Chin. J. Struct. Chem.* **2005**, *24*, 568. (c) Kulkarni, P.; Padhye, S.; Sinn, E. *Inorg. Chim.*



*Acta*. **2003**, 321, 193. (d) Yang, H.-J. Kou, H.-Z. Gao, F.; Cui, A. L.; Wang, R.-J. *Acta Cryst.*, 2004, **E60**, m611. (e) Menon, S.; Rajasekharan, M. V. *Inorg. Chem.* **1997**, 36, 4983. (f) Menon, S.; Rajasekharan, M. V. *Polyhedron*. **1998**, 17, 2463. (g) Menon, S.; Rajasekharan, M. V. *Polyhedron*. **1998**, 17, 2463. (h) Hu, J.; Tang, H.; He, S.-Y.; Zhao, J.-S.; Sun, J.; Liu, J.-N. *Chin. Acta Chim. Sinica* **2001**, 59, 1158. (i) Zhang, R.-L.; Hu, J.; Zhao, J.-S. He, S.-Y.; Liu, J.-N.; Shi, Q.-Z. *Chin. Acta Chim. Sinica*. **2004**, 62, 2259. (j) Zhang, R.-L.; Zhao, J.-S.; Gu, A.-P.; He, S.-Y. *Chin. Acta Chim. Sinica*. **2003**, 61, 262 (k) Gu, A.-P.; Zhang, R.-L.; Zhang, G.; Zhao, J.-S.; He, S.-Y. Dou, J.-M.; Wang, D.-Q. *Chin. J. Chem.* **2002**, 20, 1616. (l) Zhao, J.-S.; Zhang, R.-L.; He, S.-Y. Xue, G.-L.; Dou, J.-M.; Wang, D.-Q. *Chin. J. Struct. Chem.* **2003**, 22, 577 (m) Zhu, X.; Zhu, L.-M.; Li, B.-L.; Zhang, Y. *Chin. Chem. Res. Appln.* **2003**, 15, 832. (n) Song, Y.-H.; Zhang, R.-L.; Sun, Q.-L.; Xu, Z.-W.; Gao, Q.-C.; Liu, H.-Q. Zhao, J.-S. *Chin. J. Chem.* 2007, 25, 1508. (o) Miao S.; Kang, H.; Du, C.; Ji, B. *Anal. Sci.: X-Ray Struct. Anal. Online* **2006**, 22, x45 (p) Kulkarni, P.; Padhye, S.; Sinn, E.; Anson, C. E.; Powell, A. K. *Inorg. Chim. Acta*. **2002**, 332, 167. (q) Zhao, J.-S.; Zhang, R.-L.; Su, B.-Y.; Gu, A.-P.; He, S.-Y.; Xue, G.-n.; Liu, J.-N.; Dou, J.-M.; Wang, D.-Q. *Chin. Acta Chim. Sinica*. **2002**, 60, 2069. (r) He, X.-Y.; Liu, X.-G.; Li, B.-L.; Zhang, Y. *Chin. J. Struct. Chem.* **2005**, 24, 831. (s) Yang, G.; Yu, X.-L.; Chen, X.-M.; Ji, L.-N. *Cryst. Res. Technol.* **2000**, 35, 993. (t) Lu, Z.-L.; Duan, C.-y.; Tian, Y.-p.; You, X.-

- z.; Huang, X.-y. *Inorg. Chem.* **1996**, 35, 2253. (u) Li, M.; Huang, J.; Zhou, X.; Fang, H.; Ding, L. *Acta Cryst.* **2008**, C64, m250. (v) Li, Y.-P.; Yang, P.; Huang, Z.-X.; Xie, F.-X.; *Acta Cryst.* **2005**, C61, m7.
21. Hu, N.-L.; Bi, J.-H.; Huang, Z.-X.; Shen, Y.-H. *Asian J. Chem.* **2005**, 17, 1989.
22. (a) Procter, I. M.; Hathaway, B. J.; Nicholls, P. *J. Chem. Soc. A* **1968**, 1678-1684.  
(b) Hathaway, B. J.; Billing, D. E.; Nicholls, P.; Procter, I. M. *J. Chem. Soc. A* **1969**, 319-325.
23. (a) Hathaway, B. J. *Struct. Bonding.* **1984**, 57, 55-118. and references therein. (b) Hathaway, B. J.; Billing, D. E. *Coord. Chem. Rev.* **1970**, 5, 143. and references therein.
24. Holger Dobbek, H.; Svetlitchnyi, V.; Gremer, L. Huber, R.; Meyer, O. *Science.* **2001**, 293, 1281.
25. Barondeau, D. P.; Kassmann, C. J.; Bruns, C. K.; Tainer, J. A.; Getzoff, E. D. *Biochemistry*, **2004**, 43, 8038.
26. He, M. M.; Clugston, S. L.; Honek, J. F.; Matthews, B. W. *Biochemistry.* **2000**, 39, 8719.
27. Byun, J. C.; Han, C. H.; Kim, K. J. *Inorg. Chem. Commun.* **2006**, 9, 171.
28. Bobicz, D.; Kristiansson, O.; Persson, I. *J. Chem. Soc. Dalton Trans.* **2002**, 4201.
29. Fritz, M.; Rieger, D.; Bar, E.; Beck, G.; Fuchs, J.; Holzmann, G.; Fehlhammer, W. P. *Inorg. Chim. Acta* **1992**, 198, 513.

30. Podberezskaya, N. V.; Doronina, V. P.; Bakakin, V. V.; Yakovlev, N. N. *Russ. J. Struct. Chem.* **1984**, 25, 182.
31. Jóna, E. J. *Therm. Anal.* 1988, 34, 1053.
32. (a) Frammel, T.; Peters, W.; Wunderlich, H.; Kuchen, W. *Angew. Chem.* **1992**, 104, 632. (b) Frammel, T.; Peters, W.; Wunderlich, H.; Kuchen, W. *Angew. Chem.* **1993**, 105, 926.
33. (a) Dakternieks, D. A. Orlandini, D.; Sacconi, L. *Inorg. Chim. Acta* **1978**, 29, L205. (b) Yin, L.-H.; Bu, P.-Y. Cheng, P.; Li, J.; Yan, S.-P.; Jiang, Z.-H.; Liao, D.-Z. *J. Coord. Chem.* **2002**, 55, 537. (c) Wen, D.-C.; Liu, S.-X.; Lin, M. *J. Mol. Struct.* **2008**, 876, 154. (d) Patel, R. N.; Singh, N.; Gundla, V. L. N. *Polyhedron* **2007**, 26, 757. (e) Calatayud, M. L.; Sletten, J.; Castro, I.; Julve, M.; Seitz, G.; Mann, K. *Inorg. Chim. Act.* **2003**, 353, 159. (e) Wu, A.-Q.; Zheng, F.-K.; Guo, G.-C.; Huang, J.-S. *Acta Cryst.* **2004**, E60, m373. (f) Zhao, S.-M.; Wu, T.-X. *Acta Cryst.* **2005**, E61, m2544. (g) Freire, E.; Baggio, S.; Baggio, R.; Suescun, L. *Acta Cryst.* **1999**, C55, 1780. (h) Ferbinteanu, M.; Cimpoesu, F.; Andruh, M.; Rochon, F. D. *Polyhedron* **1998**, 17, 3671. (i) Travnický, Z.; Pastorek, R.; Slovak, V. *Polyhedron* **2008**, 27, 411. (j) Gandara, F.; Fortes-Revilla, C.; Snejko, N.; Gutierrez-Puebla, E.; Iglesias, M.; Monge, M. A. *Inorg. Chem.* **2006**, 45, 9680. (k) Zhong, H.; Zeng, X.-R.; Luo, Q.-Y. *Acta Cryst.* **2006**, E62, m3429. (l) Wu, H.-H.; Lian, F.-Y.; Yuan, D.-Q.; Hong, M.-C. *Acta Cryst.* **2007**, E63, m67.

34. (a) Cocker, T. M.; Bachman, R. E. *Chem. Commun.* **1999**, 875. (b) Hoberg, H.; Herrera, A. *Angew. Chem., Int. Ed.* **1981**, 20, 876. (c) Rodriguez-Martin, Y.; Lorenzo-Luis, P. A.; Gili, P.; Ruiz-Perez, C. *J. Coord. Chem.* **2003**, 56, 181. (d) Chesnut, D. J.; Haushalter, R. C.; Zubieta, J. *Inorg. Chim. Acta* **1999**, 292, 41. (e) Freire, E.; Baggio, S.; Baggio, R.; Suescun, L. *Acta Cryst.* **1999**, C55, 1780. (f) Ferbinteanu, M.; Cimpoesu, F.; Andruh, M.; Rochon, F. D. *Polyhedron* **1998**, 17, 3671. (g) Cabaleiro, S.; Castro, J.; Vazquez-Lopez, E.; Garcia Vazquez, J. A.; Romero, J.; Sousa, A. *Polyhedron* **1999**, 18, 1669. (h) Healy, P. C.; Patrick, J. M.; White, A. H. *Aust. J. Chem.* **1984**, 37, 921. (i) Kopel, P.; Travnick, Z.; Marek, J.; Mrozinski, J. *Polyhedron* **2004**, 23, 1573. (j) Tadokoro, M.; Kanno, H.; Kitajima, T.; Shimada-Umemoto, H.; Nakanishi, N.; Isobe, K.; Nakasuji, K. *Proc. Nat. Acad. Sci.* **2002**, 99, 4950. (k) Ruiz-Perez, C.; Luis, P. A. L.; Lloret, F.; Julve, M. *Inorg. Chim. Acta* **2002**, 336, 131. (l) Yao, J.-C.; Yao, F.-J.; Guo, J.-B.; Huang, W. Gou, S.-H. *Chin. J. Struct. Chem.* **2007**, 26, 541. (m) Liu, X.-P.; Zhang, C. *Acta Cryst.* **2007**, E63, m3063. (n) Walmsley, F.; Pinkerton, A. A.; Walmsley, J. A. *Polyhedron* **1989**, 8, 689. (o) Grirrane, A.; Pastor, A.; Ienco, A.; Mealli, C. Galindo, A. *J. Chem. Soc., Dalton Trans.* **2002**, 3771. (p) Baruah, A. M.; Karmakar, A.; Baruah, J. B. *Polyhedron* **2007**, 26, 4479. (q) Yu, M.; Liu, S.-X.; Xie, L.-H.; Cao, R.-G.; Ren, Y.-H. *Acta Cryst.* **2007**, E63, m2110. (r) Plater,

- M. J.; Foreman, M. R. St. J.; Skakle, J. M. S.; Howie, R. A. *Inorg. Chim. Acta* **2002**, 332, 135.
35. Xiong, R. -G.; Zuo, J.-Z.; Xu, E.-J.; You, X.-Z.; Huang, X.-H. *Acta Cryst.* **1996**, C52, 521.
36. Takeda, K.; Awaga, K. *Phys. Rev. B.* **1997**, 56, 14560.
37. (a) Ruiz, E.; Cano, J.; Alvarez, S. P.; Alemany, P. *J. Am. Chem. Soc.* **1998**, 120, 1122. (b) Aebersold, M. A.; Gillon, B.; Plantevin, O.; Pardi, L.; Kahn, O.; Bergerat, P.; Von Seggern, I.; Tuczek, F.; Ohrstrom, L. A.; Grand, A.; Lelievre-Berna, E. *J. Am. Chem. Soc.* **1998**, 120, 5238. (c) Charlot, M. F.; Kahn, O.; Chaillet, M.; Larrieu, M. *J. Am. Chem. Soc.* **1986**, 108, 2574.
38. (a) Sain, S.; Bid, S.; Usman, A.; Fun, H. K.; Aromi, G.; Solans, X.; Chandra, S. K. *Inorg. Chim. Acta* **2005**, 358, 3362. (b) Barandika, M. G.; Cortes, R.; Lezama, L.; Urtiaga, M. K.; Arriortua, M. I.; Rojo, T. *J. Chem. Soc. Dalton Trans.* **1999**, 2971. (c) Arriortua, M. I.; Cortes, R.; Lezam, L.; Rojo, T.; Solans, X.; Font Bardia, M. *Inorg. Chim. Acta* **1990**, 174, 263. (d) Cortes, R. C.; de Larramendi, J. I. R.; Lezama, L.; Rojo T.; Urtiaga, K. *J. Chem. Soc., Dalton Trans.* **1992**, 2723. (e) Lin, X. J.; Shen Song, Y.; Xu, H. J.; Li, Y. Z.; You, X. Z. *Inorg. Chim. Acta* **2005**, 358, 1963. (f) Vicente, R.; Escuer, A.; Ribas, J.; El Fallah, M. S.; Solans, X.; Font- Bardia, M. *Inorg. Chem.* **1993**, 32, 920. (g) Dey, S. K.; Mondal, N.; El Fallah, M. S.; Vicente, R.; Escuer, A.; Solans, X.; Font-Bardia, M.; Matsushita,

- T.; Gramlich, V.; Mitra, S. *Inorg. Chem.* **2004**, *43*, 2427. (g) Ribas, M.; Monfort, C.; Diaz, C.; Bastos, X.; Solans, X. *Inorg. Chem.* **1994**, *33*, 484. (h) Escuer, A.; Vicente, R.; El Fallah, M. S.; Solans, X.; Font-Bardia, M. *Inorg. Chim. Acta* **1996**, *247*, 85.
39. Kahn, O. *Molecular Magnetism*, Wiley-VCH, New York, **1993**.
40. Zhang, Y.; Wang, X. T.; Zhang, X. M.; Liu T. F.; Xu, W. G.; Gao, S. *Inorg Chem.* **2010**, *49*, 5868.
41. Godbole, M. D.; Roubeau, O.; Mills, A. M.; Kooijman, H.; Spek, A. L.; Bouwman, E. *Inorg Chem.* **2006**, *45*, 6713.
42. Lee, C. S.; Wu, C. Y.; Hwang, W. S.; Dinda, J. *Polyhedron* **2006**, *25*, 1791.
43. Ronson, T. K.; Adams, H.; Ward, M. D. *Eur. J. Inorg. Chem.* **2005**, 4533.
44. Yang, E. C.; Wernsdorfer, W.; Hill, S.; Edwards, R. S.; Nakano, M.; Maccagnano, S.; Zakharov, L. N.; Rheingold, A. L.; Christou, G.; Hendrickson, D. N. *Polyhedron* **2003**, *22*, 1727.
45. Delhaes, P., Drillon, M., Eds. *Organic and Inorganic Low-Dimensional crystalline Materials*; NATO ASI Series 168; Plenum: New York, **1987**.
46. Zhi-Guo, G.; Jing-Lin, Z.; Xiao-Zeng, Y. *Dalton Trans.* **2007**, 4067.
47. Mukherjee, S.; Bappaditya, G.; Chakrabarty, R.; Mukherjee, P. S. *Inorg.chem.* **2009**, *48*, 11325.
48. Zhang, N.; Zhong-Lu, Y. *Transition Met Chem.* **2010**, *35*, 437.

49. Koner, S.; Saha, S.; Mallah, T.; Okamoto, K. I. *Inorg. Chem.* **2004**, *43*, 840.
50. Dominguez-Vera, J. M.; Suarez-Varela, J.; Maimoun, I. B.; Colacio, E. *Eur. J. Inorg. Chem.* **2005**, *26*, 1907.
51. Monfort, M.; Resino, I.; Ribas, J.; Solans, X.; Font-Bardia, M.; Stoeckli-Evans, H. *New J. Chem.* **2002**, *26*, 1601.
52. Murugesu, M.; Habrych, M.; Wernsdorfer, W.; Abboud, K. A.; Christou, G. *J. Am. Chem. Soc.* **2004**, *126*, 4766.
53. Karmakar, T. K.; Chandra, S. K.; Ribas, J.; Mostafa, G.; Lu, T. H.; Ghosh, B. K. *Chem. Commun.* **2002**, 2364.
54. Goher, M. A. S.; Cano, J.; Journaux, Y.; Abu-Youssef, M. A. M.; Mautner, F. A.; Escuer, A.; Vicente, R. *Chem. Eur. J.* **2000**, *6*, 778.
55. Meyer, F.; Kircher, P.; Pritzkow, H. *Chem. Commun.* **2003**, 774.
56. Papaefstathiou, G. S.; Perlepes, S. P.; Escuer, A.; Vicente, R.; Font-Bardia, M.; Solans, X. *Angew. Chem. Int. Ed.* **2001**, *40*, 884.
57. Papaefstathiou, G. S.; Escuer, A.; Vicente, R.; Font-Bardia, M.; Perlepes, S.P.; Solans, X. *Chem. Commun.* **2001**, *23*, 2414.
58. Mialane, P.; Dolbecq, A.; Marrot, J.; Riviere, E.; Secheresse, F. *Chem. Eur. J.* **2005**, *11*, 1771.
59. Escuer, A.; Vicente, R.; Ribas, J.; Fallah, M. S. E.; Solans, X.; Font-Bardia, M. *Inorg. Chem.* **1993**, *32*, 3727.

60. Debiani, F. F.; Ruiz, E.; Cano, J.; Novoa, J. J.; Alvarez, S. *Inorg. Chem.* **2000**, 39, 3221.
61. Ribas, J.; Monfort, M.; Diaz, C.; Bastos, C.; Solans, X. *Inorg. Chem.* **1993**, 32, 3557.
62. Cortes, R.; Urtiaga, M. K.; Lezama, L.; Pizarro, J. L.; Goni, A.; Arriortua, M. I.; Rojo, T. *Inorg. Chem.* **1994**, 33, 4009.
63. (a) Kahn, O.; Sikorov, S.; Gouteron, J.; Jeannin, S.; Jeannin, Y. *Inorg. Chem.* **1983**, 22, 2877. (b) Comarmond, P.; Plumere, P.; Lehn, J. M.; Agnus, Y.; Louis, R.; Weiss, R.; Kahn, O.; Morgenstern-Badarau, I. *J. Am. Chem. Soc.* **1982**, 104, 6330. (c) Waksman, I. B.; Boillot, M. L.; Kahn, O.; Sikorov, S. *Inorg. Chem.* **1984**, 23, 4454.
64. (a) Agnus, Y.; Lewis, R.; Gisselbrecht, J. P.; Weiss, R. *J. Am. Chem. Soc.* **1984**, 106, 93. (b) Mckee, V.; Zvagulis, M.; Dagdigian, J. V.; Bau, R.; Patch, M. G.; Reed, C. A. *J. Am. Chem. Soc.* **1984**, 106, 4765.
65. Cortes, R.; Urtiga, M. K.; Lezma, L.; Larramendi, J. S. R.; Arriortua, M. I.; Rojo, T. *J. Chem. Soc. Dalton Trans.* **1993**, 3685.
66. Depree, C. V.; Beckmann, U.; Heslop, K.; Brooker, S. *J. Chem. Soc. Dalton Trans.* **2003**, 3071.
67. (a) Solomon, E. I.; Sundrama, U. M.; Machonkin, T. E. *Chem. Rev.* **1996**, 96, 2563. (b) Solomon, E. I.; Baldwin, M. J.; Lowery, M. D. *Chem. Rev.* **1992**, 92,



521. (c) Karlin, K. D.; Tyeklár, Z. (Eds.), *Bioinorganic Chemistry of Copper*, Chapman & Hall, New York, **1993**. (d) Kitajima, N.; Moro-oka, Y. *Chem. Rev. Washington DC*. **1994**, 94, 737.
68. Burmeister, J. L. *Coordin. Chem. Rev.* **1968**, 3, 225.
69. Soldatov, D.V.; Enright, G.D.; Ripmeester, J. A. *Cryst. Growth Des.* **2004**, 4, 185.
70. Kruszynski, R.; Machura, B.; Wolff, M.; Kusz, J.; Mrozinski, J.; Bienko, A. *Inorg. Chim. Acta* **2009**, 362, 1369.
71. Mukhopadhyay, U.; Bernal, I.; Massoud, S. S.; Mautner, F. A. *Inorg. Chim. Acta* **2004**, 357, 673.
72. (a) Mautner, F. A.; Vicente, R.; Massoud, S. S. *Polyhedron* **2006**, 25, 673. (b) Massoud, S. S.; Mautner, F. A. *Inorg. Chim. Acta* **2005**, 358, 3334.
73. Plieger, P. G.; Downard, A. J.; Moubaraki, B.; Murray, K. S.; Brooker, S. J. *Chem. Soc. Dalton. Trans.* **2004**, 2157.

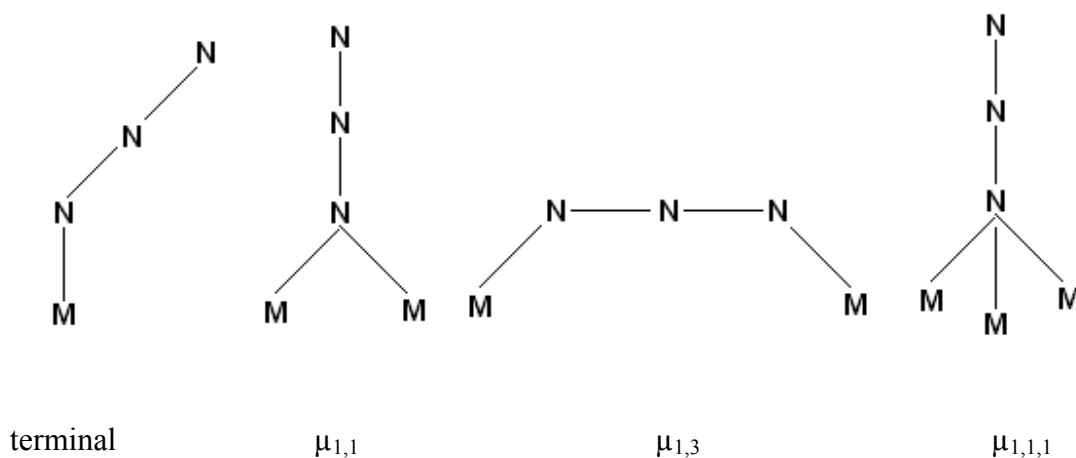


## CHAPTER II

### Tetranuclear copper azide complex of 4,5-Diazafluoren-9-one

#### 2.1 Introduction

Multinuclear copper(II) complexes occupy an important position in modern inorganic and materials chemistry. They are ubiquitous in nature as active sites in a variety of metallo-enzymes and this recognition has fuelled considerable efforts in the synthesis of multi-copper complexes that serve as spectroscopic, structural and functional mimics of the active sites of these proteins.<sup>1</sup> Tetra-nuclear copper(II) complexes represent a class of compounds that are useful in understanding magneto-structural correlations in such compounds.<sup>2</sup> Even though many mononuclear complexes of Cu-dafone were reported,<sup>3</sup> no multinuclear complexes were reported. Among the various bridging ligands available, azide has a special place because it can mediate magnetic exchange interaction through different bridging modes. In addition to the terminal mode, it can function as a  $\mu_{1,1}$ ,  $\mu_{1,3}$ , or  $\mu_{1,1,1}$  bridge (Scheme1). In certain cases the  $\mu_{1,1}$  (end-on) bridge leads to ferromagnetic coupling while the  $\mu_{1,3}$  (end-to-end) bridging mode generally gives rise to antiferromagnetic exchange coupling between the metal centers.<sup>4</sup>



**Scheme 1.** Different bridging modes of azide ligand

Here we report the crystal structure, DFT studies and magnetic properties of  $\text{Cu}_4(\text{dafone})_4(\text{N}_3)_8(\mathbf{1})$ . 4,5 diazafluorene-9-one (dafoane) is known to coordinate with Cu(II) in an unsymmetrical fashion due to its larger chelate bite compared to 2,2'-bipyridine or 1,10-phenanthroline.

## 2.2. Experimental

### 2.2.1 Reagents

All chemicals were purchased from Ranbaxy chemicals and used without further purification. Dafone was prepared using a reported procedure.<sup>5</sup>

### 2.2.2 Synthesis of $(\text{Cu})_4(\text{dafone})_4(\text{N}_3)_8$ (1)

A solution of  $\text{Cu}(\text{ClO}_4)_2 \cdot 6\text{H}_2\text{O}$  (0.185g, 0.500 mmol) in water (3 ml) was added to a long glass tube (20 cm) as a first layer, then a solution of dafone (0.186g, 1.00 mmol) in methanol (15 ml) was added as the middle layer.  $\text{NaN}_3$  (0.065g, 1.0 mmol) in methanol (5 ml) was then carefully added to form the top layer. The tube was closed and left for crystallization in a refrigerator. After two days, dark green coloured needle shaped crystals formed at the middle of the tube. The crystals were filtered and washed with cold water and cold methanol. Yield: 0.080 g (0.061 mmol, 49 %). Anal. calcd for  $\text{Cu}_4\text{C}_{44}\text{H}_{24}\text{N}_{32}\text{O}_4$  (1319.047): C,40.07; H,1.38; N, 33.98; Found: C,39.53; H,1.40; N,33.23. IR (KBr disk,  $\text{cm}^{-1}$ ): 3034, 2068, 2037, 1716, 1589.

### 2.3. Measurements

IR spectra were obtained with a Shimadzu FT-IR 8000 spectrometer. Elemental analysis was obtained using a FLASH EA 1112 SERIES CHNS analyzer. Diffuse reflectance spectra were recorded on Shimadzu UV/Vis/NIR spectrophotometer. The magnetic susceptibility was measured in the 1.98–300 K temperature range using a Quantum Design MPMS SQUID susceptometer.<sup>6, 7</sup>

**2.3.1 Crystallographic data collection and structure determination** X-ray data were collected on a Bruker SMART APEX CCD X-ray diffractometer using graphite monochromated Mo  $\text{K}\alpha$  radiation. The data was reduced using SAINTPLUS,<sup>8</sup> and

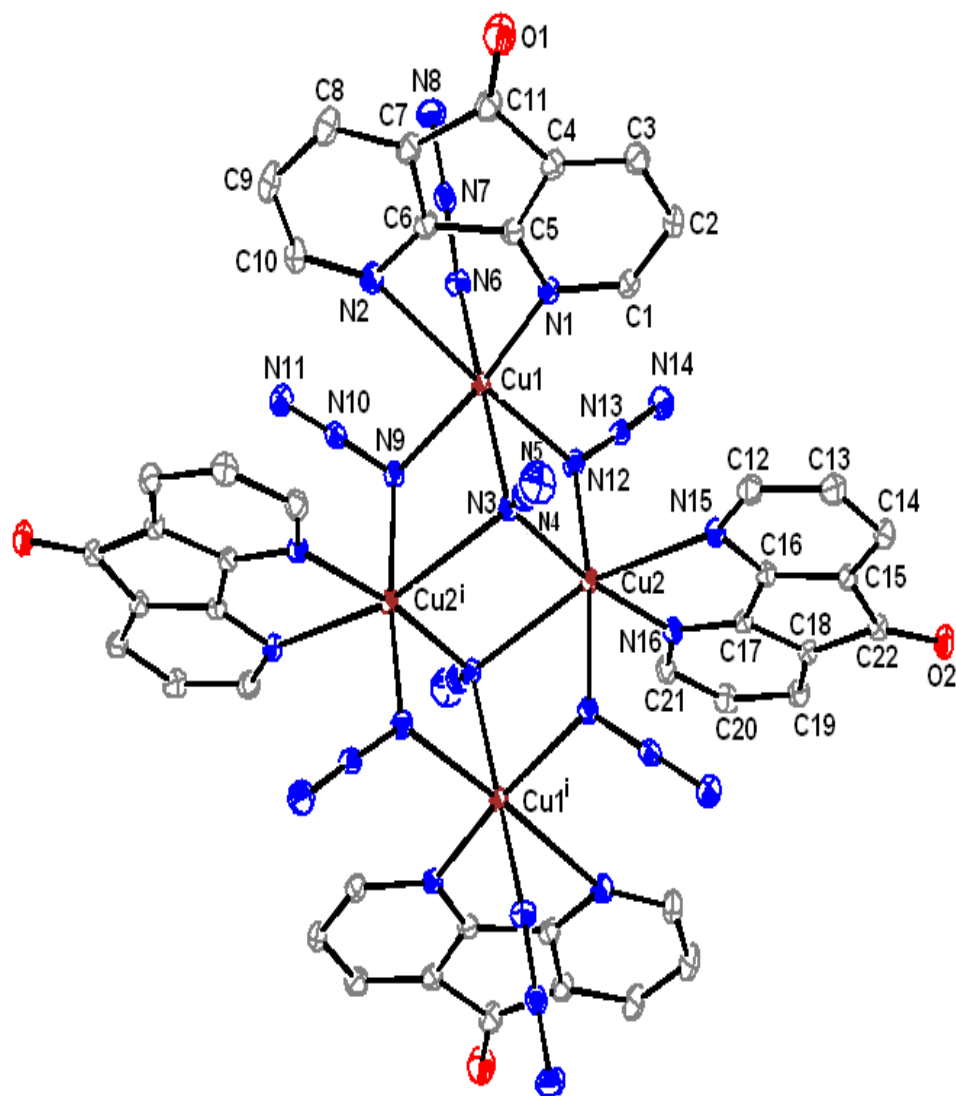
multiscan absorption corrections using SADABS<sup>9</sup> were applied. The structures was solved using SHELXS-97 and refined using SHELXL-97.<sup>10</sup> All ring hydrogen atoms were assigned on the basis of geometrical considerations and were allowed to ride upon the respective carbon atoms. Crystal data are in Table 2.1 and important interatomic distances and angles in Table 2.2.

#### 2.4 Crystal structure of $(\text{Cu})_4(\text{dafone})_4(\text{N}_3)_8$ (**1**):

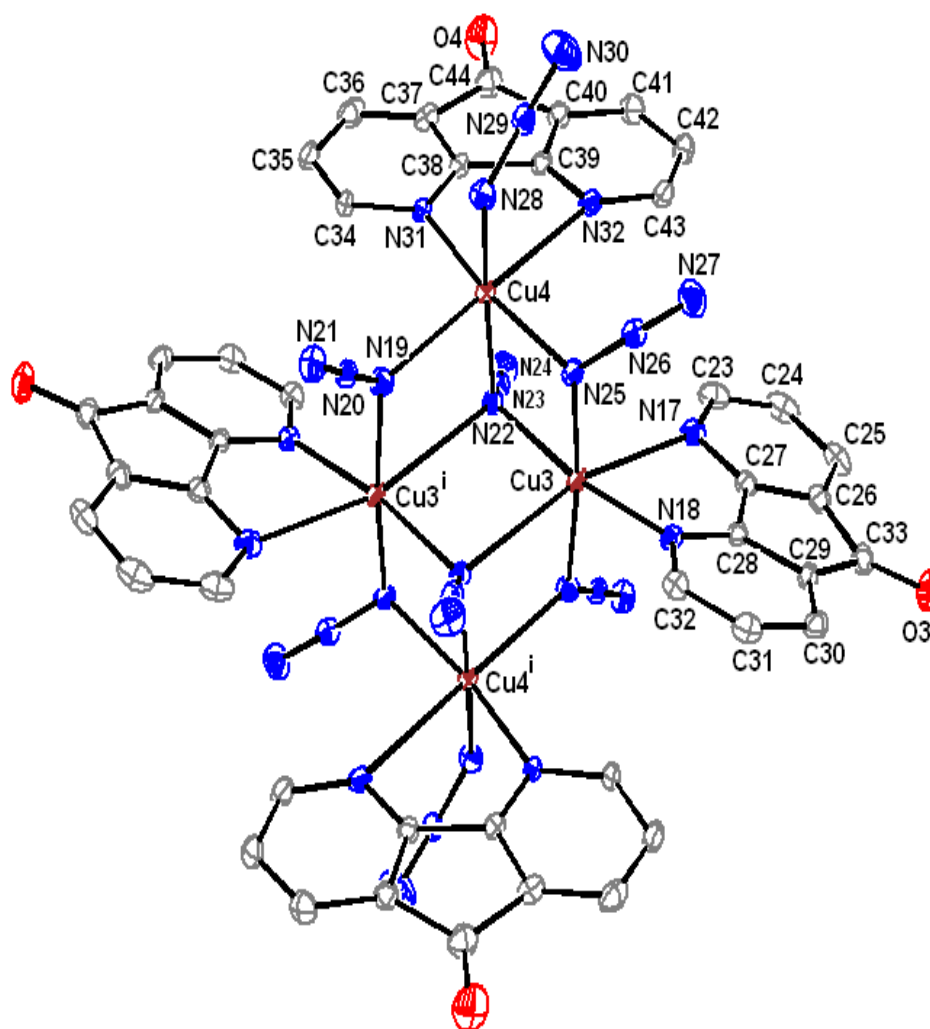
Crystals of **1** contain two crystallographically different centrosymmetric tetranuclear Cu(II) complexes (Fig 2.1). Each azide bridged cluster may be viewed as a face showing  $\text{Cu}_6\text{N}_6$  bicubane in which two Cu(II) sites are missing. The clusters having composition  $(\text{Cu})_4(\text{dafone})_4(\text{N}_3)_8$  are therefore, distortion isomers of the same open bicubane form. The isomeric structures (A and B) excluding carbon and hydrogen atoms are depicted in figure 2.2. Each copper atom in the clusters is chelated to a dafone molecule in a highly unsymmetrical fashion (Cu-N(Å) 2.02, 2.76, 2.06, 2.59 in A and 2.02, 2.68, 2.05, 2.67 in B). There are four  $\mu_{1,1}$  azide bridges, two of which are symmetric (Cu-N(Å); 1.99, 2.04 in A and 1.98, 2.01 in B), the other two being slightly unsymmetrical (Cu-N(Å); 1.96, 2.27 in both A and B). In each cluster there are also two  $\mu_{1,1,1}$  azide bridges which are unsymmetrical (Cu-N(Å); 2.07, 2.07, 2.50 in A and 2.10, 2.58, 2.04 in B). Two terminal azide ions (Cu-N(Å); 1.97 in A and 1.98 in B) complete the structure.

**Table 2.1** Crystallographic data and structure refinement for **(Cu)<sub>4</sub>(dafone)<sub>4</sub>(N<sub>3</sub>)<sub>8</sub> (1)**

Formula	C <sub>44</sub> H <sub>24</sub> Cu <sub>4</sub> N <sub>32</sub> O <sub>4</sub>
Formula weight	1319.11
Crystal system	Triclinic
Space group	$P\bar{1}$
$a$ (Å)	13.864(7)
$b$ (Å)	13.870(9)
$c$ (Å)	14.322(10)
$\alpha$ (°)	112.72(4)
$\beta$ (°)	95.63(5)
$\gamma$ (°)	94.01(5)
$V$ (Å <sup>3</sup> )	2511(3)
$Z$	2
$T$ (K)	298(2)
$D_{calc}$ (g cm <sup>-3</sup> )	1.745
$\mu$ (mm <sup>-1</sup> )	1.752
$F(000)$	1320
Crystal size (mm)	0.48 x 0.32 x 0.16
$\theta$ Range (°)	1.56 to 27.49
$h/k/l$	-5, 17/ -17, 17/ -18, 18
Reflection collected	12138
Unique reflect., [R <sub>int</sub> ]	11467 [ 0.0225]
Goodness of fit	0.942
$R_I$ [I>2 $\sigma$ (I)]	0.0585
$wR_2$	0.1420

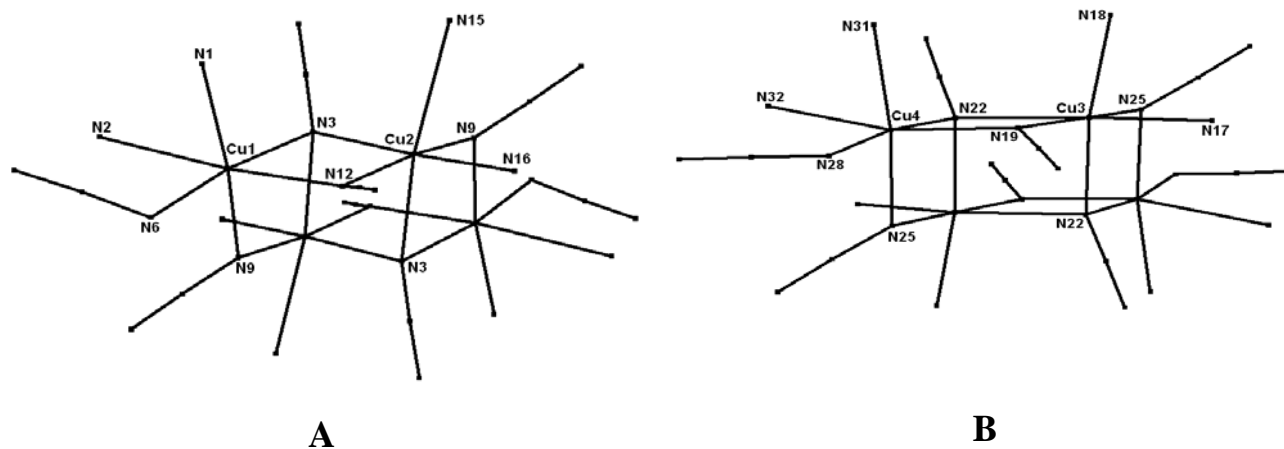




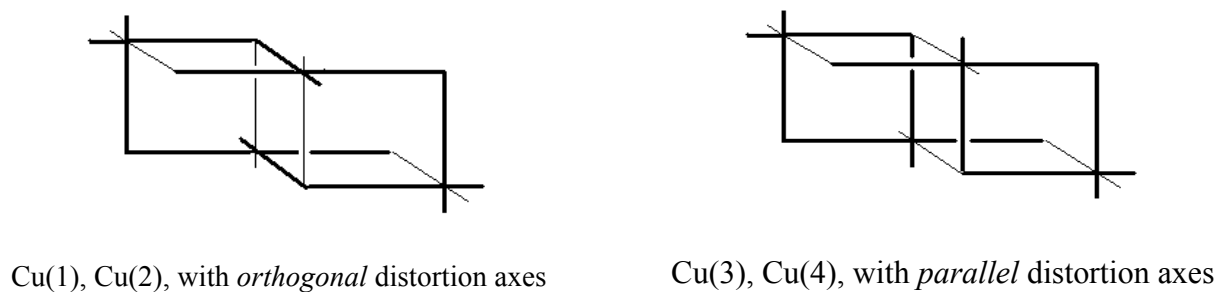


**Figure 2.1.** Thermal ellipsoid plot of the coordination environment of the distortion isomers of **1**: Atoms are represented as 30% probability ellipsoids and ring hydrogen's have been omitted for clarity. Symmetry code: (i)  $-x+1, -y+1, -z$ .

The two isomers differ in the location of the long Cu-N bond of the triply bridging azide ligands. In combination with the long Cu-N bond of dafone, in isomer A the tetragonal elongation axes of the Cu(II) polyhedral are orthogonal while in B they are parallel as schematically shown in figure 2.3.



**Figure 2.2.** The isomeric structures of complex  $(\text{Cu})_4(\text{dafone})_4(\text{N}_3)_8$  (**1**) [Excluding carbon and hydrogens]



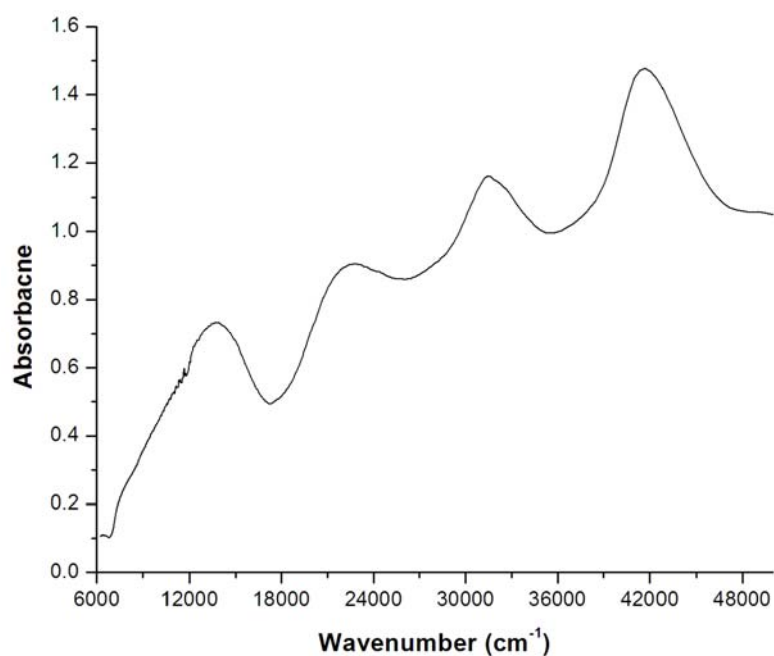
**Figure 2.3.** Schematic diagram of coordination mode of distortion isomers of  $(\text{Cu})_4(\text{dafone})_4(\text{N}_3)_8$

Table 2.2 Selected bond lengths [ $\text{\AA}$ ] and angles [ $^\circ$ ] for  $(\text{Cu})_4(\text{dafone})_4(\text{N}_3)_8$  (**1**)<sup>a</sup>

Cu(1)-N(1)	2.020(2)	Cu(2)-N(3)	2.069(2)	Cu(3)-N(17)	2.671(2)
Cu(1)-N(2)	2.758(2)	Cu(2)-N(3) #2	2.503(2)	Cu(3)-N(18)	2.048(2)
Cu(1)-N(3)	2.065(2)	Cu(2)-N(9)	1.992(2)	Cu(3)-N(19)	1.965(2)
Cu(1)-N(6)	1.966(2)	Cu(2)-N(12)	1.956(2)	Cu(3)-N(22)	2.037(2)
Cu(1)-N(9)	2.036(2)	Cu(2)-N(15)	2.587(2)	Cu(3)-N(22) #1	2.579(2)
Cu(1)-N(12)	2.270(2)	Cu(2)-N(16)	2.060(2)	Cu(3)-N(25)#1	1.982(2)
Cu(4)-N(19)	2.272(2)	Cu(4)-N(25)	2.014(2)	Cu(4)-N(31)	2.022(2)
Cu(4)-N(22)	2.100(2)	Cu(4)-N(28)	1.980(2)	Cu(4)-N(32)	2.679(2)
Cu(1)-Cu(2)	3.2038(4)	Cu(2)-Cu(2) #2	3.4933(5)	Cu(3)-Cu(4) #1	3.1070(4)
Cu(1)-Cu(2)#2	3.2958(5)	Cu(3)-Cu(4)	3.4409(5)	Cu(3)-Cu(4) #1	3.5043(4)
N(1)-Cu(1)-N(3)	90.09(8)	N(3)-Cu(2)-N(16)	172.01(8)	N(19)Cu(4)-N(28)	96.05(8)
N(1)-Cu(1)-N(6)	95.30(8)	N(12)-Cu(2)-N(16)	90.72(8)	N(19)-Cu(4)-N(31)	93.73(8)
N(1)-Cu(1)-N(9)	161.93(8)	N(9)-Cu(2)-N(3)#2	93.48(8)	N(22)-Cu(4)-N(19)	81.18(8)
N(1)-Cu(1)-N(12)	98.49(8)	N(9)-Cu(2)-N(12)#2	170.96(8)	N(22)-Cu(4)-N(28)	172.23(8)
N(3)-Cu(1)-N(6)	171.98(8)	N(9)-Cu(2)-N(16)#2	93.06(8)	N(25)-Cu(4)-N(31)	164.09(8)
N(3)-Cu(1)-N(9)	83.69(8)	N(19)-Cu(3)-N(18)	93.44(9)	N(25)-Cu(4)-N(22)	79.14(8)
N(3)-Cu(1)-N(12)	76.26(8)	N(19)-Cu(3)-N(22)#1	96.05(9)	N(28)-Cu(4)-N(25)	94.18(9)
N(6)-Cu(1)-N(9)	92.84(8)	N(19)-Cu(3)-N(25)#1	171.78(9)	N(28)-Cu(4)-N(31)	94.43(9)
N(6)-Cu(1)-N(12)	97.03(8)	N(22)-Cu(3)-N(18)#1	169.96(8)	N(19)-Cu(4)-N(25)	98.63(8)
N(9)-Cu(1)-N(12)	96.48(8)	N(25)-Cu(3)-N(18)#1	89.63(8)	N(31)-Cu(4)-N(22)	93.00(8)
N(3)-Cu(2)-N(12)	83.48(8)	N(25)#1-Cu(3)-N(22)#1	81.40(8)	a #1 -x,-y+1,-z, #2 -x+1,-y,-z+1	

## 2.5 Electronic Spectra

The three broad bands below  $24000\text{ cm}^{-1}$  may be assigned to  $d-d$  transitions between the split components of the  $^2E$  and  $^2T_2$  states of the  $d^9$  ion as follows:  $8347\text{ cm}^{-1}$  ( $d_{z^2} \rightarrow d_{x^2-y^2}$ ),  $13927\text{ cm}^{-1}$  ( $d_{xy} \rightarrow d_{x^2-y^2}$ ),  $22727\text{ cm}^{-1}$  ( $d_{xz}, d_{yz} \rightarrow d_{x^2-y^2}$ ). The bands  $31447\text{ cm}^{-1}$  and  $41667\text{ cm}^{-1}$  are ligand centered transitions are shown in the figure 2.4.



**Figure 2.4.** Diffuse reflectance spectrum of  $(\text{Cu})_4(\text{dafone})_4(\text{N}_3)_8$ .

## 2.6 Magnetic properties

The variation of molar magnetic susceptibility ( $\chi$ ) and  $\chi T$  in temperature range 2 - 300K is shown in Figure 2.5. The effective magnetic moment ( $\mu/B.M$  per tetramer) increases from 3.89 at 300K to 4.24 at 20 K and then decreases. Due to the complexity of the system it

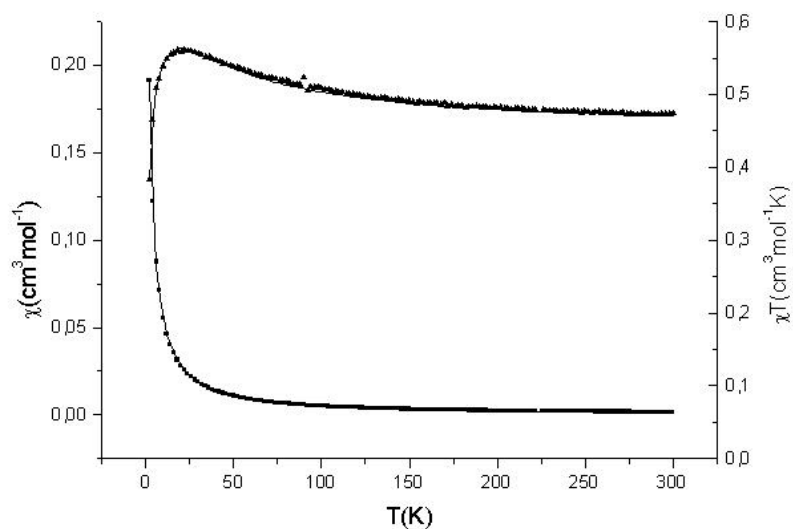
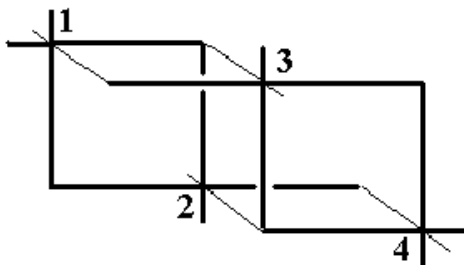


**Figure 2.5.** Molar paramagnetic susceptibility ( $\chi_M$ ) and product of molar paramagnetic susceptibility per tetramer and temperature ( $\chi_M T$ ) vs. temperature curves for **1**. The continuous lines represent Bleaney-Bowers fit.

is unreasonable to expect a unique fit using a general spin Hamiltonian which should include at least three independent exchange parameters ( $J_{12}$ ,  $J_{13}$ ,  $J_{23}$ ) for each distortion isomer (Figure 2.6) leading to a total of six parameters. As shown in Figure 2.5, the



$$J_{12} (=J_{34}) = J_1 ; \quad J_{13}(=J_{24}) = J_3 ; \quad J_{23} = J_2$$

**Figure 2.6.** Coupling modes in the tetranuclear complex

Bleaney-Bowers model including molecular field correction gives an excellent fit to the data with  $J = 20.2$ ;  $zJ' = -0.58 \text{ cm}^{-1}$  and  $g = 2.193$  indicating an overall ferromagnetic interaction. A refined fitting based on complete diagonalisation of the exchange Hamiltonian is shown in Figure 2.7. This fitting makes use of the simplifying assumption that both isomers can be modelled by the same set of parameters. It is further assumed that  $J_2 = 0$  (fixed). The fitting, however, is not unique. A contour plot showing two minima in the ( $J_1$ ,  $J_3$ ) parameter space is shown in Figure 2.8. The minimum on the right hand side of

the drawing with  $J_1 = 22.84 \text{ cm}^{-1}$  and  $J_3 = -8.2 \text{ cm}^{-1}$  is considered to be consistent with the azide bridging geometry.

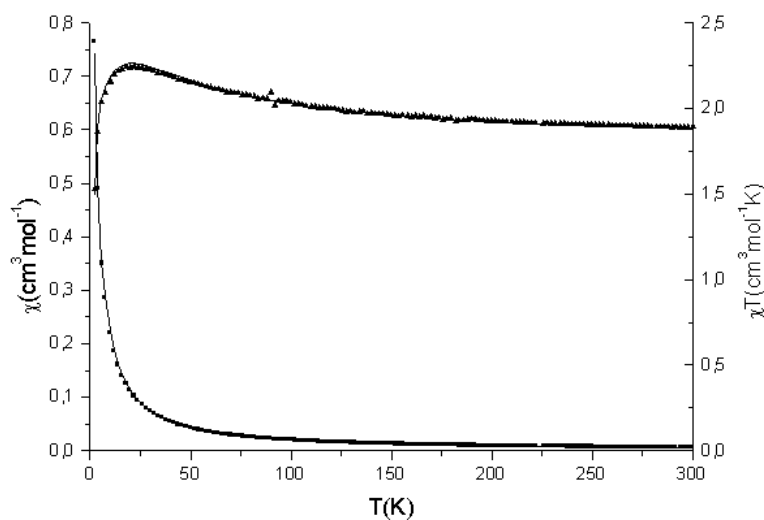


**Figure 2.7.** Molar paramagnetic susceptibility ( $\chi_M$ ) and product of molar paramagnetic susceptibility per tetramer and temperature ( $\chi_M T$ ) vs. temperature curves for **1**. The continuous lines represent the fit obtained by diagonalisation as mentioned in the text.

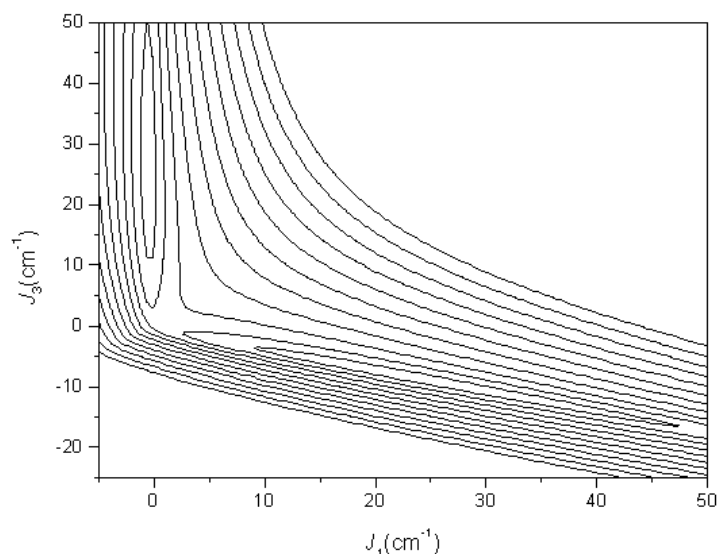


**Figure 2.8.** The contour plot showing two minima in the  $J_1, J_3$  space ( $J_2$  fixed to zero)

### 2.7 Estimation of the Exchange Integrals by DFT Calculations

Since there are two chemically distinguishable isomeric tetramers in the crystal with negligible interaction with each other, identification of the individual ground states by magnetic measurements alone is not possible. We have therefore, calculated magnetic exchange integrals by broken symmetry method using the software package ORCA developed by F. Neese.<sup>9</sup> For that purpose the tetrameric molecule was simplified by placing C=O of dafone with CH<sub>2</sub>. Coordinates from the X-ray structure of **1** were used for all other atoms, and the structure was not optimized by DFT. Six separate calculations were performed. In each of them two of the four copper ions were replaced by zinc, thus



leaving a system with only one exchange interaction between the remaining two copper ions. The calculation utilized the basis Ahlrichs-VDZ<sup>10</sup> and polarization functions from the Ahlrichs polarization basis. The magnetic properties of a system comprising two interacting magnetic centres with fictitious local spins  $\mathbf{S}_A$  and  $\mathbf{S}_B$  are typically interpreted in the context of the phenomenological Heisenberg–Dirac–van Vleck spin-Hamiltonian

$$H = -2JS_AS_B \quad (1)$$

In each case the exchange integrals were calculated according to the convention<sup>11</sup>

$$J = (E_{HS} - E_{BS}) / (S(S + 1)),$$

where HS and BS denote the high-spin state and the broken-symmetry state, respectively. Calculations were done for three azide bridged Cu(II) pairs in each distortion isomer. The resulting exchange parameters are correlated with bridge geometry in Table 2.3.

**Table 2.3** Correlation of the geometry of the azide bridge with the calculated exchange parameter for the Cu-N3-Cu pairs in the two distortion isomers.

	Cu-N (Å)	Cu-N-Cu(°)	Cu-Cu (Å)	$J$ (cm <sup>-1</sup> )
Isomer A				
Cu1-Cu2	2.06, 2.07; 2.27, 1.96	102; 98	3.20	17.63
Cu1-Cu2'	1.99, 2.04; 2.50, 2.06	110; 92	3.30	14.24
Cu2-Cu2'	2.50, 2.07; 2.07, 2.50	99; 99	3.49	1.75
Isomer B				
Cu3-Cu4	2.10, 2.58; 2.27, 1.97	94; 108	3.44	-1.13
Cu3-Cu4'	1.98, 2.01; 2.10, 2.04	102; 97	3.11	34.73
Cu3-Cu3'	2.04, 2.58; 2.58, 2.04	98; 98	3.50	0.08

It is seen that in isomer A (with orthogonal distortion axes) there are two nearly equal ferromagnetic exchanges while the third interaction is comparatively insignificant. In isomer B (with parallel distortion axes) there is one ferromagnetic pair with an exchange parameter about twice as large as in isomer A, while the coupling in other two pairs are comparatively negligible. As expected, symmetric azide bridges produce ferromagnetic coupling whose magnitude is rapidly reduced with reduction in symmetry at the bridge. The overall ferromagnetic nature of the tertranuclear complex is as observed

experimentally. However, the results show that fitting of magnetic data through exact diagonalisation considering only a single cluster is not entirely satisfactory.

## **2.8 Conclusion**

For the first time a cluster complex of copper-dafone system was reported. Two distortion isomers were present in the crystal lattice of which one shows orthogonal distortion axes and another one shows parallel distortion axes. Calculations on orthogonally distorted tetramer gave three J values corresponds to ferromagnetic interactions and calculations on parallelly distorted tetramer gave J values corresponds to one antiferro and two ferromagnetic interactions. Magnetic measurements showed an overall ferromagnetic interaction which is analysed using Bleaney-Bowers model as well as by full diagonalisation of the spin matrix.

## 2.9 References

1. (a). Tolman, W. B. *Acc. Chem. Res.*, **1997**, 30, 227; (b) Stack, T. D. P. *Dalton Trans.*, **2003**, 1881; (c) Kruse, T.; Weyhermuller, T.; Wieghardt, K. *Inorg. Chim. Acta*, **2002**, 331, 81; (d) Chaudhuri, P.; Hess, M.; Weyhermuller, T.; Wieghardt, K. *Angew. Chem., Int. Ed.*, **1999**, 38, 1095; (e) Kaim, W. *Dalton Trans.*, **2003**, 761; (f) Yoon, J.; Solomon, E. I. *Coord. Chem. Rev.*, **2007**, 251, 379; (g) Battaini, G.; Granata, A.; Monzani, F.; Gullotti, M.; Casella, L. *Adv. Inorg. Chem.*, **2006**, 58, 185; (h) Solomon, E. I.; Sundaram, U. M.; Machonkin, T. E. *Chem. Rev.*, **1996**, 96, 2563; (i) Holm, R. H.; Solomon, E. I. *Chem. Rev.*, **2004**, 104, 347; (j) Yoon, J.; Mirica, L. M.; Stack, T. D. P.; Solomon, E. I. *J. Am. Chem. Soc.*, **2005**, 127, 13680; (k) Kruger, P. E.; Moubaraki, B.; Fallon, G. D.; Murray, K. S. *J. Chem. Soc., Dalton Trans.*, **2000**, 713.
2. (a) Colacio, E.; Ghazi, M.; Kivekäs, R.; Moreno, J. M. *Inorg. Chem.* **2000**, 39, 2882. (b) Kruger, P. E.; Moubaraki, B.; Fallon, G. D.; Murray, K. S. *J. Chem. Soc. Dalton Trans.* **2000**, 713. (c) Mukherjee, A.; Saha, M. K.; Rudra, I.; Ramasesha, S.; Nethaji, M.; Chakravarty, A. R. *Inorg. Chim. Acta* **2004**, 357, 1077.
3. (a) Menon, S.; Balagopalakrishna, C.; Rajasekharan, M. V.; Ramakrishna, B. L. *Inorg. Chem.* **1994**, 33, 950. (b) Balagopalakrishna, C.; Rajasekharan, M. V.; Bott,

- S.; Atwood, J. L.; Ramakrishna, B. L. *Inorg. Chem.* **1992**, *31*, 2843. (c) Menon, S.; Rajasekharan. M. V. *Inorg. Chem.* **1997**, *36*, 4983. (d) Menon, S.; Rajasekharan. M. V. *Polyhedron* **1998**, *17*, 2463. (e) Miao, S.; Kang, H.; Du, C.; Ji. B. *X-Ray Struct. Anal. Online*, **2006**, *22*, 45. (f) Lu, Z.; Duan, C.; Tian, Y.; You, X. *Inorg. Chem.* **1996**, *35*, 2253. (g) Wang, Y.; Jackman, D. C.; Woods, C.; Rillema, D. P. *J. Chem. Crystal.* **1995**, *25*, 549.
4. (a) Thompson, L. K.; Tandon, S. S.; Lloret, F.; Cano, J.; Julve, M. *Inorg. Chem.* **1997**, *36*, 3301. (b) Ribas, J.; Monfort, M.; Solans, X.; Drillon, M. *Inorg. Chem.* **1994**, *33*, 742.
5. Henderson Jr. L. J.; Fronczek, F. R.; Cherry, W. R. *J. Am. Chem. Soc.* **1984**, *106*, 5876.
6. Connor, C.J.O. *Prog. Inorg.Chem.* **1982**, *29*, 203.
7. Ginsberg, A.P.; Lines, M.E. *Inorg. Chem.* **1972**, *11*, 2289.
8. SAINTPLUS, Bruker AXS Inc. Madison, Wisconsin, USA.
9. Sheldrick, G.M. SADABS Programm for Empirical Absorption Correction, University of Gottingen, Germany, **1996**.
10. M. Sheldrick, *Acta Cryst.* **2008**, *A64*, 112.

11. Neese, F. *ORCA*, an ab initio, Density Functional and Semiempirical Program Package, Version 2.6-35, 2008; Universität Bonn: Bonn, Germany; free download from <http://www.thch.uni-bonn.de/tc/orca/>, registration required.
12. (a) Schaefer, A.; Horn, H.; Ahlrichs, R. *J. Chem. Phys.* **1992**, 97, 2571. (b) Ahlrichs et al. Unpublished work. (c) The Ahlrichs auxiliary basis sets were obtained from the TurboMole basis set library under [ftp.chemie.uni-karlsruhe.de/pub/jbasen](ftp://ftp.chemie.uni-karlsruhe.de/pub/jbasen). (d) Eichkorn, K.; Treutler, O.; Ohm, H.; Haser, M.; Ahlrichs, R. *Chem. Phys. Lett.* **1995**, 240, 283. (e) Eichkorn, K.; Weigend, F.; Treutler, O.; Ahlrichs, R. *Theor. Chem. Acc.* **1997**, 97, 119.
13. Bencini, A.; Gatteschi, D. *J. Am. Chem. Soc.* **1980**, 102, 5763.

# Copper complexes of 4,5-Diazafluoren-9-one

### 3.1 Introduction

Copper (II) exhibits a wide array of structural varieties due to various reasons like Jahn-Teller instability of the single hole  $e_g$  and steric effect of the ligands etc. In search for the structural varieties of copper, we have synthesised few complexes of 4,5-diazafluoren-9-one (dafone). Dafone is a bidentate ligand similar to phen and bpy. However, its coordination chemistry is still restricted to a few metals.<sup>1-7</sup>

### 3.2. Experimental

**3.2.1 Reagents:** All chemicals were purchased from Ranbaxy chemicals and used without further purification. Dafone was prepared using a reported procedure.<sup>8</sup>

#### 3.2.2 Synthesis

**Synthesis of  $\text{Cu(dafone)}_2(\text{NCS})_2$  (1):**  $\text{Cu}(\text{ClO}_4)_2(\text{H}_2\text{O})_6$  (0.370 g, 1.00 mmol) was dissolved in water (6 mL). Dafone (0.182 g, 1.00 mmol) and KSCN (0.044 g, 0.5 mmol) were dissolved in methanol (20 mL). Water solution was transferred to a long glass tube

followed by the methanolic solution added slowly through the walls of the tube and kept for crystallisation at 5 ° C. Green coloured crystals formed with in one day. Yield 0.410 g (0.75 mmol, 75 %). Anal. Calcd.  $C_{24}H_{12}CuN_6O_2S_2$  (M. W. 544.06) C, 52.98; H, 2.22; N 15.45. Found: C, 52.85; H, 2.26; N, 15.38. Important IR absorptions (KBr disk,  $cm^{-1}$ ): 2071, 1732, 1589, 1257, 760 and 628.

**Synthesis of  $Cu(dafone)_2(NCO)_2 \cdot CH_3CN$  (2):**  $Cu(ClO_4)_2(H_2O)_6$  (0.370 g, 1.00 mmol) and sodium cyanate (0.130 g, 2.00 mmol) were dissolved in acetonitrile (20 mL) and resulting green solution was transferred to a long glass tube. Acetonitrile solution of dafone (0.364 g, 1.00 mmol) was added slowly to the above tube. Upon mixing the colour of the solution became blue and it was kept for crystallization at 28 ° C. After few hours blue coloured crystals separated. Yield 0.205 g (0.39 mmol, 39 %). Anal. Calcd.  $C_{28}H_{18}CuN_8O_4$  (M. W. 594.02). C, 56.61; H, 3.05; N 18.86. Found: C, 56.71; H, 3.11; N, 18.75. Important IR absorptions (KBr disk,  $cm^{-1}$ ): 3431, 2183, 2156, 1736, 1589, 1568, 1466, 1408, 1259, 1103, 916, 839, 761, 690, 617 and 524.

**Synthesis of  $[Cu_2(dafone)_4(OH)_2](ClO_4)_2$  (3):** The methanolic solution (7ml) of dafone (0.182 g, 1.00 mmol) was added slowly to the aqueous solution of sodium cyanate ( 0.046 g, 0.70 mmol). The resulting yellow coloured solution was taken in a long tube. The methanolic solution of  $Cu(ClO_4)_2 \cdot 6H_2O$  (0.185 g, 0.500 mmol) was added slowly to the



above tube. Upon mixing the colour of the solution became blue. After one day dark blue crystals were separated. Yield 0.202 g (0.19 mmol, 76 %) Anal. Calcd.  $\text{Cu}_2\text{C}_{44}\text{H}_{26}\text{N}_8\text{O}_{14}\text{Cl}_2$  (M.W. 1088.723) C, 48.5; H, 2.40; N, 10.29. Found: C, 48.42; H, 2.41; N, 10.45 Important IR absorptions (KBr disk,  $\text{cm}^{-1}$ ): 3522, 3069, 1840, 1726, 1593, 1570, 1464, 1410, 1263, 1089, 918, 837, 758, 621 and 507.

**Synthesis of  $[\text{Cu}_2(\text{dafone})_2(\text{oxalate})_2] (\text{H}_2\text{O})_{0.5}$  (4):** Sodium oxalate was dissolved in water (5 mL). It was taken in a long tube. The methanolic solution (18 mL) of  $\text{Cu}(\text{ClO}_4)_2(\text{H}_2\text{O})_6$  (0.186 g, 0.5 mmol) and dafone (0.182 g, 1.00 mmol) were added slowly to the above and kept at 5 °C for crystallization. Green coloured crystals were formed within three weeks. Yield. 0.020 g. (0.030 mmol, 11.8 %). Anal. Calcd.  $\text{C}_{26}\text{H}_{13}\text{Cu}_2\text{N}_4\text{O}_{10.50}$  (M. W. 676.48) C, 46.16; H, 1.94; N, 8.28. Found: C, 50.99; H, 2.30; N, 10.15. Important IR absorptions (KBr disk,  $\text{cm}^{-1}$ ): 2359, 1724, 1593 and 1261.

### 3.3. Measurements

IR spectra were obtained with a Shimadzu FT-IR 8000 spectrometer. Elemental analysis was obtained using a FLASH EA 1112 SERIES CHNS analyzer. Diffuse reflectance spectra were recorded on Shimadzu UV/Vis/NIR spectrophotometer. The magnetic susceptibility was measured in the 1.98–300 K temperature range using a Quantum Design MPMS SQUID susceptometer.

### 3.3.1 Crystallographic data collection and structure determination

X-ray data for **4** was collected for the on an Enraf-Nonius CAD4 diffractometer at room temperature using graphite monochromated Mo K $\alpha$  radiation. Data for **1**, **2** and **3** were collected on a Bruker SMART APEX CCD X-ray diffractometer using graphite monochromated Mo K $\alpha$  radiation. The data for **1**, **2** and **3** was reduced using SAINTPLUS<sup>9</sup>, and multiscan absorption corrections using SADABS<sup>10</sup> were applied. The structures were solved using SHELXS-97 and refined using SHELXL-97<sup>11</sup>. All ring hydrogen atoms were assigned on the basis of geometrical considerations and were allowed to ride upon the respective carbon atoms. All water hydrogen atoms were located from the difference Fourier maps and bond length constraints were applied. Crystal data are in Table 3.1, 3.4 and important interatomic distances and angles in Table 3.2, 3.3, 3.5 and 3.6.

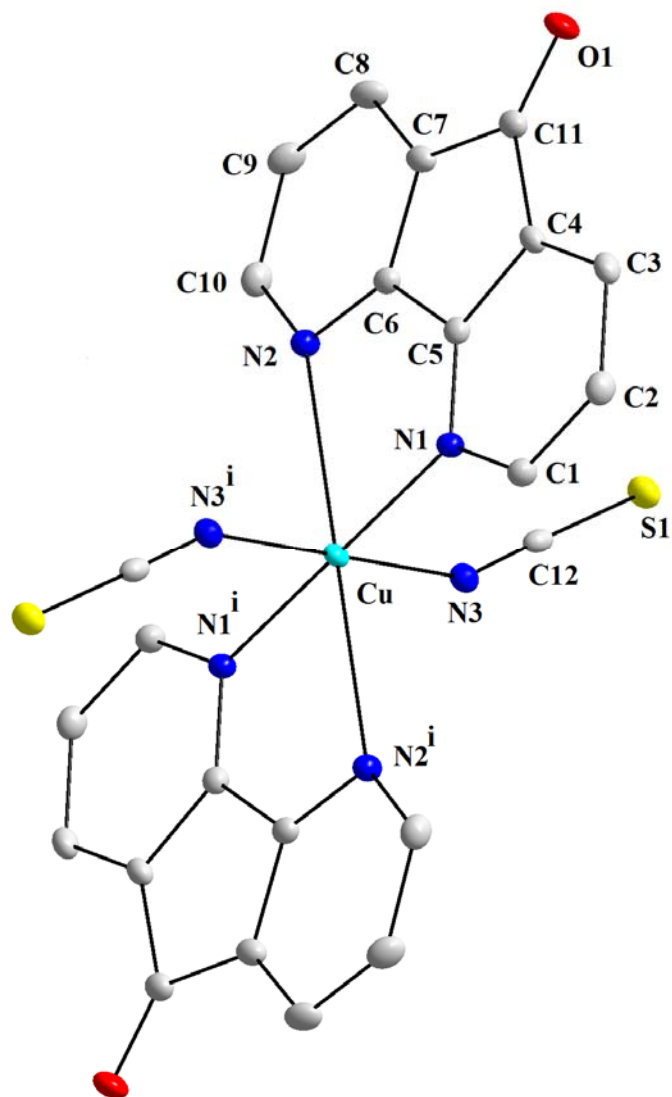
**Table 3.1** Crystallographic data and structure refinement for **1** and **2**

	<b>1</b>	<b>2</b>
Formula	C <sub>24</sub> H <sub>12</sub> CuN <sub>6</sub> O <sub>2</sub> S <sub>2</sub>	C <sub>28</sub> H <sub>18</sub> CuN <sub>8</sub> O <sub>4</sub>
Formula weight	544.06	594.04
Crystal system	Monoclinic	Monoclinic
Space group	<i>P</i> 2 <sub>1</sub> / <i>c</i>	<i>P</i> 2 <sub>1</sub> / <i>c</i>
<i>a</i> (Å)	8.7202(6)	7.8011(5)
<i>b</i> (Å)	13.5501(10)	24.5545(16)
<i>c</i> (Å)	10.4393(5)	7.5058(5)
<i>α</i> (°)	90	90
<i>β</i> (°)	116.024(4)	115.6850(10)
<i>γ</i> (°)	90	90
<i>V</i> (Å <sup>3</sup> )	1108.44(12)	1295.69(15)
<i>Z</i>	2	2
<i>T</i> (K)	100(2)	298(2)
<i>D</i> <sub>calc</sub> (g cm <sup>-3</sup> )	1.630	1.523
<i>μ</i> (mm <sup>-1</sup> )	1.211	0.895
<i>F</i> (000)	550	606
Crystal size (mm)	0.20 x 0.18 x 0.10	0.19 x 0.16 x 0.12
θ Range (°)	2.60 – 26.03	1.66 – 28.28
<i>h</i> / <i>k</i> / <i>l</i>	–10, 10/ –16, 16/ –12, 12	–10, 10/ –32, 32/ 9, 9
Reflection collected	10815	14980
Unique reflect., [ <i>R</i> <sub>int</sub> ]	2172 [0.0348]	3127 [0.0501]
Goodness of fit	1.098	1.090
<i>R</i> <sub><i>I</i></sub> [ <i>I</i> > 2σ( <i>I</i> )]	0.0331	0.0321
<i>wR</i> <sub>2</sub>	0.0763	0.0903

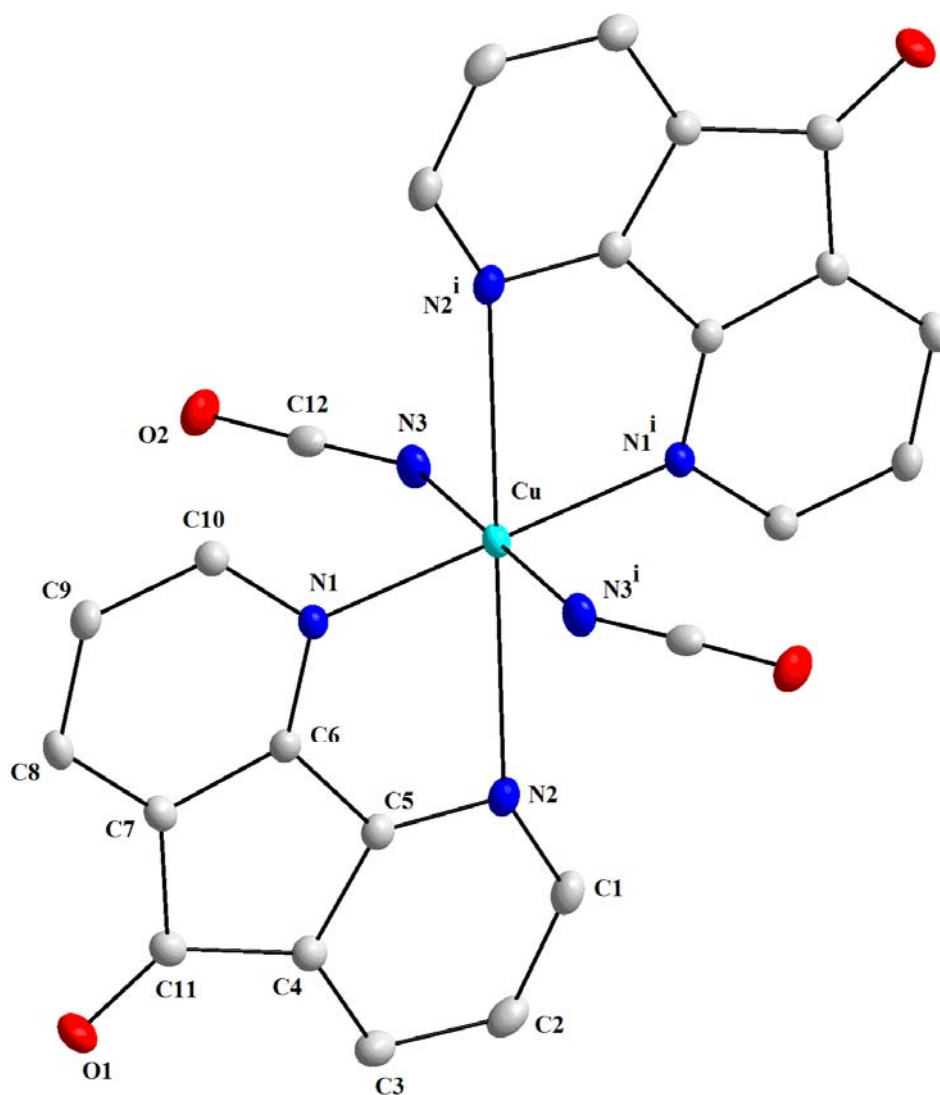
### 3.4 Crystal structures

#### 3.4.1 Crystal structures of $\text{Cu}(\text{dafone})_2(\text{NCS})_2$ (**1**) and $\text{Cu}(\text{dafone})_2(\text{NCO})_2\text{CH}_3\text{CN}$ (**2**)

Molecular diagram of the complexes **1** and **2** were given in Figures 3.1 and 3.2. The crystallographic parameters are comparable to the previously reported complexes<sup>6,8</sup> viz of  $\text{Cu}(\text{dafone})_2\text{Cl}_2$  and  $\text{Cu}(\text{dafone})_2\text{Br}_2$ . In both complexes **1** and **2** copper lie on crystallographic inversion centres. Both structures are having coplanar  $\text{CuN}_4$  coordination in which strain is relieved by lengthening of one pair of *trans* Cu-N bonds. In both cases two distinct Cu-N distances are observed. Cu-N1, 2.035 Å; Cu-N2, 2.644 Å for **1** and Cu-N1, 2.013 Å; Cu-N2, 2.756 Å for **2**. For **2** Cu-N2 distance is slightly longer by 0.112 Å. Consequently the Cu-N1 distance is shorter by 0.022 Å. The remaining coordination is completed by two NCS ligands (Cu-N3, 1.946 Å) in case of **1** and by two NCO ligands (Cu-N3, 1.960 Å) in case of **2**.



**Figure 3.1:** Thermal ellipsoid plot of the coordination environment of the complex molecules **1**: Atoms are represented as 50% probability ellipsoids and ring hydrogen's have been omitted for clarity. Symmetry code: (i)  $-x, y, -z$ .

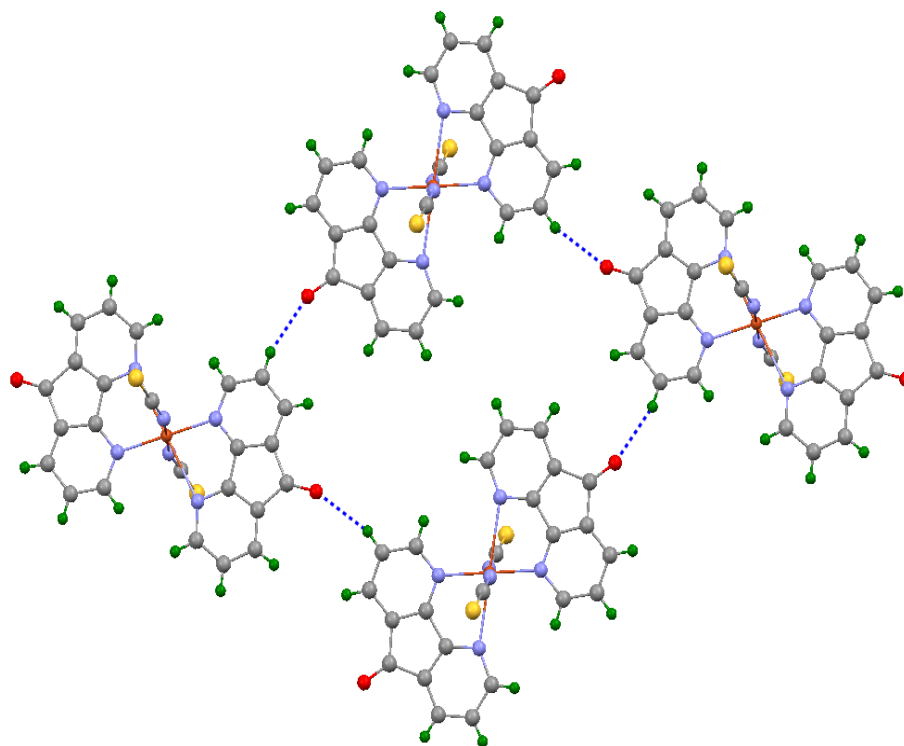


**Figure 3.2:** Thermal ellipsoid plot of the coordination environment of the complex molecules **2**: Atoms are represented as 50% probability ellipsoids and ring hydrogen's have been omitted for clarity. Symmetry code: (i)  $-x, y, -z$ .

**Table 3.2** Selected bond lengths [ $\text{\AA}$ ] and angles [ $^\circ$ ] for  $\text{Cu}(\text{dafone})(\text{NCS})_2$  (**1**)<sup>a</sup>

Cu-N(1)	2.035(2)	Cu-N(2)	2.644(2)	Cu-N(3)	1.946(2)
N(1)-Cu-N(2)	78.49(6)	N(1)-Cu-N(2)#1	101.5(1)	N(1)#1-Cu-N(2)#1	78.49(6)
N(1)-Cu-N(3)	90.53(8)	N(1)-Cu-N(3)#1	89.47(8)	N(1)#1-Cu-N(3)#1	90.53(8)
N(2)-Cu-N(3)	83.51(7)	N(2)#1-Cu-N(2)	180.00(3)	N(3)-Cu-N(2)#1	96.49(7)
N(1)-Cu-N(1)#1	180.0(1)	N(3)-Cu-N(3)#1	180.0(1)	N(3)#1-Cu-N(2)#1	83.51(7)

<sup>a</sup> #1  $-x, y, -z$ .

**Figure 3.3** A view of the supramolecular synthon  $R_4^4(32)$  of the complex **1**

**Table 3.3** Selected bond lengths [Å] and angles [°] for Cu(dafone)(NCO)<sub>2</sub> (**2**)<sup>a</sup>

Cu-N(1)	2.013(2)	Cu-N(2)	2.756(1)	Cu-N(3)	1.960(2)
N(1)-Cu-N(2)	76.92(5)	N(1)#1-Cu-N(1)	180.0(1)	N(3)#1-Cu-N(2)	90.62(5)
N(1)-Cu-N(3)	88.95(6)	N(1)#1-Cu-N(2)	103.1(1)	N(3)-Cu-N(3)#1	180.0(1)
N(2)-Cu-N(3)	89.38(5)	N(1)#1-Cu-N(3)	91.1(1)	N(3)#1-Cu-N(1)#1	88.95(6)
a #1 -x, -y, -z+1					

Coming to the crystal packing, compound **1** forms two-dimensional networks with help of C-H...O interactions (C2-H2...O1, 2.480 Å). Supramolecular synthon  $R_4^4$  (32)<sup>12</sup> (Figure 3.3) build 0-dimensional motif into two-dimensional networks (Figure 3.4). These two dimensional networks develop into 3-dimension by C-H...S (C9-H9...S1, 2.868 Å) and  $\pi$ -stacking interactions (C9...C5 and C12...C7, 3.432 Å). Compound **2** form 2-dimensional networks (Figure 3.5) with C-H...O interactions (C3-H3...O1, 2.598 Å and C10-H10...O2, 2.510 Å). 2-dimensional networks are further build into three-dimension with the help of a solvent acetonitrile (C13-H13...O1, 2.548 Å and C2-H2...N4, 2.563 Å interactions).



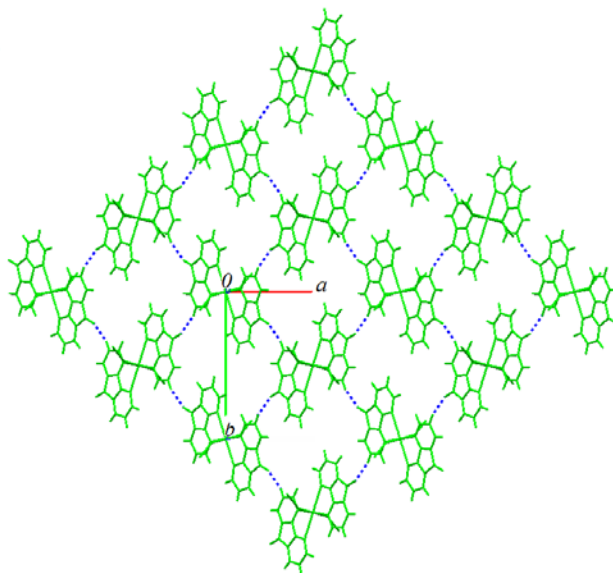


**Figure 3.4** Down the *c* axis view of the two-dimensional networks of **1**, it was formed by C-H...O interactions.

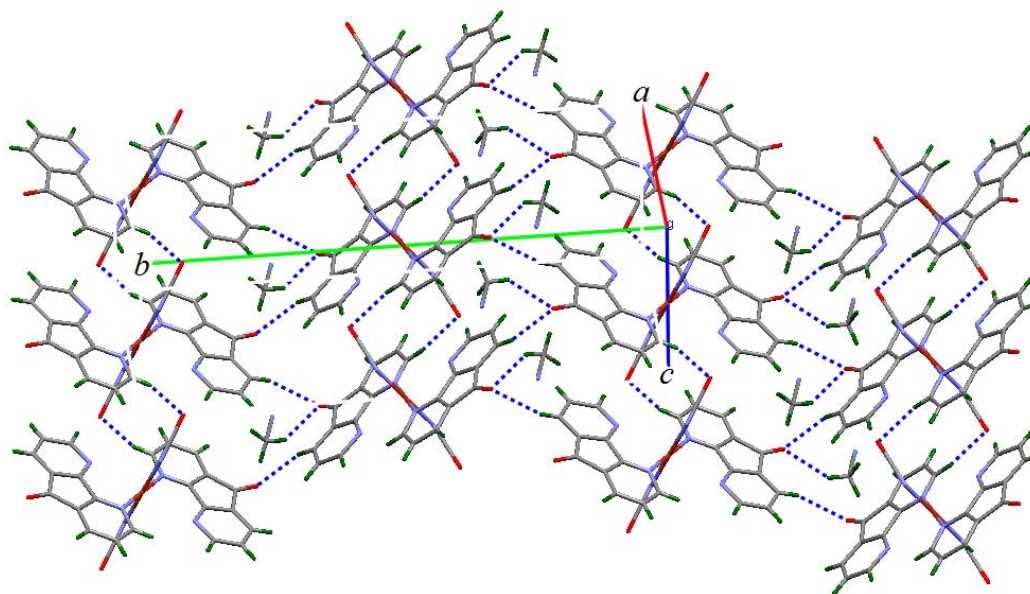


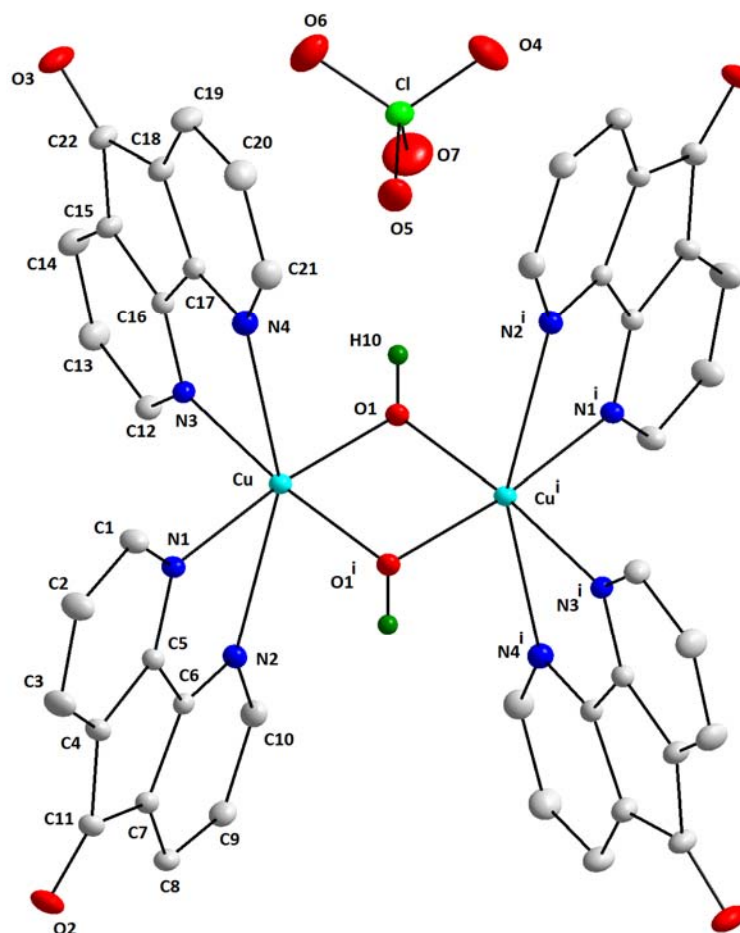
**Figure. 3.5.** A view of the two-dimensional networks of **2** formed by C-H...O interactions.

**Table 3.4** Crystallographic data and structure refinement for **3** and **4**

	<b>3</b>	<b>4</b>
Formula	C <sub>44</sub> H <sub>26</sub> Cl <sub>2</sub> Cu <sub>2</sub> N <sub>8</sub> O <sub>14</sub>	C <sub>26</sub> H <sub>13</sub> Cu <sub>2</sub> N <sub>4</sub> O <sub>10.50</sub>
Formula weight	1088.71	676.48
Crystal system	Triclinic	Monoclinic
Space group	$P\bar{1}$	$C2/c$
<i>A</i> (Å)	8.6067(6)	16.548(8)
<i>B</i> (Å)	11.5112(7)	21.819(7)
<i>C</i> (Å)	12.0715(8)	15.415(13)
<i>A</i> (°)	70.257(6)	90
<i>B</i> (°)	77.191(6)	116.84(6)
<i>Γ</i> (°)	71.479(6)	90
<i>V</i> (Å <sup>3</sup> )	1058.56(12)	4966(5)
<i>Z</i>	1	8
<i>T</i> (K)	298(2)	298(2)
<i>D</i> <sub>calc</sub> (g cm <sup>-3</sup> )	1.708	1.810
<i>M</i> (mm <sup>-1</sup> )	1.214	1.786
<i>F</i> (000)	550	2712
Crystal size (mm)	0.60 x 0.50 x 0.12	0.50 x 0.35 x 0.20
Θ Range (°)	3.28 – 31.94	1.77 – 27.47
<i>h/k/l</i>	–12, 12/ –16, 17/ –17, 13	0, 21/ 0, 28/ –20, 17
Reflection collected	11139	5988
Unique reflect., [R <sub>int</sub> ]	6672 [ 0.0376 ]	5685 [0.0167]
Goodness of fit	1.073	0.984
<i>R</i> <sub>I</sub> [I>2σ(I)]	0.0373	0.0480
<i>wR</i> <sub>2</sub>	0.1020	0.1067

### 3.4.2 Crystal structure of $[\text{Cu}_2(\text{dafone})_4(\text{OH})_2](\text{ClO}_4)_2$ (**3**)

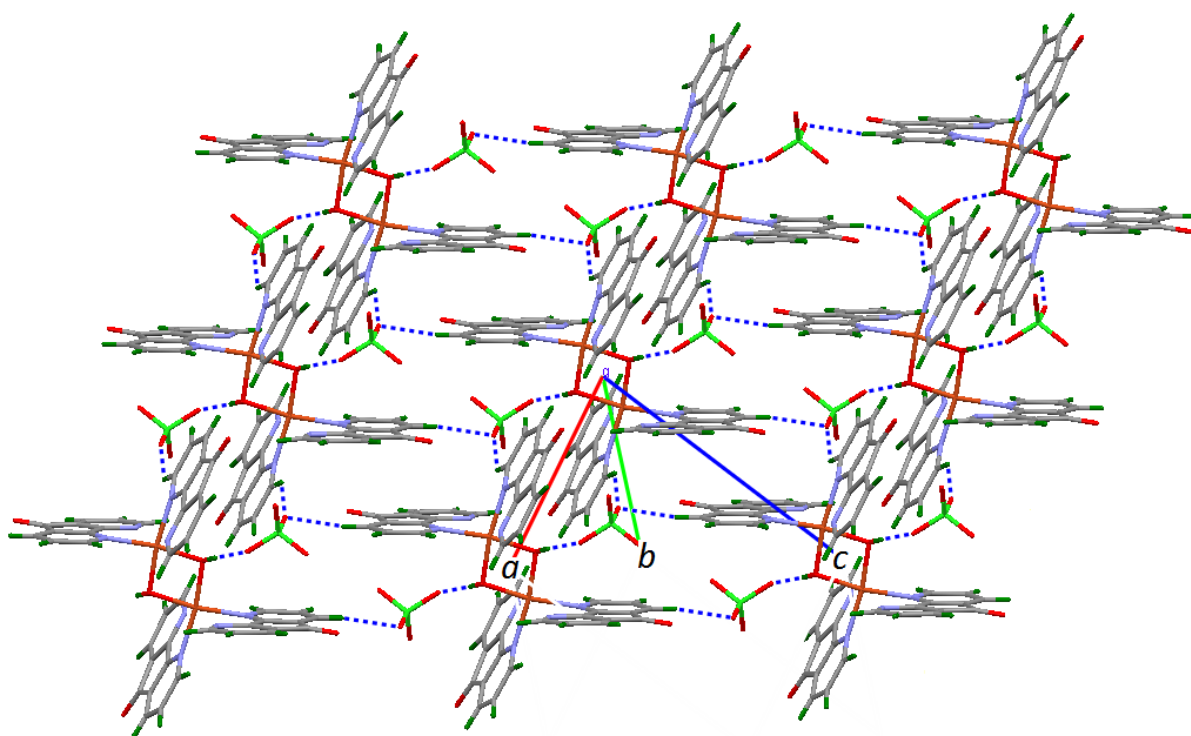
In acetonitrile when sodium thiocyanate was used, it was coordinated to the copper(II) centre but when used in methanol media, it was hydrolysed and hydroxyl bridged dinuclear complex was formed. The complex  $[\text{Cu}_2\text{L}_4(\text{OH})_2]^{2+}$  features are hydroxyl bridged Cu(II) dimer complex as shown in Figure 3.6. The cation is dinuclear with crystallographic inversion centre. The copper(II) has a distorted octahedral geometry in which equatorial plane consist of  $\text{CuN}_2\text{O}_2$  chromophore comprised of two nitrogen atoms from the dafone ligand (Cu-N1, 2.005 Å and Cu-N3, 2.017 Å) and two oxygen atoms from hydroxo group (Cu-O1, 1.920 Å). The axial directions are occupied by two nitrogen atoms from two dafone molecules (Cu-N2, 2.943 Å and Cu-N4, 2.790 Å). Since the complex is Jan-Teller active, the axial bond distances are quite large when compared to other bond distances. The N4-Cu-N2 bond angle shows a considerable deviation of 158.75°. The bite angles for the dafone ligands are 75.46° for N4-Cu-N3 and 72.85° for N1-Cu-N2. The Cu...Cu distance is 2.942 Å. The two Cu-O-Cu bridges are nearly symmetric with a bridge angle of 99.7°. Coming to the crystal packing, **3** form two-dimensional networks (Figure 3.7) with the help of  $\text{O}_1\text{-H}_{10}\dots\text{O}_5$  (2.17 Å) and  $\text{C-H}\dots\text{O}$  (2.172-2.436 Å) interactions.  $\pi$ -stacking interactions (3.314-3.498 Å) build the above network into a three-dimensional network.



**Figure 3.6.** Thermal ellipsoid plot of the coordination environment of the complex molecules **3**: Atoms are represented as 50% probability ellipsoids and ring hydrogen's have been omitted for clarity. Symmetry code: (i)  $-x, -y, -z$ .

**Table 3.5** Selected bond lengths [ $\text{\AA}$ ] and angles [ $^\circ$ ] for  $[\text{Cu}_2(\text{dafone})_4(\text{OH})_2](\text{ClO}_4)$  (**3**)<sup>a</sup>

Cu-O(1)	1.9200(13)	Cu-N(1)	2.0048(15)	Cu-N(3)	2.0173(14)
Cu-O(1)#1	1.9288(12)	Cu-N(2)	2.943(15)	Cu-N(4)	2.790(15)
Cu-Cu#1	2.9417(4)				
O(1)-Cu-N(1)	91.41(6)	N(1)-Cu-N(3)	92.74(6)	Cu-O(1)-Cu#1	99.69(6)
O(1)-Cu-N(2)	87.24(6)	N(1)-Cu-N(2)	72.84(2)	O(1)#1-Cu-N(1)	171.40(5)
O(1)-Cu-N(3)	171.27(5)	N(3)-Cu-N(4)	75.46(8)	O(1)#1-Cu-N(3)	171.27(6)
O(1)-Cu-N(4)	107.41(6)	N(1)-Cu-N(3)	97.13(6)	a #1 -x, -y, -z	

**Figure 3.7.** Two-dimensional networks of **3** formed by C-H...O interactions.

### 3.4.3 Crystal structure of $[\text{Cu}_2(\text{dafone})_2(\text{oxalate})_2] (\text{H}_2\text{O})_{0.5}$ (4)

Molecular diagram of the complex is shown in figure 3.8. The crystal structure consist of polymeric chains of  $[\text{Cu}(\text{dafone})]^{2+}$  ions bridged by oxalate anions. The copper atom is coordinated with two nitrogen atom of the dafone and four oxygen atoms of the two oxalato groups, and the coordination geometry of the copper is described by an elongated rhombic octahedron. There is considerable asymmetry in the oxalate chelation. Three oxygen atoms from the oxalate group and one nitrogen atom of the dafone stay in equatorial plane with average Cu-O distances are 1.978 Å for Cu1 and 1.968 Å for Cu2. One oxygen atom from the oxalate group and one nitrogen atom from the dafone stay in axial directions (Cu1-N2, 2.687; Cu1-O5, 2.257; Cu2-N4, 2.773 and Cu2-O6, 2.330 Å).  $[\text{Cu}_2(\text{dafone})_2(\text{ox})_2]$  forms polymeric zig-zag chains down the c axis. The lattice water molecule interconnects two such chains by hydrogen bond interaction (Figure 3.9).

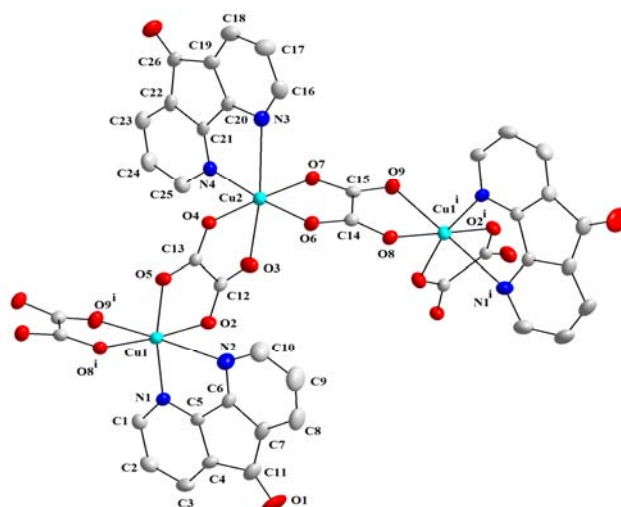


**Figure 3.8.** Thermal ellipsoid plot of the coordination environment of the complex molecules **4**: Atoms are represented as 50% probability ellipsoids and ring hydrogen's have been omitted for clarity. Symmetry code: (i)  $-x, y, -z$ .

**Table 3.6** Selected bond lengths [ $\text{\AA}$ ] and angles [ $^\circ$ ] for  $[\text{Cu}_2(\text{dafone})_2(\text{ox})_2](\text{H}_2\text{O})_{0.5}$  (**4**)<sup>a</sup>

Cu(1)-N(1)	2.027(3)	Cu(2)-N(3)	2.020(4)	Cu(2)-O(3)	1.978(3)
Cu(1)-N(2)	2.688(4)	Cu(2)-N(4)	2.772(3)	Cu(2)-O(7)	1.977(3)
Cu(2)-O(4)	1.947(3)	Cu(2)-O(2)	1.982(3)	Cu(2)-O(6)	2.329(3)
Cu(1)-O(5)	2.258(3)	Cu(1)-O(9)#1	1.998(3)	O(4)-Cu(2)-O(6)	99.62(10)
Cu(1)-O(8)#1	1.955(3)	O(4)-Cu(2)-O(7)	176.31(10)	O(7)-Cu(2)-O(6)	78.62(10)
N(1)-Cu(1)-O(5)	100.99(11)	O(4)-Cu(2)-O(3)	84.83(12)	O(3)-Cu(2)-N(3)	174.53(12)
O(5)-Cu(1)-N(2)	177.26(11)	O(7)-Cu(2)-O(3)	91.84(12)	O(9)#1-Cu(1)-N(2)	89.57(11)
N(1)-Cu(1)-N(2)	77.62(11)	O(4)-Cu(2)-N(3)	92.09(13)	O(8)#1-Cu(1)-O(2)	174.28(10)
O(8)#1-Cu(1)-N(2)	86.47(13)	O(7)-Cu(2)-N(3)	91.35(13)	a, #1 $x, -y+1, z-1/2$	

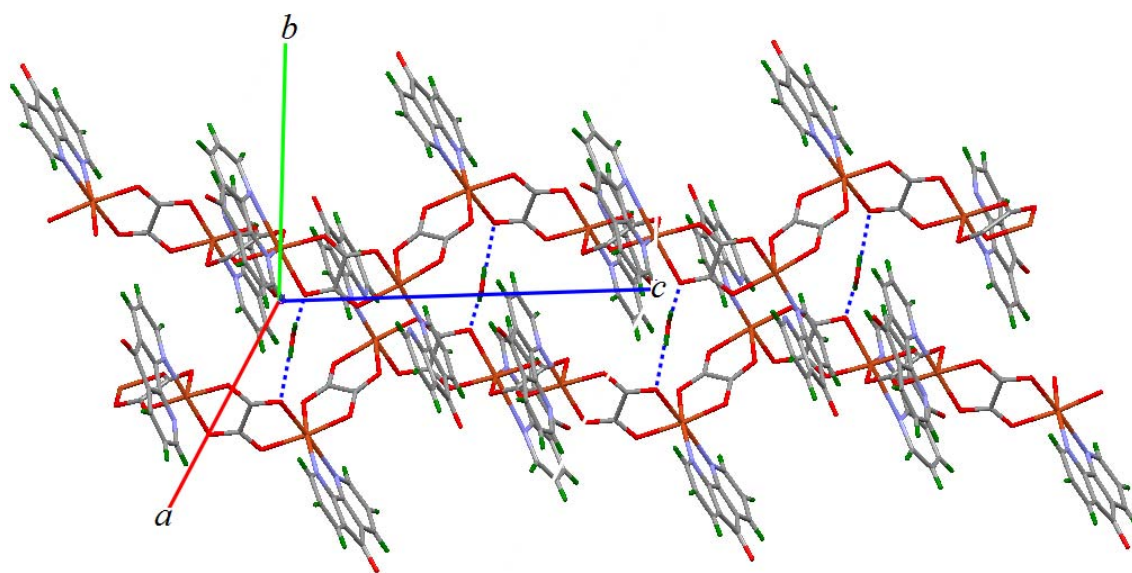


**Figure 3.9.** Two zig-zag chains of **4** are interconnected hydrogen bond interaction of a water molecule.



### 3.5. Electronic spectra

#### 3.5.1 Electronic spectrum of Cu(dafone)<sub>2</sub>NCS<sub>2</sub> (**1**)

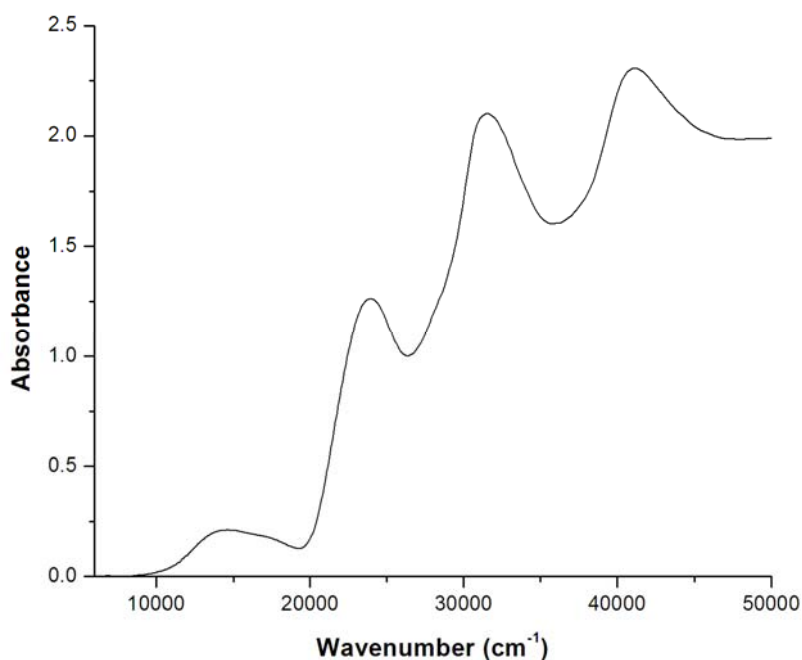


**Figure 3.10.** Diffuse reflectance spectrum of **1**

Diffuse reflectance spectrum of **1** is shown in Figure 3.10. The three broad bands below 24000 cm<sup>-1</sup> may be assigned to *d-d* transitions between the split components of the <sup>2</sup>*E* and <sup>2</sup>*T*<sub>2</sub> states of the *d*<sup>9</sup> ion as follows: 14326 cm<sup>-1</sup> (*d*<sub>z<sup>2</sup></sub> → *d*<sub>x<sup>2</sup>-y<sup>2</sup></sub>), 17123 cm<sup>-1</sup> (*d*<sub>xy</sub> → *d*<sub>x<sup>2</sup>-y<sup>2</sup></sub>), 23923 cm<sup>-1</sup> (*d*<sub>xz</sub>, *d*<sub>yz</sub> → *d*<sub>x<sup>2</sup>-y<sup>2</sup></sub>). The assignments are consistent with the previously reported octahedral copper(II) complexes.<sup>13</sup> The bands 31446 cm<sup>-1</sup> and 41322 cm<sup>-1</sup> are ligand centred transitions.

### 3.5.2 Electronic spectrum of $[\text{Cu}(\text{dafone})_2(\text{NCO})_2]\text{CH}_3\text{CN}$ (**2**)

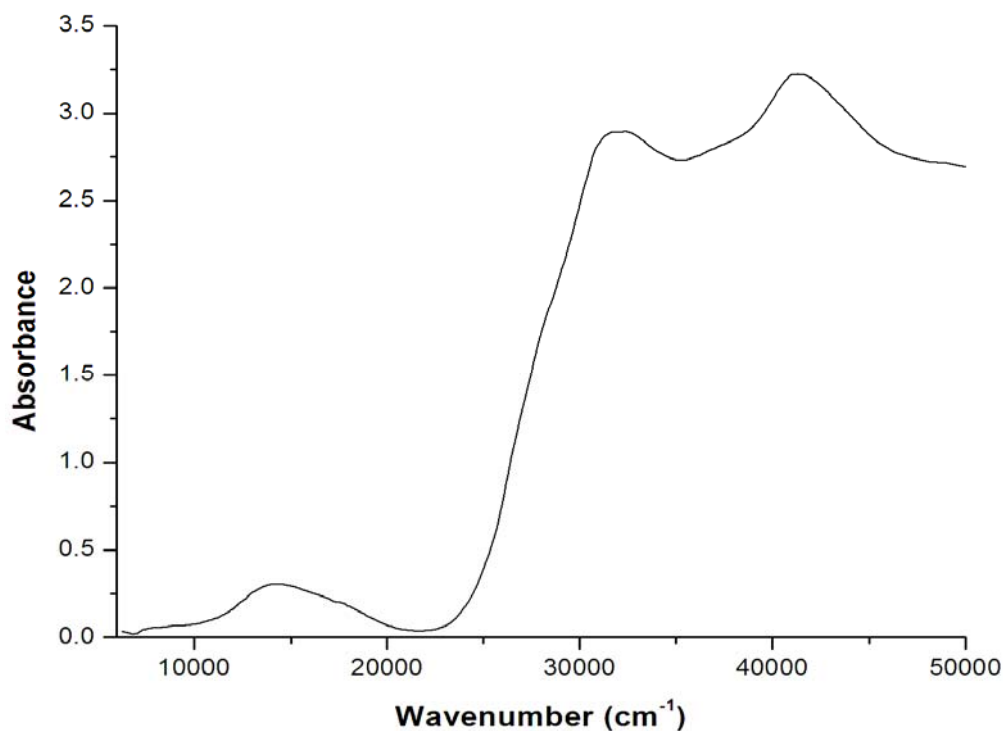


**Figure 3.11.** Diffuse reflectance spectrum of **2**

Diffuse reflectance spectrum of **2** is shown in Figure 3.11. The two broad bands below  $24000\text{ cm}^{-1}$  may be assigned to  $d-d$  transitions between the split components of the  $^2E$  and  $^2T_2$  states of the  $d^9$  ion as follows:  $14164\text{ cm}^{-1}$  ( $d_{z^2} \rightarrow d_{x^2-y^2}$ ) and  $17667\text{ cm}^{-1}$  ( $d_{xy} \rightarrow d_{x^2-y^2}$ ). The bands  $31646\text{ cm}^{-1}$  and  $41322\text{ cm}^{-1}$  are ligand centred transitions.

### 3.5.3 Electronic spectrum of $[\text{Cu}_2(\text{dafone})_4(\text{OH})_2](\text{ClO}_4)_2$ (**3**)

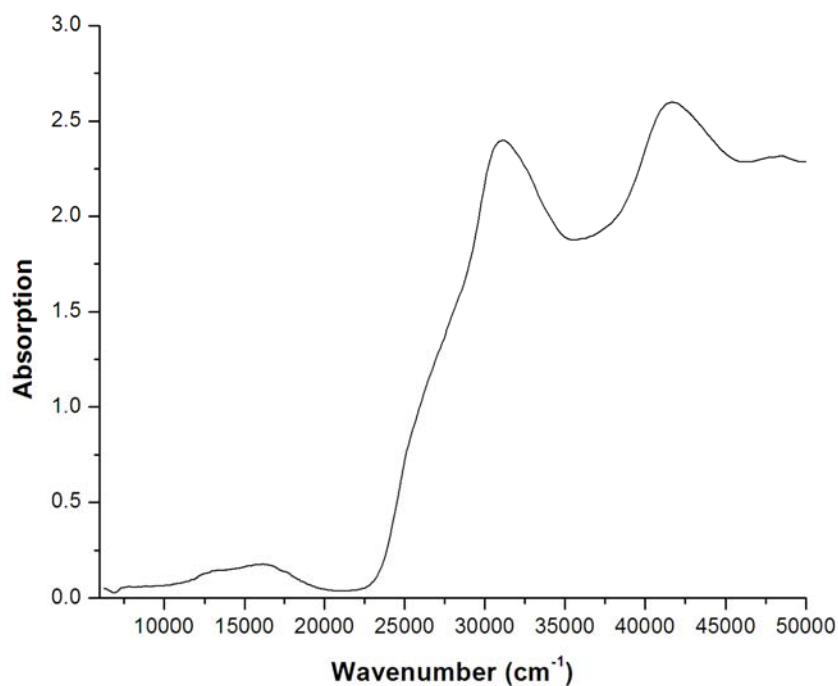


**Figure 3.12.** Diffuse reflectance spectrum of **3**

Diffuse reflectance spectrum of **3** is shown in Figure 3.12. The two broad bands below  $24000\text{ cm}^{-1}$  may be assigned to  $d-d$  transitions between the split components of the  $^2E$  and  $^2T_2$  states of the  $d^9$  ion as follows:  $12920\text{ cm}^{-1}$  ( $d_{z^2} \rightarrow d_{x^2-y^2}$ ) and  $16393\text{ cm}^{-1}$  ( $d_{xy} \rightarrow d_{x^2-y^2}$ ). The bands  $28902\text{ cm}^{-1}$ ,  $31506\text{ cm}^{-1}$  and  $41667\text{ cm}^{-1}$  are ligand centered transitions.

### 3.5.4 Electronic spectrum of $[\text{Cu}_2(\text{dafone})_2(\text{oxalate})_2] (\text{H}_2\text{O})_{0.5}$ (**4**)

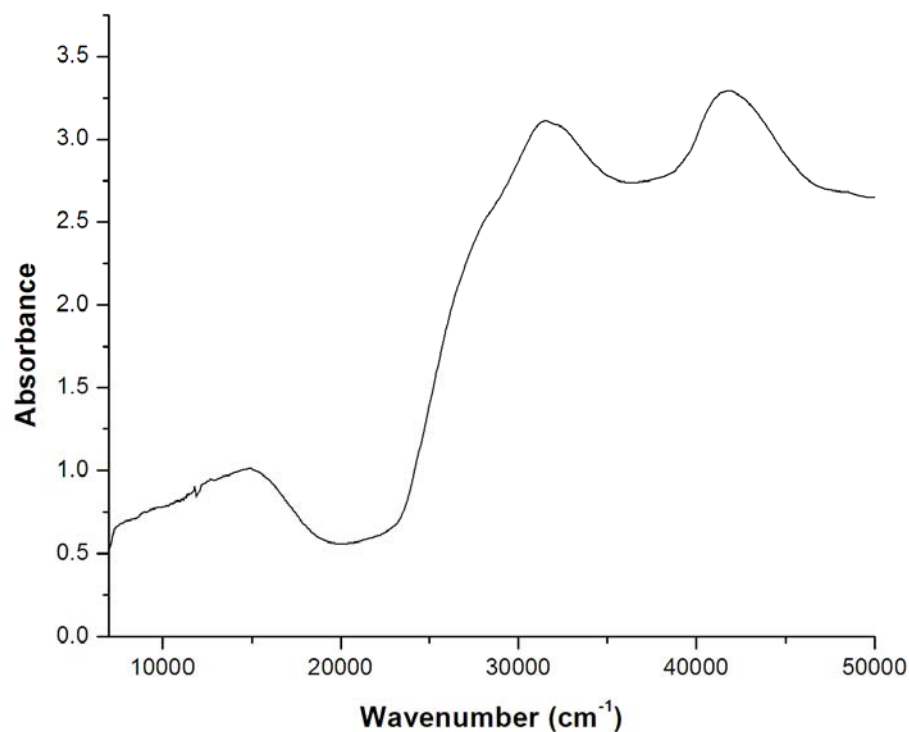


**Figure 3.13.** Diffuse reflectance spectrum of **4**

Diffuse reflectance spectrum of **4** is shown in Figure 3.13. The two broad bands below  $24000\text{ cm}^{-1}$  may be assigned to  $d-d$  transitions between the split components of the  $^2E$  and  $^2T_2$  states of the  $d^9$  ion as  $14970\text{ cm}^{-1}$  ( $d_{z^2} \rightarrow d_{x^2-y^2}$ ). The remaining absorptions  $28571\text{ cm}^{-1}$ ,  $31446\text{ cm}^{-1}$  and  $41966\text{ cm}^{-1}$  are ligand centered transitions.

### 3.6 Magnetic properties

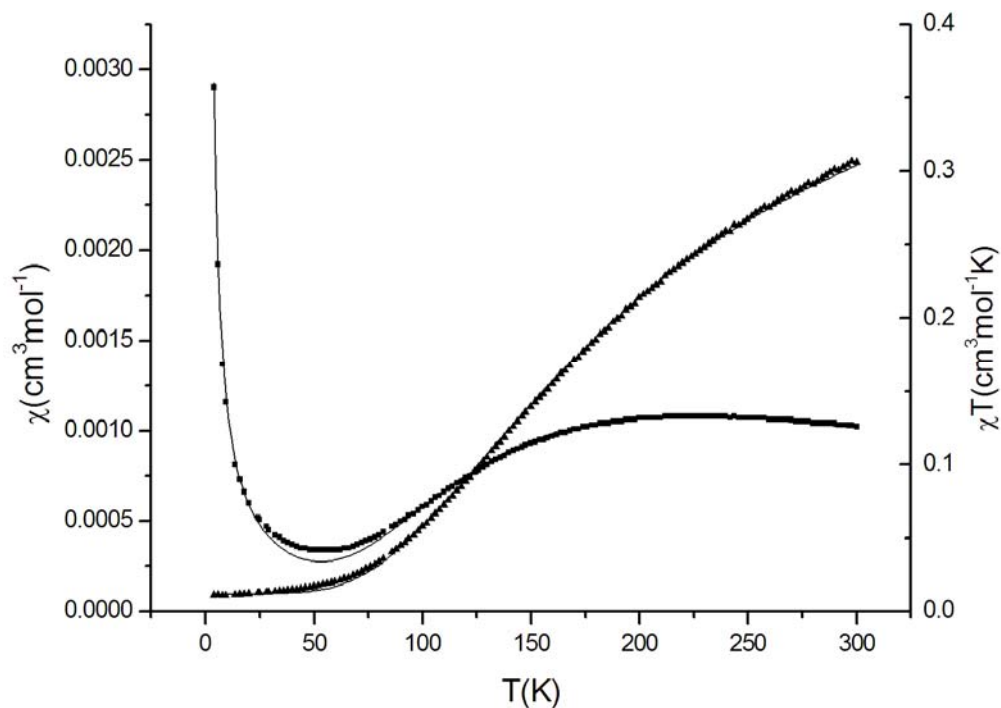


**Figure 3.14.** Molar paramagnetic susceptibility ( $\chi_M$ ) and product of molar paramagnetic susceptibility per mole of  $\text{Cu}^{2+}$  and temperature ( $\chi_M T$ ) vs. temperature curves for **3**.

Magnetic susceptibility data was recorded for compound **3** from 299.9 K to 3.84 K (Figure 3.14). The  $\chi_M T$  product is  $0.304 \text{ cm}^3 \text{ mol}^{-1} \text{ K}$  (per mol of  $\text{Cu}^{2+}$ ) at 299.9 K which can be seen to be much lower than the calculated value of  $0.37 \text{ cm}^3 \text{ mol}^{-1} \text{ K}$  for two uncoupled

spins ( $S_1 = 1/2$ ,  $S_2 = 1/2$ ) with  $g = 2$ . This suggests anti-ferromagnetic coupling in the dimers as confirmed by the variable temperature susceptibility study. With decrease of temperature,  $\chi_M T$  decreases slowly reaching a value  $0.011 \text{ cm}^3 \text{ mol}^{-1} \text{ K}$  at 3.84 K. The magnetic data was fitted by using dimer model including inter-dimer interactions within the molecular field approximation. For complex **3** it was found that a good fit of the  $\chi_M T$  vs temperature data could be obtained, except at the lowest temperatures where the theoretical values of  $\chi_M T$  were found to be smaller than the observed. In the case of antiferromagnetically-coupled complexes, it is frequently the presence of a small amount of paramagnetic impurity that causes this deviation. Thus, in the fitting of the data, we have included a susceptibility term (Curie law behavior) for a paramagnetic  $S = 1/2$  impurity (2 %). The parameters obtained by least square fitting<sup>14</sup> are:  $J = -126.80 \text{ cm}^{-1}$ ,  $zJ = -0.971 \text{ cm}^{-1}$ ,  $g = 2.26$ ,  $\text{TIP} = 0.00006 \text{ emu mol}^{-1}$  (fixed), ( $\hat{H} = -2JS_1S_2$ ).

### 3.7 Estimation of the Exchange Integrals by DFT Calculations

Since there are two chemically distinguishable isomeric tetramers in crystal, identification of the ground state by magnetic measurements alone is not possible. To overcome this we have calculated magnetic exchange integrals by broken symmetry method. “Broken symmetry” calculations were attempted by using the free software package ORCA

developed by F. Neese.<sup>15</sup> For that purpose the dimeric molecule was simplified by placing two hydrogen atoms on the C=O position of the dafone. Coordinates from the X-ray structure of **3** were used for all other atoms, and the structure was not optimized by DFT. The calculation utilized the basis Ahlrichs-VDZ<sup>16</sup> and polarization functions from the Ahlrichs polarization basis. The magnetic properties of a system comprising two interacting magnetic centres with fictitious local spins  $\mathbf{S}_A$  and  $\mathbf{S}_B$  are typically interpreted in the context of the phenomenological

Heisenberg–Dirac–van Vleck spin-Hamiltonian

$$H = -2JS_AS_B \quad (1)$$

In each case the exchange integrals were calculated according to the convention<sup>17</sup>

$$J = (E_{HS} - E_{BS})/(S(S+1))$$

Where, HS and BS denote the high-spin state and the broken-symmetry state, respectively.

Calculation shows  $J = -159.21 \text{ cm}^{-1}$  which is slightly above the experimentally reported value of  $-126.80 \text{ cm}^{-1}$ .

### 3.8 Conclusion

Four new Cu(II) complexes of dafone were synthesised. Two mononuclear complexes form  $\text{CuN}_4$  coordination by cleverly avoiding steric strain with the elongation of one pair of Cu-N bonds. Unlike in acetonitrile, sodium thiocyanate hydrolyses under the given reaction conditions in methanol media and forms hydroxo bridged Cu(II) dimer. With the

help of oxalate anion copper-dafone complex forms a coordination polymer. The hydroxo bridged complex,  $[\text{Cu}_2(\text{dafone})_4(\text{OH})_2](\text{ClO}_4)_2$  (**3**) is strongly antiferromagnetically coupled with a  $|2J|$  value more than  $250 \text{ cm}^{-1}$ . The centrosymmetric dimer has a bridge angle of  $99.7^\circ$  and Cu-Cu distance of  $2.94 \text{ \AA}$ . Magneto structural correlation of hydroxo bridged Cu(II) complexes has been reported based on experimental data<sup>18</sup> as well as DFT calculations.<sup>19</sup> Based on magnetic and structural data on several complexes having very nearly coplanar  $\text{Cu}_2(\text{OH})_2$  unit, like in the present case, the following expression was proposed to evaluate  $2J$  value with bridge angle ( $\Phi$ )<sup>18</sup>

$$2J = -74.53 \Phi + 7270$$

This would mean compound **3** should have a  $2J$  value of  $-80 \text{ cm}^{-1}$ , which is much less than the value actually observed. Theoretical calculations based on DFT (B3LYP)<sup>19</sup> showed that besides the bridging angle, the torsion ( $\tau$ ) defining the out-of-plane displacement of the hydroxyl hydrogen atoms also plays an important role in determining the singlet-triplet splitting ( $\tau = 49^\circ$  in **3**). However, for  $\tau \sim 0$  the calculations predict a much larger  $|2J|$  value ( $320\text{--}480 \text{ cm}^{-1}$ ) for a bridge angle of  $99^\circ$ . The present calculation yielded  $2J = -318 \text{ cm}^{-1}$  somewhat greater in magnitude than the experimental value of  $-254 \text{ cm}^{-1}$ .



### 3.9 References

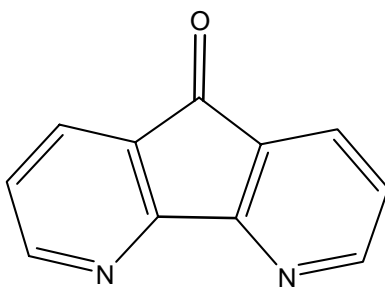
1. Menon, S.; Balagopalakrishna, C.; Rajasekharan, M. V.; Ramakrishna, B. L. *Inorg. Chem.* **1994**, *33*, 950.
2. Balagolalakrishna, C.; Rajasekharan, M. V.; Bott, S.; Atwood, J. L.; Ramakrishna, B. L. *Inorg. Chem.* **1992**, *31*, 2843.
3. Menon, S.; Rajasekharan, M. V. *Inorg. Chem.* **1997**, *36*, 4983.
4. Menon, S.; Rajasekharan, M. V. *Polyhedron* **1998**, *17*, 2463.
5. Miao, S.; Kang, H.; Du, C.; Ji, B. *X-Ray Struct. Anal. Online*, **2006**, *22*, 45.
6. Lu, Z.; Duan, C.; Tian, Y.; You, X. *Inorg. Chem.* **1996**, *35*, 2253.
7. Wang, Y.; Jackman, D. C.; Woods, C.; Rillema, D. P. *J. Chem. Crystal.* **1995**, *25*, 549.
8. Henderson Jr. L. J.; Fronczek, F. R.; Cherry, W. R. *J. Am. Chem. Soc.* **1984**, *106*, 5876.
9. SAINTPLUS, Bruker AXS Inc. Madison, Wisconsin, USA.
10. Sheldrick, G. M. *SADABS, Program for Empirical Absorption Correction*, University of Gottingen, Germany, **1996**.
11. M. Sheldrick, *Acta Cryst.* **2008**, *A64*, 112.

12. Kunz, P. C.; Huber, W.; Spingler, B. *J. Chem. Crystallogr.* DOI 10.1007/s10870-010-9845-0.
13. Manch, W.; Ferneliuss, W. C. *J. Chem. Educ.* **1961**, 38, 192.
14. Chandramouli, G. V. R.; Balagopalakrishna, C.; Rajasekharan, M. V.; Manoharan, P. T. *Comput. Chem.* **1996**, 20, 353.
15. Neese, F. *ORCA*, an ab initio, Density Functional and Semiempirical Program Package, Version 2.6-35, 2008; Universita't Bonn: Bonn, Germany; free download from <http://www.thch.uni-bonn.de/tc/orca/>, registration required.
16. (a) Schaefer, A.; Horn, H.; Ahlrichs, R. *J. Chem. Phys.* **1992**, 97, 2571. (b) Ahlrichs et al. Unpublished work. (c) The Ahlrichs auxiliary basis sets were obtained from the TurboMole basis set library under <ftp://chemie.uni-karlsruhe.de/pub/jbasen>. (d) Eichkorn, K.; Treutler, O.; Ohm, H.; Haser, M.; Ahlrichs, R. *Chem. Phys. Lett.* **1995**, 240, 283. (e) Eichkorn, K.; Weigend, F.; Treutler, O.; Ahlrichs, R. *Theor. Chem. Acc.* **1997**, 97, 119.
17. (a) Ginsberg, A. P. *J. Am. Chem. Soc.* **1980**, 102, 111. (b) Noodleman, L. *J. Chem. Phys.* **1981**, 74, 5737. (c) Noodleman, L.; Davidson, E. R. *Chem. Phys.* **1985**, 109, 131.
18. Van, H.; Crawford, V. H.; Richardson, H. W.; Wasson, J. H.; Hodgson, D. J.; Hatfield, W. E. *Inorg. Chem.* **1976**, 15, 2107.
19. Ruiz, E.; Alemany, P.; Alvarez, S.; Cano, J. *J. Am. Chem. Soc.* **1997**, 119, 1297.

### Nickel complexes of 4, 5-Diazafluoren-9-one

#### 4.1 Introduction

4,5-Diazafluoren-9-one (dafone) is a bidentate ligand. It is a derivative of 1,10-phenanthroline (phen), having an exocyclic keto function<sup>1</sup>. Dafone attracted attention of researchers due perhaps to its DNA intercalation properties<sup>2</sup>.



(dafone)

Unlike phen / bpy (1,10-phenanthroline/2,2'-bipyridine), coordination chemistry of bidentate, neutral ligand dafone is still restricted to a few metals<sup>3-9</sup>. The differences in the binding properties of phen and dafone may be attributed to the reduced overlap of nitrogen orbitals with the appropriate metal orbitals due to the larger bite distance in dafone<sup>10</sup>. Nickel plays numerous roles in the biology of microorganisms and plants, the main

constituent of various enzymes and coenzymes like carbon monoxide dehydrogenase<sup>11</sup>. Even though many mononuclear complexes of bpy<sup>12</sup> and phen<sup>13</sup> have been structurally characterised, only one structure<sup>14</sup> was reported with dafone. Due to intrinsic interest for the various structural varieties of mononuclear nickel complexes, we have synthesised two complexes.

## 4.2 Experimental

### 4.2.1 Reagents

All chemicals were purchased from Ranbaxy chemicals and used without further purification. Dafone was prepared using a reported procedure<sup>1</sup>.

### 4.2.2 Synthesis

#### Synthesis of Ni(dafone)<sub>2</sub>(NCS)<sub>2</sub> (1)

Ni(ClO<sub>4</sub>)<sub>2</sub>(H<sub>2</sub>O)<sub>6</sub> (0.370 g, 1.00 mmol) was dissolved in water and taken in a long tube. Methanolic solution of dafone (0.182 g, 1.00 mmol) was added slowly to the above solution. Methanolic solution of KSCN (0.097 g, 1.0 mmol) was added slowly to the top the above solution and was kept for crystallization at 5° C. After two days green coloured crystals were separated. Yield 0.270 g (0.501 mmol, 50 %). Anal. Cald. C<sub>24</sub>H<sub>12</sub>N<sub>6</sub>NiO<sub>2</sub>S<sub>2</sub> (M.Wt. 539.23) C, 53.46; H, 2.24; N, 15.58. Found: C, 53.35; H, 1.69; N, 15.22. Important IR absorptions (KBr disk, cm<sup>-1</sup>): 2081, 1809, 1738, 1597, 1292, 839, 534 and 476.

**Synthesis of [Ni(dafone)(H<sub>2</sub>O)<sub>4</sub>]NO<sub>3</sub> (2)**

Ni(NO<sub>3</sub>)<sub>2</sub>(H<sub>2</sub>O)<sub>6</sub> (0.207 g, 1.00 mmol) and dafone (0.182 g, 1.00 mmol) were dissolved in acetonitrile (10 mL) and kept for crystallization. The green coloured solution was kept for crystallization at room temperature. Green coloured crystals were formed within few days. Yield 0.266 g (0.61 mmol, 61 %). Anal. Cald. For. C<sub>11</sub>H<sub>14</sub>N<sub>4</sub>NiO<sub>11</sub> (M.Wt. 436.97) C, 30.23; H, 3.23; N, 12.82. Found: C, 30.11; H, 3.31; N, 13.12. Important IR absorptions (KBr disk, cm<sup>-1</sup>): 3269, 2399, 1822, 1736, 1643, 1583, 1413, 1359, 1246, 1103, 906, 831 and 760.

**4.3. Measurements**

IR spectra were obtained with a Shimadzu FT-IR 8000 spectrometer. Elemental analysis was obtained using a FLASH EA 1112 SERIES CHNS analyzer. Diffuse reflectance spectra were recorded on Shimadzu UV/Vis/NIR spectrophotometer.

**4.3.1. Crystallographic data collection and structure determination**

Data were collected on a Bruker SMART APEX CCD X-ray diffractometer using graphite monochromated Mo K $\alpha$  radiation. The data were reduced using SAINTPLUS<sup>15</sup>, and multiscan absorption corrections using SADABS<sup>16</sup> were applied. The structures were solved using SHELXS-97 and refined using SHELXL-97<sup>17</sup>. All ring hydrogen atoms were assigned on the basis of geometrical considerations and were allowed to ride upon the respective carbon atoms. All water hydrogen atoms were located from the difference Fourier maps and bond length constraints were applied. Crystal data are in Table 4.1 and important interatomic distances and angles in Table 4.2 and 4.3.

**Table 4.1** Crystallographic and structure refinement data for **1** and **2**

	<b>1</b>	<b>2</b>
Formula	C <sub>24</sub> H <sub>12</sub> N <sub>6</sub> NiO <sub>2</sub> S <sub>2</sub>	C <sub>11</sub> H <sub>14</sub> N <sub>4</sub> NiO <sub>11</sub>
Formula weight	539.23	436.97
Crystal system	Orthorhombic	Monoclinic
Space group	<i>Pbcn</i>	<i>C2/c</i>
<i>a</i> (Å)	13.3910(10)	12.905(3)
<i>b</i> (Å)	10.0420(7)	10.204(2)
<i>c</i> (Å)	16.3809(12)	13.110(3)
$\alpha$ (°)	90	90
$\beta$ (°)	90	105.874(3)
$\gamma$ (°)	90	90
<i>V</i> (Å <sup>3</sup> )	2202.8(3)	1660.5(6)
<i>Z</i>	4	4
<i>T</i> (K)	100(2)	293(2)
$\rho_{\text{calcd}}$ (g cm <sup>-3</sup> )	1.626	1.748
$\mu$ (mm <sup>-1</sup> )	1.108	1.238
<i>F</i> (000)	1096	896
Crystal size (mm)	0.24 x 0.20 x 0.18	0.38 x 0.37 x 0.25
$\theta$ Range (°)	2.49 – 26.02	2.58 – 28.30
<i>h</i> / <i>k</i> / <i>l</i>	–16, 16/ –12, 12/ –20, 20	–17, 17/ –13, 13/ –17, 17
Reflection collected	18947	9371
Unique reflect., [ <i>R</i> <sub>int</sub> ]	2176 [ 0.0327]	2006 [0.0621]
Goodness of fit	1.130	1.079
<i>R</i> <sub><i>I</i></sub> [ <i>I</i> > 2σ( <i>I</i> )]	0.0391	0.0322
<i>wR</i> <sub>2</sub>	0.0928	0.0866

## 4.4 Crystal structure

### 4.4.1 Crystal structure of Ni(dafone)<sub>2</sub>(NCS)<sub>2</sub> (1)

Molecular diagram of the complex is shown in Figure. 4.1. The octahedral Ni(II) centre is located on a special position. Two dafone ligands chelate in cis-mode with an average Ni-N distance of 2.176 Å. The ambidentate ligand NCS<sup>−</sup> coordinates through the hard end ie through the nitrogen atom. The average Ni-N<sub>NCS</sub> distance is 2.002 Å. Ni-NCS bond distances are slightly shorter than the Ni-N distances of chelating dafone ligands. Coming to the crystal packing, molecules form two dimensional networks by a S1...O1 (3.118 Å) contact. A C2-H2...O1 contact further develops these 2-dimensional networks into 3-dimensional porous [4, 4] networks (Figure 4.2).

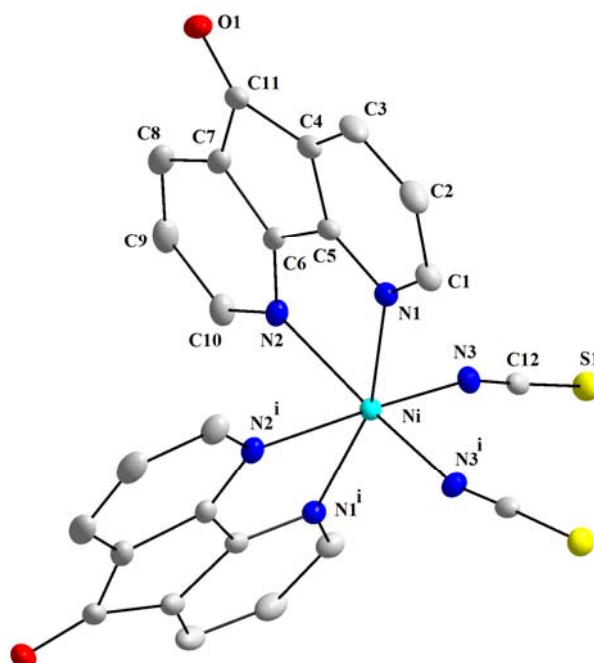


**Figure 4.1.** Thermal ellipsoid plot of the coordination environment of the complex molecules **1**: Atoms are represented as 50% probability ellipsoids and ring hydrogen's have been omitted for clarity. Symmetry code: (i)  $-x, y, -z+1/2$ .

**Table 4.2** Selected bond lengths [ $\text{\AA}$ ] and angles [ $^\circ$ ] for  $\text{Ni}(\text{dafone})(\text{NCS})_2$  (**1**)<sup>a</sup>

Ni-N(1)	2.162(2)	Ni-N(2)	2.190(2)	Ni-N(3)	2.002(2)
N(1)-Ni-N(2)	82.12(8)	N(1)-Ni-N(1)#1	163.8(1)	N(2)-Ni-N(2)#1	87.7(11)
N(1)-Ni-N(3)	90.21(8)	N(1)-Ni-N(2)#1	86.18(8)	N(2)-Ni-N(3)#1	89.30(8)
N(2)-Ni-N(3)	171.9(8)	N(1)-Ni-N(3)#1	100.8(1)	a #1 $-x, y, -z+1/2$	



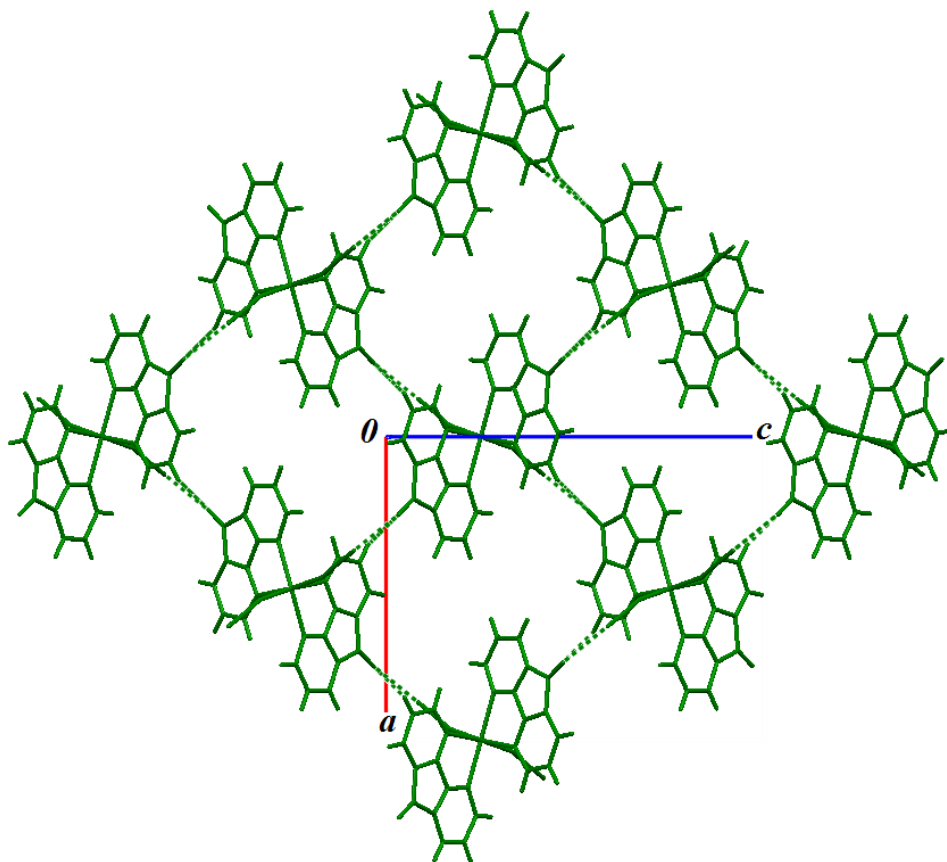


**Figure 4.2.** View of (4,4) networks of **1** formed by S...O and C-H...O contacts, with rectangular voids down the *b* axis.

The voids are blocked by a two-fold parallel interpenetration of identical networks (Figure 4.3). The adjacent nets are connected by  $\pi$ -stacking interactions (3.305–3.487 Å). Of late, interpenetrating networks<sup>18</sup> are studied more extensively in crystal engineering of coordination polymers and metal organic frameworks.

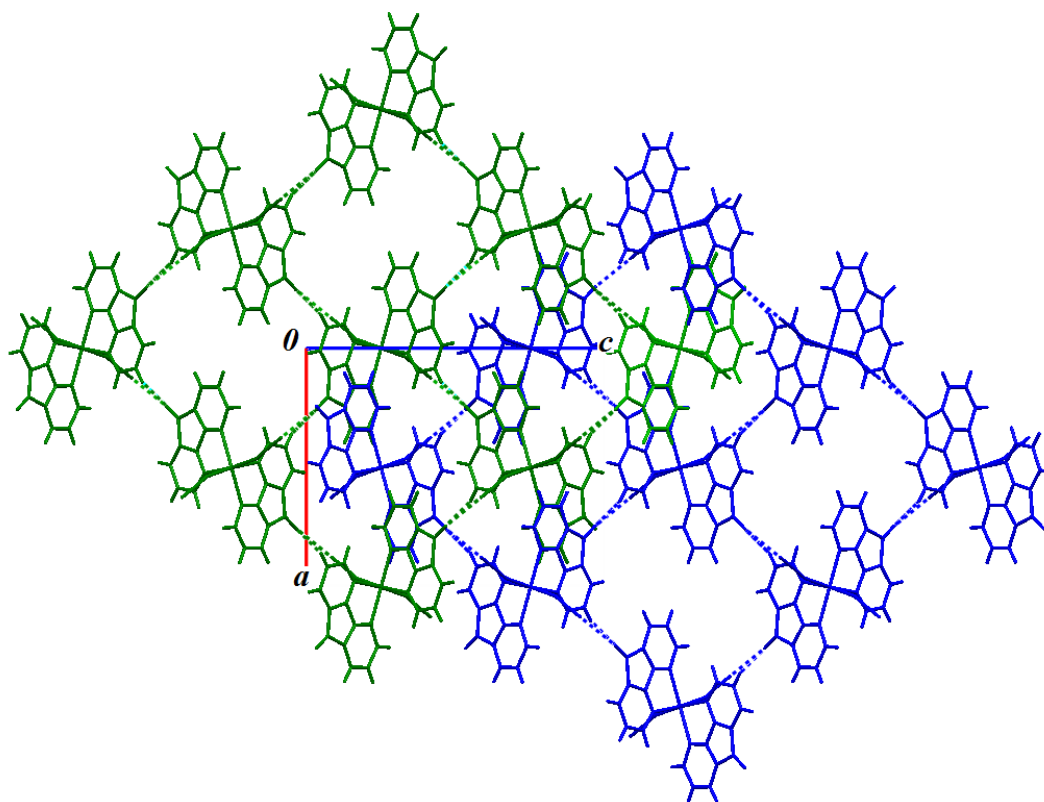


**Figure 4.3.** Two-fold parallel interpenetrating (4,4) networks of **1**.

#### 4.4.2 Crystal structure of $[\text{Ni}(\text{dafone})(\text{H}_2\text{O})_4](\text{NO}_3)_2$ (**2**)

The cation in **2** is situated on a crystallographic special position. The cation (Figure 4.4) has distorted octahedral structure with dafone ligand and two coordinated water molecules in the equatorial plane. The axial directions are filled by two water molecules. The in-plane

average bond distance for Ni-N<sub>dafone</sub> is 2.156 Å and for Ni-O<sub>water</sub> is 2.059 Å. The axial Ni-O<sub>water</sub> average distance is 2.041 Å.

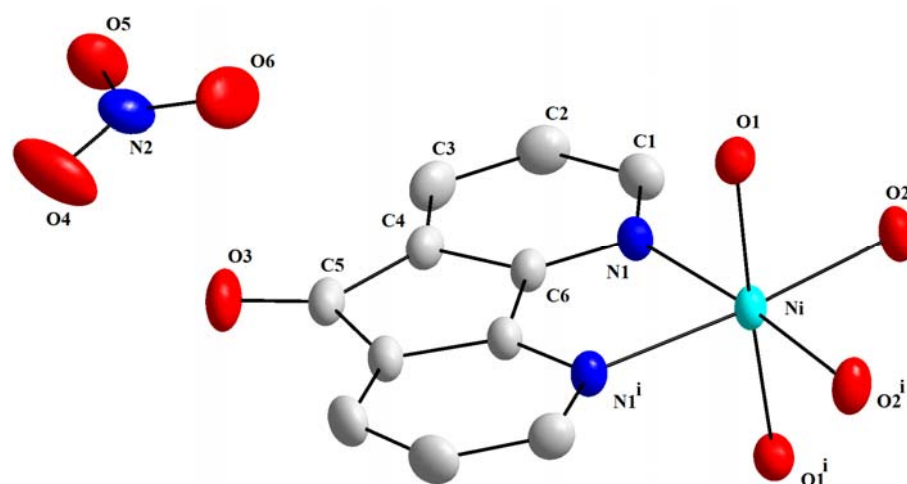
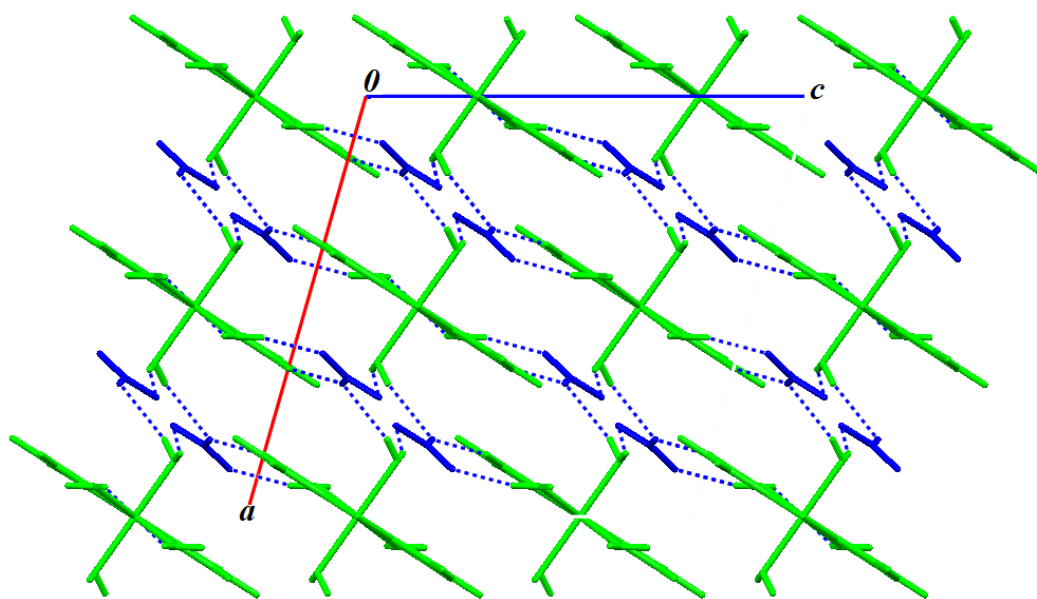


**Figure 4.4.** Thermal ellipsoid plot of the coordination environment of the complex molecules **2**: Atoms are represented as 50% probability ellipsoids and ring hydrogen's have been omitted for clarity. Symmetry code: (i)  $-x, y, -z+1/2$

**Table 4.3** Selected bond lengths [Å] and angles [°] for [Ni(dafone)(H<sub>2</sub>O)<sub>4</sub>](NO<sub>3</sub>)<sub>2</sub> (**2**)<sup>a</sup>

Ni-N(1)	2.156(2)	Ni-O(1)	2.041(2)	Ni-O(2)	2.059(1)
O(1)-Ni-O(2)	87.69(6)	O(1)-Ni-N(1)#1	89.89(6)	O(2)-Ni-O(2)#1	90.47(9)
O(1)-Ni-N(1)	92.07(6)	O(2)-Ni-N(1)#1	175.37(5)	O(2)#1-Ni-N(1)	175.37(5)
O(1)#1-Ni-O(2)	90.47(6)	O(1)-Ni-O(1)#1	177.39(7)	O(2)#1-Ni-N(1)#1	93.50(6)
N(1)#1-Ni-N(1)	82.63(8)	O(2)-Ni-N(1)	93.50(6)	a #1 $-x, y, -z+1/2$	

The complex forms 3-dimensional network with help of various hydrogen bonds (Table 4.4). A view of the hydrogen bonded networks down the  $b$  axis has given in Figure. 4.5.



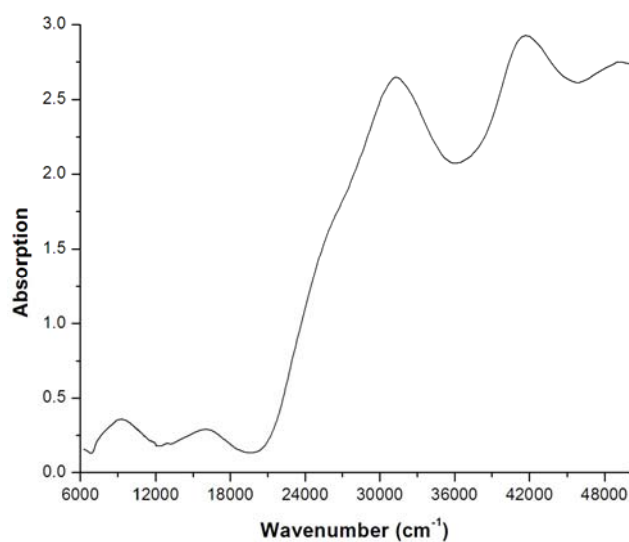
**Figure 4.5.** A view of hydrogen bonded networks of complex **2** down the  $b$  axis

Table 4.4 Hydrogen bonding parameters for  $[\text{Ni}(\text{dafone})(\text{H}_2\text{O})_4](\text{NO}_3)_2$  (**2**).

Donor-H...acceptor	D-H (Å)	H...A (Å)	D...A (Å)	D - H...A (°)	Symmetry code
O(2)-H(21)...O(5)	0.80(2)	2.12(3)	2.849(3)	151(4)	1/2-x, 1/2-y, -z
O(1)-H(12)...O(6)	0.76(2)	2.14(2)	2.856(3)	157(2)	
O(1)-H(11)...O(4)	0.766(18)	2.160(19)	2.898(2)	162(3)	1/2-x, 1/2+y, 1/2-z
O(2)-H(22)...O(3)	0.79(2)	2.23(3)	2.975(2)	158(4)	x, 1+y, z
O(1)-H(11)...O(5)	0.766(18)	2.42(2)	3.071(3)	143(2)	1/2-x, 1/2+y, 1/2-z
O(1)-H(12)...O(4)	0.76(2)	2.40(2)	3.076(2)	148(2)	

## 4.5 Electronic spectra

**4.5.1 Electronic spectrum of Ni(dafone)<sub>2</sub>(NCS)<sub>2</sub> (1):** Diffuse reflectance spectrum of **1** is shown in Figure 4.6. Two broad bands at 9310 cm<sup>-1</sup>, 16077 cm<sup>-1</sup> are due to d-d transitions as expected for six coordinate Nickel(II) complexes.<sup>19, 20</sup> The bands at 27624 cm<sup>-1</sup>, 31250 cm<sup>-1</sup> and 41667 cm<sup>-1</sup> are ligand centered transitions.



**Figure 4.6.** Diffuse reflectance spectrum of **1**

#### 4.5.2. Electronic spectrum of $[\text{Ni}(\text{dafone})(\text{H}_2\text{O})_4](\text{NO}_3)_2$ (**2**)

Diffuse reflectance spectrum of **2** is shown in Figure 4.7 Two broad bands at  $8976\text{ cm}^{-1}$  and  $15432\text{ cm}^{-1}$  are due to d-d transitions as expected for six coordinate nickel(II) complexes. The bands at  $28409\text{ cm}^{-1}$ ,  $31250\text{ cm}^{-1}$  and  $42016\text{ cm}^{-1}$  are ligand centered transitions.

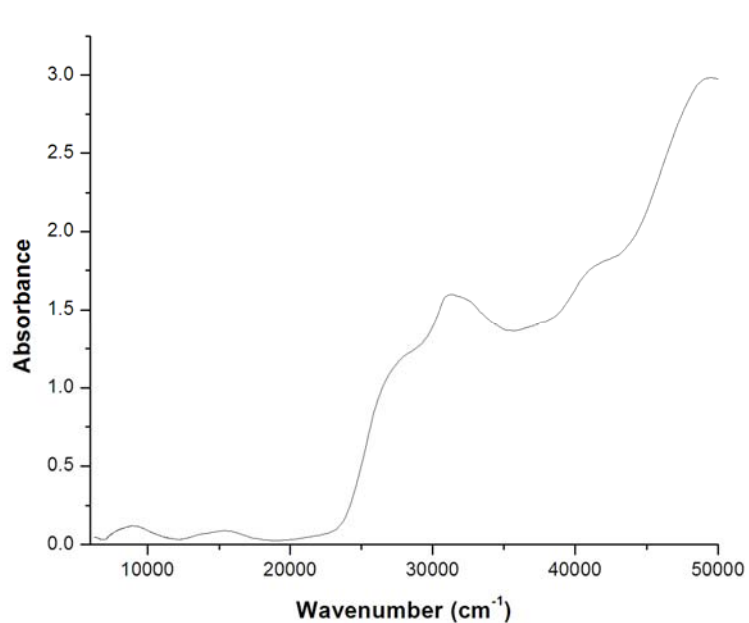


**Figure 4.7.** Diffuse reflectance spectrum of **2**

#### 4.6 Conclusion

Two new complexes of Ni(II) were synthesised and structurally characterised. Ambidentate ligand NCS has coordinated to Ni(II) through the hard end *ie* through the N atom. Intermolecular S...O contacts play a major role in the network formation. Structure **1** forms 2-fold parallel interpenetrating network. Structure **2** forms 3-dimensional networks with the help various hydrogen bond interactions.

#### 4.7 References

1. Henderson Jr. L. J.; Fronczek, F. R.; Cherry, W. R. *J. Am. Chem. Soc.* **1984**, *106*, 5876.
2. Pyle, M.; Rahman, R.; Meshoyrer, J. P.; Kumar, C. V.; Turro, N. J.; Barton, J. K. *J. Am. Chem. Soc.* **1989**, *111*, 3051.
3. Menon, S.; Balagopalakrishna, C.; Rajasekharan, M. V.; Ramakrishna, B. L. *Inorg. Chem.* **1994**, *33*, 950.
4. Balagolalakrishna, C.; Rajasekharan, M. V.; Bott, S.; Atwood, J. L.; Ramakrishna, B. L. *Inorg. Chem.* **1992**, *31*, 2843.
5. Menon, S.; Rajasekharan, M. V. *Inorg. Chem.* **1997**, *36*, 4983.

6. Menon, S.; Rajasekharan. M. V. *Polyhedron* **1998**, *17*, 2463.
7. Miao, S.; Kang, H.; Du, C.; Ji. B. *X-Ray Struct. Anal. Online*, **2006**, *22*, 45.
8. Lu, Z.; Duan, C.; Tian, Y.; You, X. *Inorg. Chem.* **1996**, *35*, 2253.
9. Wang, Y.; Jackman, D. C.; Woods, C.; Rillema, D. P. *J. Chem. Crystal.* **1995**, *25*, 549.
10. D. E. Marx, A. J. Lees, *Inorg. Chem.* **1987**, *26*, 620.
11. G. Jaouen. *Bioorganometallics: Biomolecules, Labeling, Medicine*, Wiley-VCH, Weinheim (2006).
12. (a) Dakternieks, D. A.Orlandini, D.; Sacconi, L. *Inorg. Chim. Acta* **1978**, *29*, L205. (b) Yin, L.-H.; Bu, P.-Y. Cheng, P.; Li, J.; Yan, S.-P.; Jiang, Z.-H.; Liao, D.-Z. *J. Coord. Chem.* **2002**, *55*, 537. (c) Wen, D.-C.; Liu, S.-X.; Lin, M. *J. Mol. Struct.* **2008**, *876*, 154. (d) Patel, R. N.; Singh, N.; Gundla, V. L. N. *Polyhedron* **2007**, *26*, 757. (e) Calatayud, M. L.; Sletten, J.; Castro, I.; Julve, M.; Seitz, G.; Mann, K. *Inorg. Chim. Acta* **2003**, *353*, 159. (f) Wu, A.-Q.; Zheng, F.-K.; Guo, G.-C.; Huang, J.-S. *Acta Cryst.* **2004**, *E60*, m373. (g) Zhao, S.-M.; Wu, T.-X. *Acta Cryst.* **2005**, *E61*,



- m2544. (h) Freire, E.; Baggio, S.; Baggio, R.; Suescun, L. *Acta Cryst.* **1999**, C55, 1780. (i) Ferbinteanu, M.; Cimpoesu, F.; Andruh, M.; Rochon, F. D. *Polyhedron*, **1998**, 17, 3671. (i) Travnicek, Z.; Pastorek, R.; Slovak, V. *Polyhedron*, **2008**, 27, 411. (j) Gandara, F.; Fortes-Revilla, C.; Snejko, N.; Gutierrez-Puebla, E.; Iglesias, M.; Monge, M. A. *Inorg. Chem.* **2006**, 45, 9680. (k) Zhong, H.; Zeng, X.-R.; Luo, Q.-Y. *Acta Cryst.* **2006**, E62, m3429. (l) Wu, H.-H.; Lian, F.-Y.; Yuan, D.-Q.; Hong, M.-C. *Acta Cryst.* **2007**, E63, m67.
13. (a) Cocker, T. M.; Bachman, R. E. *Chem. Commun.* **1999**, 875. (b) Hoberg, H.; Herrera, A. *Angew. Chem., Int. Ed.* **1981**, 20, 876. (c) Rodriguez-Martin, Y.; Lorenzo-Luis, P. A.; Gili, P.; Ruiz-Perez, C. *J. Coord. Chem.* **2003**, 56, 181. (d) Chesnut, D. J.; Haushalter, R. C.; Zubieta, J. *Inorg. Chim. Acta* **1999**, 292, 41. (e) Freire, E.; Baggio, S.; Baggio, R.; Suescun, L. *Acta Cryst.* **1999**, C55, 1780. (f) Ferbinteanu, M.; Cimpoesu, F.; Andruh, M.; Rochon, F. D. *Polyhedron* **1998**, 17, 3671. (g) Cabaleiro, S.; Castro, J.; Vazquez-Lopez, E.; Garcia Vazquez, J. A.; Romero, J.; Sousa, A. *Polyhedron* **1999**, 18, 1669. (h) Healy, P. C.; Patrick, J. M.; White, A. H. *Aust. J. Chem.* **1984**, 37, 921. (i) Kopel, P.; Travnicek, Z.; Marek, J.; Mrozinski, J. *Polyhedron* **2004**, 23, 1573. (j) Tadokoro, M.;

- Kanno, H.; Kitajima, T.; Shimada-Umemoto, H.; Nakanishi, N.; Isobe, K.; Nakasuji, K. *Proc. Nat. Acad. Sci.* **2002**, *99*, 4950. (k) Ruiz-Perez, C.; Luis, P. A. L.; Lloret, F.; Julve, M. *Inorg. Chim. Acta* **2002**, *336*, 131. (l) Yao, J.-C.; Yao, F.-J.; Guo, J.-B.; Huang, W. Gou, S.-H. *Chin. J. Struct. Chem.* **2007**, *26*, 541. (m) Liu, X.-P.; Zhang, C. *Acta Cryst.* **2007**, *E63*, m3063. (n) Walmsley, F.; Pinkerton, A. A.; Walmsley, J. A. *Polyhedron* **1989**, *8*, 689. (o) Grirrane, A.; Pastor, A.; Ienco, A.; Mealli, C. Galindo, A. *J. Chem. Soc., Dalton Trans.* **2002**, 3771. (p) Baruah, A. M.; Karmakar, A. Baruah, J. B. *Polyhedron* **2007**, *26*, 4479. (q) Yu, M.; Liu, S.-X.; Xie, L.-H.; Cao, R.-G.; Ren, Y.-H. *Acta Cryst.* **2007**, *E63*, m2110. (r) Plater, Foreman, M. R. St. J.; Skakle, J. M. S.; Howie, R. A. *Inorg. Chim. Acta* **2002**, *332*, 135.
14. Xiong, R.-G.; Zuo, J.-L.; Xu, E.-J.; You, X.-Z.; Huang, X.-Y *Acta Cryst.*, **1996**, *52*, 521.
15. SAINTPLUS, Bruker AXS Inc. Madison, Wisconsin, USA.
16. Sheldrick, G.M. SADABS Programm for Empirical Absorption Correction, University of Gottingen, Germany, **1996**.
17. M. Sheldrick, *Acta Cryst.* **2008**, *A64*, 112.

18. Batten, S. R.; Robson, R. *Angew. Chem.; Int. Ed.* **1998**, 37, 1461.
19. Hay, R.W.; Jeragh, B.; Ferguson, G.; Kaitnar, B.; Ruhl, B. L. *J. Chem. Soc. Dalton Trans.* **1982**, 1531.
20. Bembi, R.; Singh, R.; Aftab, S.; Roy, T. G.; Jhanjee, A. K. *J. Coord. Chem.* **1985**, 14, 119.



## CHAPTER V

### Nickel complexes of 1,10-phenanthroline ligand

#### 5.1 Introduction

Nickel plays numerous roles in the biology of microorganisms and plants, the main constituent of various enzymes and coenzymes like carbon monoxide dehydrogenase<sup>1</sup>, superoxide dismutase<sup>2</sup> and glyoxalase.<sup>3</sup> Superoxide dismutases are metalloenzymes which disproportionate the  $O_2^-$  radical into molecular oxygen. The superoxide radical is an inevitable by-product of aerobic metabolism which if not eliminated may cause significant cellular damage. To avoid such a harmful consequence, all oxygen metabolising organisms have metalloenzymes known as superoxide dismutases (SODs). X-ray crystallographic studies<sup>4</sup> of NiSODs from *streptomyces* have shown that the active site is mononuclear. It exhibit a square pyramidal coordination in the oxidized form (NiSOD<sub>ox</sub>) and square planar coordination in reduced form ((NiSOD<sub>red</sub>)). Even though many mononuclear complexes of bpy<sup>5</sup> and phen<sup>6</sup> have been structurally characterised, only one structure<sup>7</sup> was reported with dafone. Due to intrinsic interest for the various structural varieties of mononuclear nickel complexes, we have synthesised two complexes.

## 5.2. Experimental

### 5.2.1 Reagents

All chemicals were purchased from Ranbaxy chemicals and used without further purification.

### 5.2.2 Synthesis

**Preparation of  $[\text{Ni}(\text{phen})(\text{H}_2\text{O})_3\text{Cl}]\text{Cl}\cdot\text{H}_2\text{O}$  (1):**  $[\text{Ni}(\text{NO}_3)_2](\text{H}_2\text{O})_6$  (0.290 g, 1.00 mmol) and 1,10 phenanthroline (0.200 g, 1.01 mmol) were dissolved in concentrated HCl (2 mL) by stirring. The green coloured solution was filtered and kept at room temperature for 2 days. Bluish coloured crystalline precipitate was obtained. One blue coloured crystal was carefully picked for X-ray study. Yield: 0.10 g (0.26 mmol, 26 %) Anal. Cald:  $\text{C}_{12}\text{H}_{16}\text{Cl}_2\text{N}_2\text{NiO}_4$  (M. Wt. 381.88) C, 37.74; H, 4.22; N, 7.34. Found: C, 37.85; H, 4.16; N, 7.45. Important IR absorptions (KBr disk,  $\text{cm}^{-1}$ ): 3433, 1626, 1582, 1421, 1140, 1103, 846, 725, 443, 424.

**Preparation of  $[\text{Ni}(\text{phen})(\text{H}_2\text{O})_3\text{Br}]\text{Br}$  (2) and  $[\text{Ni}(\text{phen})_3](\text{Br}_3)_2\cdot\text{Br}_2$  (3):**  $[\text{Ni}(\text{NO}_3)_2](\text{H}_2\text{O})_6$  (0.290 g, 1.00 mmol) and 1,10 phenanthroline (0.200 g, 1.01 mmol) were dissolved in 1:1 mixture of acetonitrile and methanol. 48 % hydrogen bromide (1.0 mL) solution was added to the above green coloured solution and up on adding the colour of the solution was changed to violet blue. It was filtered and kept outside at room temperature for crystallization. Close examination of the sample revealed the presence of two types of crystals. Vast majority (95 %) of the crystals were blue in colour (2) and

remaining crystals were red in colour (**3**). Yield: 0.385g (0.85 mmol, 85 %) Anal. Calcd: C, 31.83; H, 3.12; N, 6.19. Found: C, 31.85; H, 3.16; N, 6.45. Important IR absorptions (KBr disk,  $\text{cm}^{-1}$ ): 3347, 1757, 1638, 1599, 1574, 1476, 1418, 1327, 1169, 104, 1028, 817, 768, 735, 654, 556, 417.

### 5.3. Measurements

IR spectra were obtained with a Shimadzu FT-IR 8000 spectrometer. Elemental analysis was obtained using a FLASH EA 1112 SERIES CHNS analyzer.

#### 5.3.1 Crystallographic data collection and structure determination

Data were collected on a Bruker SMART APEX CCD X-ray diffractometer using graphite monochromated Mo  $K\alpha$  radiation. The data were reduced using SAINTPLUS<sup>8</sup>, and multiscan absorption corrections using SADABS<sup>9</sup> were applied. The structures were solved using SHELXS-97 and refined using SHELXL-97.<sup>10</sup> All ring hydrogen atoms were assigned on the basis of geometrical considerations and were allowed to ride upon the respective carbon atoms. All water hydrogen atoms were located from the difference Fourier maps and bond length constraints were applied. Crystal data are in Table 5.1 and 5.4 important interatomic distances and angles in Table 5.2, 5.3 and 5.5.

Table 5.1 Crystallographic data and structure refinement for **1** and **2**

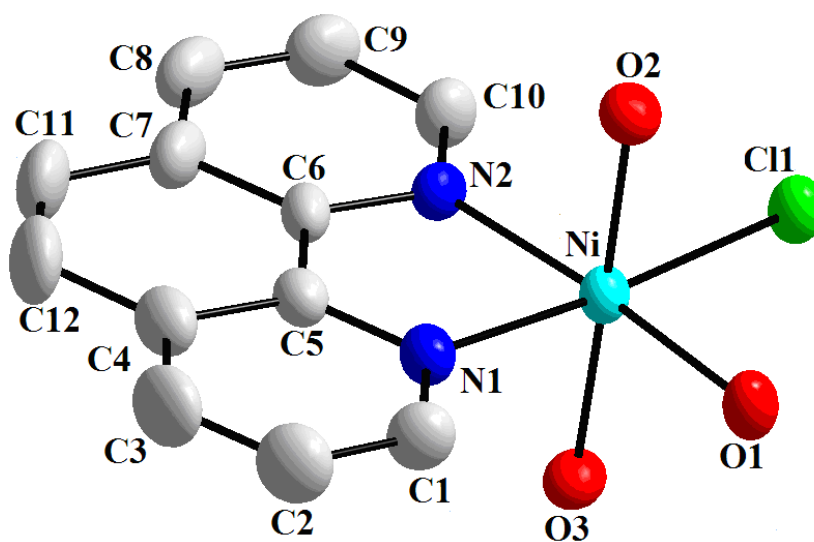
	<b>1</b>	<b>2</b>
Formula	C <sub>12</sub> H <sub>16</sub> Cl <sub>2</sub> N <sub>2</sub> NiO <sub>4</sub>	C <sub>12</sub> H <sub>14</sub> Br <sub>2</sub> N <sub>2</sub> NiO <sub>3</sub>
Formula weight	381.88	452.78
Crystal system	Monoclinic	Monoclinic
Space group	<i>P</i> 2 <sub>1</sub> / <i>c</i>	<i>P</i> 2 <sub>1</sub> / <i>c</i>
<i>a</i> (Å)	7.5921(15)	12.0650(8)
<i>b</i> (Å)	12.361(2)	9.2840(6)
<i>c</i> (Å)	16.996(3)	14.0541(9)
$\beta$ (°)	103.863(7)	107.3530(10)
<i>V</i> (Å <sup>3</sup> )	1548.5(5)	1502.57(17)
<i>Z</i>	4	4
<i>T</i> (°C)	298(2)	298(2)
$\lambda$ (Å)	0.71073	0.71073
<i>D</i> <sub>calc</sub> (g cm <sup>-3</sup> )	1.638	2.002
$\mu$ (mm <sup>-1</sup> )	1.613	6.616
<i>F</i> (000)	784	888
Crystal size (mm)	0.28 x 0.24 x 0.18	0.22 x 0.20 x 0.18
$\theta$ Range (°)	2.06 – 24.99	2.10 – 24.74
<i>h</i> / <i>k</i> / <i>l</i>	–9, 9/ –14, 14/ –20, 20	–16, 16/ –12, 12/ –18, 18
Reflection collected	14288	16894
Unique reflect., [R <sub>int</sub> ]	2714	3524
Goodness of fit on F <sup>2</sup>	1.150	1.057
<i>R</i> <sub>I</sub> [I > 2σ(I)]	0.0519	0.0308
<i>wR</i> <sub>2</sub> (all data)	0.1373	0.0843



## 5.4 Crystal Structure

### 5.4.1 Crystal structure of $[\text{Ni}(\text{phen})(\text{H}_2\text{O})_3\text{Cl}]\text{Cl}\cdot\text{H}_2\text{O}$ (**1**)

The molecular structure of  $[\text{Ni}(\text{phen})(\text{H}_2\text{O})_3\text{Cl}]\text{Cl}(\text{H}_2\text{O})$  (**1**) is shown in Figure 5.1. The structure consists of one water of hydration a chloride ion and a complex cation. The complex cation has an octahedral nickel centre coordinated by one 1, 10-phenanthroline, three water molecules and a chloride anion, with the chloride ion in the equatorial plane. The average Ni-N distance is 2.081 Å, which is comparable to the reported Ni-Phen complexes.<sup>6</sup> The bite of the phenanthroline (80.54°) is also typical. The Ni-Cl distance is 2.428 Å as expected. The average Ni-O<sub>water</sub> distance is 2.064 Å.

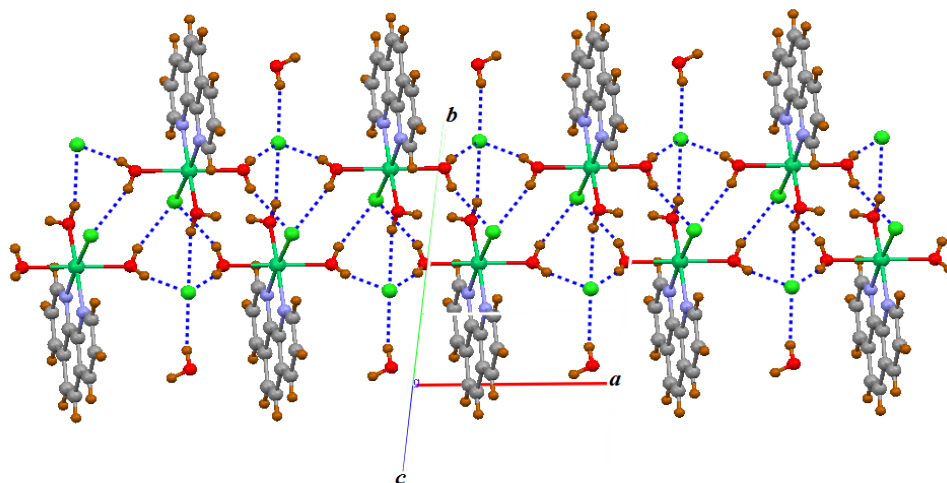


**Figure 5.1.** Thermal ellipsoid plot of the coordination environment of the complex molecules **1**: Atoms are represented as 50% probability ellipsoids and hydrogen atoms have been omitted for clarity.

**Table 5.2** Selected bond lengths [ $\text{\AA}$ ] and angles [ $^\circ$ ] for  $[\text{Ni}(\text{phen})(\text{H}_2\text{O})_3\text{Cl}]\text{Cl}\cdot\text{H}_2\text{O}$  (**1**)

Ni-N(1)	2.089(3)	Ni-O(1)	2.072(3)	Ni-O(3)	2.058(3)
Ni-N(2)	2.072(3)	Ni-O(2)	2.061(3)	Ni-Cl(1)	2.4280(11)
O(1)-Ni-O(2)	89.12(12)	O(2)-Ni-O(3)	177.80(11)	N(1)-Ni-Cl(1)	175.05(10)
O(1)-Ni-O(3)	90.11(12)	O(2)-Ni-N(1)	88.50(12)	N(2)-Ni-Cl(1)	94.66(10)
O(1)-Ni-N(1)	92.38(13)	O(2)-Ni-N(2)	90.22(12)	N(1)-Ni-N(2)	80.52(13)
O(1)-Ni-N(2)	172.89(12)	O(3)-Ni-N(1)	89.47(12)	O(2)-Ni-Cl(1)	90.37(8)
O(1)-Ni-Cl(1)	92.42(8)	O(3)-Ni-N(2)	90.28(12)	O(3)-Ni-Cl(1)	91.72(9)

Coming to the crystal packing, molecules are assembled into one-dimensional chain by O-H...Cl interactions (2.284-2.482  $\text{\AA}$ ) (Figure 5.2). However an O1-H1A...O4 (1.889  $\text{\AA}$ ) interaction interconnect this one-dimensional chains into a three-dimensional networks.

**Figure 5.2.** One-dimensional chains of **1** by O-H...Cl interactions.

#### 5.4.2 Crystal structure of [Ni(phen)(H<sub>2</sub>O)<sub>3</sub>Br]Br (2)

The molecular structure of [Ni(phen)(H<sub>2</sub>O)<sub>3</sub>Br]Br (**2**) is shown in figure 5.3. The structure consists of bromide ion and a complex cation. The complex cation has an octahedral nickel centre coordinated by one 1, 10-phenanthroline, three water molecules and a bromide anion, the bromide coordinating from the axial position. The average Ni-N distance is 2.065 Å which is comparable to the reported Ni-phen complexes.<sup>6</sup> The bite of the phenanthroline (80.72°) is also typical. The average Ni-O<sub>water</sub> distance is 2.071 Å. The Ni-Br1 distance is 2.586 Å as expected. Coming to the crystal packing, molecules are assembled into a two-dimensional networks by various O-H...Br interactions (2.455-2.610 Å) (Figure 5.4).

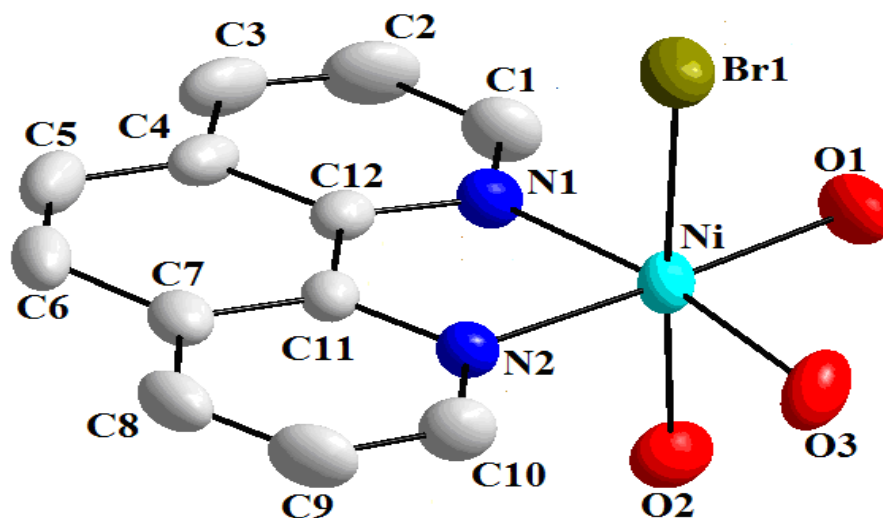


**Figure 5.3.** Thermal ellipsoid plot of the coordination environment of the complex molecules **2**: Atoms are represented as 50% probability ellipsoids and hydrogen atoms have been omitted for clarity.

**Table 5.3** Selected bond lengths [ $\text{\AA}$ ] and angles [ $^\circ$ ] for  $[\text{Ni}(\text{phen})(\text{H}_2\text{O})_3\text{Br}]\text{Br}$  (**2**)

Ni-N(1)	2.066(2)	Ni-O(1)	2.055(2)	Ni-O(3)	2.061(2)
Ni-N(2)	2.063(2)	Ni-O(2)	2.097(2)	Ni-Br(1)	2.5857(5)
O(1)-Ni-O(2)	88.29(11)	N(1)-Ni-O(2)	91.00(10)	O(2)-Ni-Br(1)	176.66(7)
O(1)-Ni-O(3)	91.78(11)	N(1)-Ni-N(2)	80.72(9)	O(3)-Ni-Br(1)	92.77(8)
O(1)-Ni-N(1)	96.21(10)	N(2)-Ni-O(2)	92.11(10)	N(1)-Ni-Br(1)	91.89(7)
O(1)-Ni-N(2)	176.91(10)	O(3)-Ni-O(2)	84.61(10)	N(2)-Ni-Br(1)	90.01(6)
O(1)-Ni-Br(1)	89.73(8)	O(3)-Ni-N(2)	91.31(10)	O(3)-Ni-N(1)	170.77(10)

$\pi$ -stacking interactions (3.310-3.477  $\text{\AA}$ ) build these two-dimensional networks into a three dimensional networks.

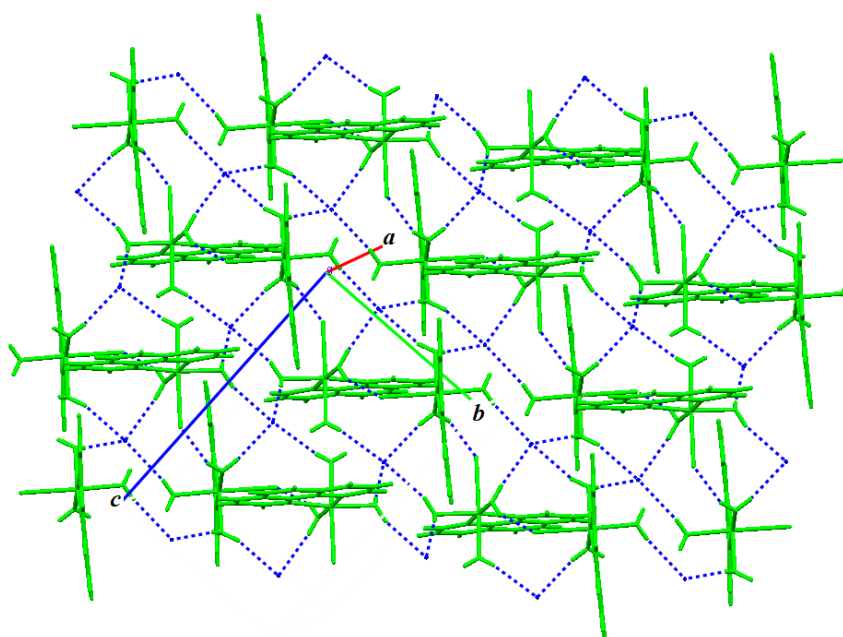
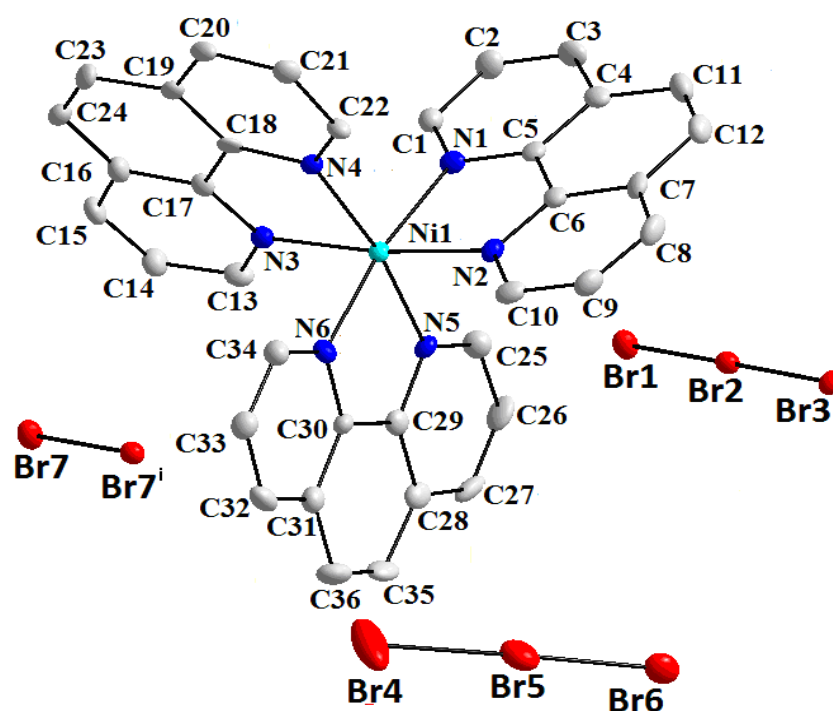
**Figure 5.4.** Two-dimensional networks of **2** formed by O-H...Br interactions.

Table 5.4 Crystallographic data and structure refinement for **3**

Formula	C <sub>36</sub> H <sub>24</sub> Br <sub>7</sub> N <sub>6</sub> Ni
Formula weight	1158.69
Crystal system	Triclinic
Space group	$P\bar{1}$
$a$ (Å)	12.5469(7)
$b$ (Å)	13.0834(7)
$c$ (Å)	13.1198(7)
$A$	79.0590(10)
$\beta$ (°)	65.1990(10)
$\Gamma$	72.1720(10)
$V$ (Å <sup>3</sup> )	1856.48(17)
$Z$	2
$T$ (K)	100(2)
$\lambda$ (Å)	0.71073
$D_{calc}$ (g cm <sup>-3</sup> )	2.073
$\mu$ (mm <sup>-1</sup> )	8.092
$F(000)$	1110
Crystal size (mm)	0.28 x 0.20 x 0.18
$\theta$ Range (°)	1.64 – 24.00
$h/k/l$	–14, 14/ –14, 14/ –15, 15
Reflection collected	16463
Unique reflect., [R <sub>int</sub> ]	5801, 0.0351
Goodness of fit on F <sup>2</sup>	1.056
$R_1$ [I > 2σ(I)]	0.0485
$wR_2$ (all data)	0.1325

### 5.4.3 Crystal structure of $[\text{Ni}(\text{phen})_3](\text{Br}_3)_2 \cdot \text{Br}_2$ (**3**)

Molecular diagram of the complex **3** is shown in figure 5.5.  $[\text{Ni}(\text{phen})_3]^{2+}$  entities exhibit a quasi  $D_3$  symmetry. The six-coordinated nitrogen atoms of three phen ligands form a distorted octahedron around the Ni(II) ions (Figure 5.5). The average value of the Ni-N bond length is 2.085 Å, which is comparable to the reported structures.<sup>11</sup> Two of the Ni-N distances are notably longer than other four which was in agreement with the previously reported  $[\text{Ni}(\text{phen})_3]^{2+}$  structures.<sup>12</sup> The average bite angle of the phenanthroline ligand is 80.16°. The bite of



**Figure 5.5.** Thermal ellipsoid plot of the coordination environment of the complex molecules **3**: Atoms are represented as 50% probability ellipsoids and ring hydrogen's have been omitted for clarity.

the phenanthroline is also typical. Average Br-Br distance is 2.547 Å for the  $\text{Br}_3^-$  anions. The Br-Br distances are consistent with the previous reports.<sup>13</sup> The Br(1)-Br(2)-Br(3) angle is 177.97(6)° and Br(4)-Br(5)-Br(6) angle is 178.84(5)°. The Br(7)-Br(#7) bond length is 2.336(2) Å. The Br-Br lengths are sensitive to the coordination polarization effects and readily elongate from 2.284 Å in a non coordinated molecule.<sup>14</sup> The Br-Br bond length varied between (2.28-2.33 Å) in the weakly coordinating solvents like acetone, dioxane and methanol.<sup>15</sup> In the absence of significant polarization the dibromine can coordinate equally well with either end. Owing to the acceptor  $\sigma^*$ -orbital which is localised on both bromine centres dibromine has often be found in crystals to be symmetrically coordinated to a pair of donor molecules. In the present case dibromine is coordinated with  $\text{Br}_3^-$  ions on either side forming a centrosymmetric  $\text{Br}_8^{2-}$  ion (Figure 5.6). The Z-shaped ion has a high degree of planarity with a Br..Br distance of 3.09 Å (between the dibromine and tribromide units) and an angle of 79° at the Z-bend.

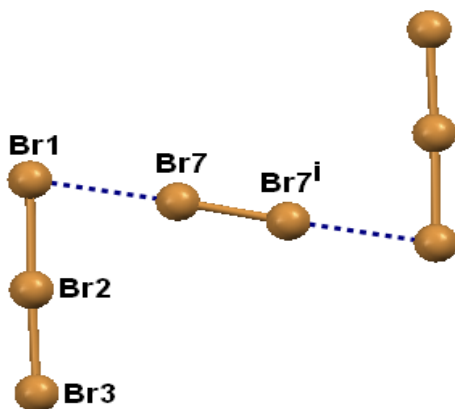


**Figure 5.6.** View of the  $\text{Br}_8^{2-}$  ion ( $i = -x, -y+1, -z+1$ ).

**Table 5.5** Selected bond lengths [Å] and angles [°] for [Ni(phen)<sub>3</sub>](Br<sub>3</sub>)<sub>2</sub>.Br<sub>2</sub>(**3**)

Ni(1)-N(1)	2.088(6)	Ni(1)-N(3)	2.104(6)	Ni(1)-N(5)	2.080(6)
Ni(1)-N(2)	2.072(6)	Ni(1)-N(4)	2.091(6)	Ni(1)-N(6)	2.076(6)
Br(1)-Br(2)	2.6174(19)	Br(4)-Br(5)	2.5977(11)	Br(7)-Br(7) <sup>i</sup>	2.3356(16)
Br(2)-Br(3)	2.4703(15)	Br(5)-Br(6)	2.5014(11)		
N(1)-Ni(1)-N(3)	80.3(2)	N(2)-Ni(1)-N(3)	172.6(2)	N(3)-Ni(1)-N(5)	93.2(2)
N(1)-Ni(1)-N(3)	95.7(2)	N(2)-Ni(1)-N(4)	94.3(2)	N(3)-Ni(1)-N(6)	91.3(2)
N(1)-Ni(1)-N(4)	92.9(2)	N(2)-Ni(1)-N(5)	93.3(2)	N(4)-Ni(1)-N(5)	170.9(2)
N(1)-Ni(1)-N(5)	93.3(2)	N(2)-Ni(1)-N(6)	93.3(2)	N(4)-Ni(1)-N(6)	93.8(2)
N(6)-Ni(1)-N(1)	171.0(2)	N(3)-Ni(1)-N(4)	79.6(2)	N(5)-Ni(1)-N(6)	80.6(2)
Br(1)-Br(2)-Br(3)	177.97(6)	Br(4)-Br(5)-Br(6)	178.84(5)	(i): -x, 1-y, 1-z	

The Br<sub>8</sub><sup>2-</sup> ion has been reported only once before in the crystal of diquinuclidinium bromide<sup>16</sup> which has a similar structure except for the obtuse angle of 107° at the Z-bend. In view of the presence of polybromide anions, a more appropriate formulation of Compound **3** is [Ni(phen)<sub>3</sub>] Br<sub>3</sub> 0.5Br<sub>8</sub>. Coming to the crystal packing C-H...Br (2.826-2.868 Å) interactions build the molecules into one-dimensional chains and  $\pi$ -stacking interaction (C23...C23, 3.316 Å) build these one-dimensional chains into two-dimensional networks (Figure 5.7).



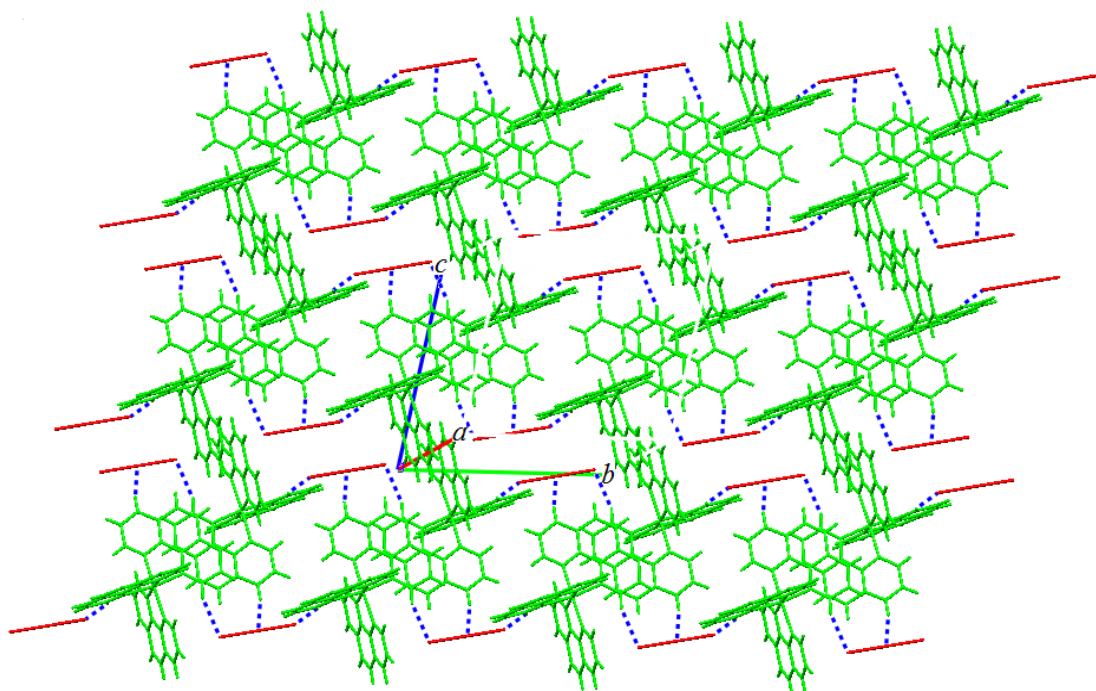


**Figure 5.7.** Two-dimensional networks of **3** formed by C-H...Br and  $\pi$ -stacking interactions.

## 5.5 Conclusion

Three new complexes of nickel 1,10-phenanthroline were synthesised. Lattice free  $\text{Br}^-$  and  $\text{Cl}^-$  anions extensively involve in hydrogen bonding with coordinated water molecules to form network structures for complexes **1** and **2**. The rarely observed polybromide ion  $\text{Br}_8^{2-}$  (previously reported only once) has been obtained in one crystal.

## 5.6 References

1. Jaouen, G. *Bioorganometallics: Biomolecules, Labeling and Medicine* **2006**, Wiley-VCH, Weinheim.
2. Szilagy, R. K.; Bryngelson, P. A.; Maroney, M. J.; Hedman, B.; Hodgson, K. O.; Solomon, E. I. *J. Am. Chem. Soc.* **2004**, *126*, 3018.
3. Thornalley, P. J. *Biochem. Soc. Trans.*, **2003**, *31*, 1343.
4. (a) Barondeau, D.P. Kassmann, C. J. Bruns, C. K.; Tainer, J. A. Getzoff, E. D. *Biochemistry* **2004**, *43*, 8038. (b) Wuerges, J. Lee, J. W.; Yim, Y.I.; Yim, H. S.; Kang, S. O.; Carugo, K. D. *Proc. Natl. Acad. Sci. USA*, **2004**, *101*, 8569.
5. (a) Dakternieks, D. A.Orlandini, D.; Sacconi, L. *Inorg. Chim. Acta* **1978**, *29*, L205. (b) Yin, L.-H.; Bu, P.-Y. Cheng, P.; Li, J.; Yan, S.-P.; Jiang, Z.-H.; Liao, D.-Z. *J. Coord. Chem.* **2002**, *55*, 537. (c) Wen, D.-C.; Liu, S.-X.; Lin, M. *J. Mol. Struct.* **2008**, *876*, 154. (d) Patel, R. N.; Singh, N.; Gundla, V. L. N. *Polyhedron* **2007**, *26*, 757. (e) Calatayud, M. L.; Sletten, J.; Castro, I.; Julve, M.; Seitz, G.; Mann, K. *Inorg. Chim. Acta* **2003**, *353*, 159. (e) Wu, A.-Q.; Zheng, F.-K.; Guo, G.-C.; Huang, J.-S. *Acta Cryst.* **2004**, *E60*, m373. (f) Zhao, S.-M.; Wu, T.-X. *Acta Cryst.* **2005**, *E61*, m2544. (g) Freire, E.; Baggio, S.; Baggio, R.; Suescun, L. *Acta Cryst.* **1999**, *C55*, 1780. (h) Ferbinteanu, M.; Cimpoesu, F.; Andruh, M.; Rochon, F. D. *Polyhedron*, **1998**, *17*, 3671. (i) Travnicek, Z.; Pastorek, R.;

- Slovak, V. *Polyhedron*, **2008**, 27, 411. (j) Gandara, F.; Fortes-Revilla, C.; Snejko, N.; Gutierrez-Puebla, E.; Iglesias, M.; Monge, M. A. *Inorg. Chem.* **2006**, 45, 9680. (k) Zhong, H.; Zeng, X.-R.; Luo, Q.-Y. *Acta Cryst.* **2006**, E62, m3429. (l) Wu, H.-H.; Lian, F.-Y.; Yuan, D.-Q.; Hong, M.-C. *Acta Cryst.* **2007**, E63, m67.
6. (a) Cocker, T. M.; Bachman, R. E. *Chem. Commun.* **1999**, 875. (b) Hoberg, H.; Herrera, A. *Angew. Chem., Int. Ed.* **1981**, 20, 876. (c) Rodriguez-Martin, Y.; Lorenzo-Luis, P. A.; Gili, P.; Ruiz-Perez, C. *J. Coord. Chem.* **2003**, 56, 181. (d) Chesnut, D. J.; Haushalter, R. C.; Zubieta, J. *Inorg. Chim. Acta.* **1999**, 292, 41. (e) Freire, E.; Baggio, S.; Baggio, R.; Suescun, L. *Acta Cryst.* **1999**, C55, 1780. (f) Ferbinteanu, M.; Cimpoesu, F.; Andruh, M.; Rochon, F. D. *Polyhedron* **1998**, 17, 3671. (g) Cabaleiro, S.; Castro, J.; Vazquez-Lopez, E.; Garcia Vazquez, J. A.; Romero, J.; Sousa, A. *Polyhedron* **1999**, 18, 1669. (h) Healy, P. C.; Patrick, J. M.; White, A. H. *Aust. J. Chem.* **1984**, 37, 921. (i) Kopel, P.; Travnicek, Z.; Marek, J.; Mrozinski, J. *Polyhedron* **2004**, 23, 1573. (j) Tadokoro, M.; Kanno, H.; Kitajima, T.; Shimada-Umemoto, H.; Nakanishi, N.; Isobe, K.; Nakasuji, K. *Proc. Nat. Acad. Sci.* **2002**, 99, 4950. (k) Ruiz-Perez, C.; Luis, P. A. L.; Lloret, F.; Julve, M. *Inorg. Chim. Acta* **2002**, 336, 131. (l) Yao, J.-C.; Yao, F.-J.; Guo, J.-B.; Huang, W. Gou, S.-H. *Chin. J. Struct. Chem.* **2007**, 26, 541. (m) Liu, X.-P.; Zhang, C. *Acta Cryst.* **2007**, E63, m3063. (n) Walmsley, F.; Pinkerton, A. A.;

- Walmsley, J. A. *Polyhedron* **1989**, 8, 689. (o) Griirane, A.; Pastor, A.; Ienco, A.; Mealli, C. Galindo, A. *J. Chem. Soc., Dalton Trans.* **2002**, 3771. (p) Baruah, A. M.; Karmakar, A. Baruah, J. B. *Polyhedron* **2007**, 26, 4479. (q) Yu, M.; Liu, S.-X.; Xie, L.-H.; Cao, R.-G.; Ren, Y.-H. *Acta Cryst.* **2007**, E63, m2110. (r) Plater, Foreman, M. R. St. J.; Skakle, J. M. S.; Howie, R. A. *Inorg. Chim. Acta.* **2002**, 332, 135.
7. Xiong, R. -G.; Zuo, J.-Z.; Xu, E.-J.; You, X.-Z.; Huang, X.-H. *Acta Cryst.* **1996**, C52, 521.
8. SAINTPLUS, Bruker AXS Inc. Madison, Wisconsin, USA.
9. Sheldrick, G.M. SADABS Programm for Empirical Absorption Correction, University of Gottingen, Germany, **1996**.
10. M. Sheldrick, *Acta Cryst.* **2008**, A64, 112.
11. (a) Frenz, B.A.; Ibers, J. A. *Inorg. Chem.* **1972**, 11, 1109. (b) Gillard, R. D.; Mitchell, S. H.; Robinson, W. T. *Polyhedron* **1989**, 8, 2649. (c) Abdel-Rahman, L.; Battaglia, L. P.; Rizzoli, C.; Sgarabotto, P. *J. Chem. Crystallogr.* **1995**, 25, 629. (c) Travnicek, Z.; Pastorek, R.; Sindelar, Z.; Klicka, R. Marek, J. *Polyhedron* **1995**, 14, 3627. (d) Decurtins, S. Schmalle, H. W.; Pellaux, R. Schneuwly, P. Hauser, A. *Inorg. Chem.* **1996**, 35, 1451. (e) Suescun, L. Mombru, A. W.; Mariezcurrena, R. A. *Acta Crystallogr.* **1999**, C55, 1991. (f) Walmsley, F. Pinkerton, A. A.; Walmsley, J. A. *Polyhedron* **1989**, 8, 689.

12. Norman, R. E.; Xie, M. *J. Coord. Chem.* **2004**, 57, 425.
13. Gall, B. L.; Conan, F.; Cosquer, N.; Kerbol, J. M.; Kubicki, M. M.; Vigieri, E.; Mest, Y. L.; Sala pala, J. *Inorg. Chim. Acta.* **2001**, 324, 300.
14. Alexandr, V.; Vasilyev, S.; Lindeman, V.; Kochi, J. K. *New J. Chem.*, **2002**, 26, 592.
15. (a) Hassel, O.; Strømme, K. O. *Acta Chem. Scand.*, **1959**, 13, 275. (b) Marstokk, K.-M.; Strømme, K. O. *Acta Crystallogr.*, Sect. B, **1968**, 24, 713. (c) Groth, P.; Hassel, O. *Acta Chem. Scand.*, **1964**, 18, 402. (d) Hassel, O.; Hvoslef, J. *Acta Chem. Scand.*, **1954**, 8, 873.
16. Robertson, K. N.; Bakshi, P. K.; Cameron, T. S.; Knop, O. *Z. anorg. allg. Chem.* **1997**, 104, 623.



## POSTERS AND WORKSHOPS

- (1) Presented a poster entitled Novel structures of Cu(II) and Ni(II) with 4,5,diazafluoren-9-one; kishore Babu, B.; Rajasekharan, M. V. at 11<sup>th</sup> National symposium on Modern Trends in inorganic Chemistry (MTIC-XI), IIT Delhi, December 8-10, (2005).
- (2) In house symposium presented a poster and oral entitled Novel structures of Cu(II) and Ni(II) with 4,5,diazafluoren-9-one; kishore Babu, B.; Rajasekharan, M. V. at University of Hyderabad, School of chemistry, Hyderabad, February 18, (2005).

## Manuscripts under preparation

- (1) Synthesis, structure, magnetic and DFT studies of tetranuclear distortion isomers of copper(II) complex with 4,5-diazafluoren-9-one; Kishore Babu, B.; Tuchuges, J.-P.; Rajasekharan, M. V.
- (2) Synthesis, structure, magnetic and DFT studies on binuclear copper(II) hydroxo-bridged acetonitrile solvated ion complex with 4,5,diazafluoren-9-one; Kishore Babu, B.; Tuchuges, J.-P.; Rajasekharan, M. V.
- (3) Nickel (II) complexes of phenanthroline. crystal structures, electronic spectra and hydrogen bonded network of [Ni(phen)(H<sub>2</sub>O)<sub>3</sub>Br]Br, [Ni(phen)<sub>3</sub>](Br<sub>3</sub>)<sub>2</sub>.Br<sub>2</sub> Ni(phen)(H<sub>2</sub>O)<sub>3</sub>Cl]Cl(H<sub>2</sub>O) Kishore Babu, B.; Rajasekharan, M. V.
- (4) Synthesis, Crystal structure, Magnetic susceptibility and single crystal EPR studies of Cu(dafone) oxalate ion bridged polymeric complex with 4,5,diazafluoren-9-one; Kishore Babu,B.; Rajasekharan, M. V.
- (5) "Structural characterization of Cu(dafone)<sub>2</sub> (NCS)<sub>2</sub> and Ni (dafone)<sub>2</sub> (NCS)<sub>2</sub>,Ni (dafone)(NO<sub>3</sub>)<sub>2</sub> H<sub>2</sub>O EPR and electronic spectral studies" Kishore Babu,B.; Rajasekharan, M. V.
- (6) "Structural characterization of Cu(dafone)<sub>2</sub> (NCO)<sub>2</sub> EPR and electronic spectral studies" Kishore Babu, B.; Rajasekharan, M. V.